Policies and Planning for Low-Carbon Power Systems

Daniel Julius Burle Olsen

A dissertation
submitted in partial fulfillment of the
requirements for the degree of

Doctor of Philosophy

University of Washington

2019

Reading Committee:

Daniel Kirschen, Chair

Miguel Ortega-Vazquez

Baosen Zhang

Program Authorized to Offer Degree:
Electrical Engineering

University of Washington

Abstract

Policies and Planning for Low-Carbon Power Systems

Daniel Julius Burle Olsen

Chair of the Supervisory Committee:
Title of Chair Daniel Kirschen
Electrical Engineering

Mitigating the effects of anthropogenic climate change is a pressing global concern which will require steep cuts in emissions of greenhouse gases, including from power systems. In line with over a century of research into environmental economics, private industry has little incentive to provide enough emissions reductions unless induced to do so by effective public policy. There has been considerable research into energy and environmental economic policies, as well as into the technical potential for power systems to be planned and operated for lower carbon emissions, but so far the literature lacks an intersection of these two areas. This dissertation is intended to fill that gap, by presenting detailed technical models of power systems embedded within policy design problems for lowering carbon emissions. Four policy design models are proposed in detail:

i) Electrification of transportation will likely lead to large increases in at-home vehicle charging, which can stress residential distributions systems that were not planned for this level of peak evening demand. The deployment of home energy management systems will tend to shift loads towards traditional off-peak hours, but may end up creating new local peaks. How can distribution system operators manage the transition of their customers to more electrified transportation and price-responsive load scheduling?

ii) Power systems present one of the most practical opportunities for quick emissions reductions, as fuel-switching on the back-end can significantly reduce emissions with no

change in the quality or quantity of power delivered to consumers. However, many power systems are operated at minimum fuel cost and allow carbon dioxide to be emitted for free, or have a price on emissions that is ineffective in driving deep decarbonization. How can we design a carbon tax rate that achieves a given emissions reduction target at minimum cost increase?

iii) Much of the world's primary energy consumption is ultimately induced by the consumption of secondary energy consumption within buildings. If we are designing campus-scale infrastructure from scratch, which energy conversion and storage equipment should we install if we have a target for induced emissions? If we only have control of equipment choices via building codes, what are the relative efficiencies of these less direct policy measures?

iv) Grid-scale energy storage is often touted as the answer to the problem of intermittent renewable generation. However, if installed in current power systems and operated without regard for marginal emissions rates, it is likely to increase carbon emissions. If we mandate an 'emissions neutrality constraint'–the impact of storage operation on power systems cannot be to increase emissions–how does this change power system emissions, operating costs, and investment in grid-scale energy storage?

The use of these policy design approaches in broader-scale decarbonization models is discussed, and several more projects in the same vein are proposed for future work.

TABLE OF CONTENTS

LIST OF FIGURES

LIST OF TABLES

ACKNOWLEDGMENTS

I have many people to thank for helping me along the way to completing this dissertation. This list is not–and could not be–exhaustive, but I have tried to make it as complete as possible and mean no offense for any omissions.

First to my blood family, who have supported me since long before this endeavor was even an idea. I owe thanks to my parents, for nurturing my interest in mathematics and the natural beauty of the world, and for setting an example of advocating for change when you see injustice in the world. To my brother, for being someone I could always turn to, in good times and in bad. To my grandparents, for funding my education. To Auntie Carol and Uncle Dave, for a childhood full of fun trips to Los Angeles. To Auntie Pidgie and Uncle Ron, for hot meals and relaxing boat days in the middle of long cross-country road trips. To my cousin Derek, for endless dumb jokes and travel adventures. To my cousins Karen and Kaz, for [what happens at Camp Rozlik, stays at Camp Rozlik].

Second, to the academic community at UW, starting with the professors who have advised me. To Miguel, for teaching me how to conduct rigorous academic research, for tolerating my long process of deciding what I wanted to work on, and for lengua tacos at Fonda La Catrina. To Daniel, for trusting me to pursue projects in the order I saw fit, for a wealth of tangential research ideas, and for many conversations about the interplay between academic research and the real world. To the professors at Tsinghua University, Ning Zhang and Chongqing Kang, for offering me a unique opportunity to work in a different group and experience everyday life in a different country, and to Jingwei, Yaohua, and Yuxiao for helping me to get settled in a foreign environment. To Baosen Zhang, for his valuable feedback during my general exam and dissertation defense. To Rich Christie, for his candid suggestions on taking

the research a step further. To Brian Johnson, for purchasing an espresso machine for the lab and stocking it with beans. To Joe Mahoney, for his focus on the real-world application of the technologies and methods that we study. To Aseem Prakash for the example he set in collaboration between academia and governance.

Next to the students and postdocs I who I worked with during my time in the REAL lab. To my co-authors: Mushfiq, for giving me my first inside look at the academic paper process from start to finish; to Yury, for sending me more papers to read than I could ever keep up with; to Ricardo for your attention to detail and warm company. To my labmates: Jesus, for being a reliable sounding board for ideas and methods; to Abeer, for consistently bringing excitement and style and grace to our office; to Ahmad, for many productive conversations about research and politics, and for making me feel less alone as a power system researcher studying climate policy; to Mareldi for her boundless leadership in orchestrating social events for the department; to Chase, for inspiring the philosophical rationale of the Introduction. To the How To crew: Agustina, Anna, Drew, James, Jesus, John (my 351 guru), Kelly, Kevin, and Ryan; for many informative nights discussing pineapples and penguins. A special thanks to Mareldi, Tinu, Yuanyuan, and Bora for invaluable feedback on the defense presentation.

Third, to my chosen family. To Heather, for whipping me into shape towards functional adulthood. To Tom, for long bikes rides when I needed them and once or twice when I really didn't. To Meb, for always having my back at the drop of a hat. To Eric, for helping me get started road-tripping around the country, to Anna, for important conversations about the value of learning from discomfort, and to both of them for opening their home to me when I needed it the most.

To my roommates (or virtual roommates) over the years, who made the houses I lived in feel like homes. To Gideon, for being relentlessly upbeat and mischevious; to Rachel, for being a constant example of the value of self-care; to Sima, for demonstrating the value of being in tune with your body; to Abe, for innumerable long conversations on inane topics;

to Will, for vigilance on meat deals; and to Brian, Gonzalo, Haley, Hanley, and Marine.

To the Seattle burner community, who helped make this city feel like home. To Danne, for being the nucleus of a group full of productive creativity; to Kendra, for endless snark; to Allison, for being the textbook example of a supportive friend; to Mark, for maintaining your sense of humor even when you're exhausted and dripping with sweat; to Lia, for many cooking and costuming adventures; and to Michael, for countless fun hours fiddling with art projects. To the build crews of Inflection, Pentaphilia, and Phlogistan, for the creativity to build big art and the patience to teach people how to make it happen.

Fourth, to the broader community who helped teach me about energy, engineering, or civic engagement. To my high school teachers, who pushed us all to be better: Parker Merrill, Maryann Wolfe, Clarence Harris, and Marietta Joe. To my mentors at Lawrence Berkeley National Laboratory: Aimee McKane, Sila Kiliccote, Peter Therkelsen, Mike Sohn, Joe Eto, and Mary Ann Piette. To my mentors at the internships I worked during my summers: Farshid Shariatzadeh, Troy Nergaard, Tess Williams, Jesse Gantz, and Alex Rudkevich.

Finally, to the people responsible for the logistics of this bizarre endeavor. To the restaurateurs of the U-district and beyond, who kept me nourished through my studies: Saigon Deli, Chili's South Indian Cuisine, Teriyaki 1st, Sultan Gyro, Toronado Seattle, The College Inn Pub, and Ravenna Brewing Company. To the EE main office, who made sure that all us students were getting paid and had access to the resources we need. To the UW library, taking care of hundred-year old books for whenever we may need them. Last but not least, to the maintainers of the Lake Washington Loop and the other bike routes in the Seattle area.

Chapter 1

INTRODUCTION

If it is economically advantageous to a nation to keep up forests, on account of their beneficial effects in moderating and equalizing rainfall, the advantage is one which private enterprise has no tendency to provide; since no one could appropriate and sell improvements in climate.

– Henry Sidgwick, *The Principles of Political Economy*, 1887

1.1 Motivation

Worldwide, approximately 25% of greenhouse gas (GHG) emissions responsible for anthropogenic climate change are produced by electricity generation [1]. Limiting global average temperature rises to 2°C is widely assumed to avoid the worst effects of climate change, although there is a growing consensus that even a rise of 1.5°C would have significant negative effects [2]. However, the most recent pledges for the Paris Climate Accords are projected to result in end-of-century warming of 2.7-3.0°C, as shown in Figure 1.1 [3]. Worse still, the currently enacted policies are projected to result in end-of-century warming of 3.1-3.5°C. In order to stay below either the 1.5°C or 2°C limit, large sustained reductions in GHG emissions are needed, and power systems will need to contribute to this effort.

This is a problem unprecedented in human history. Similar problems of global scope have been encountered before, notably the exhaustion of certain natural resources, and innovative solutions have always been found. However, this is a problem not of resource exhaustion, but of pollution. In a resource exhaustion problem, the scarcity of supply drives market prices for

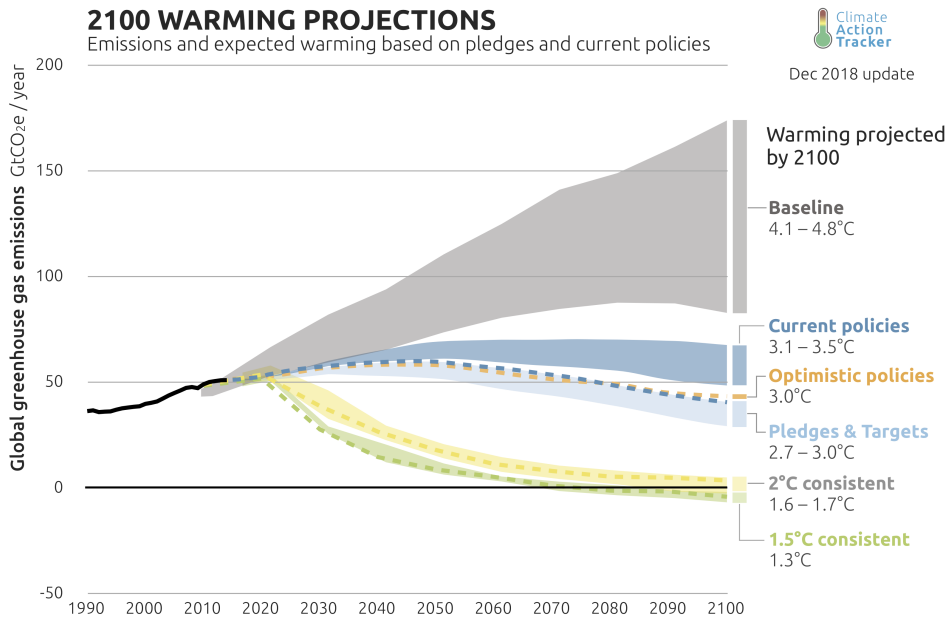

Figure 1.1: GHG emissions trajectories and estimated temperature rises. Source: Climate Action Tracker [3]

the resource upward, creating a strong incentive to reduce consumption and to develop and deploy alternative products. In a pollution problem, there is no such feedback loop, since the costs of pollution are borne by society as a whole, not by producers or consumers of pollution-causing goods and services.

Only by unprecedented levels of international cooperation has a similar global atmospheric pollution problem been solved in the past: the banning of clorofluorocarbons (CFCs) with the Montreal Protocol on Substances that Deplete the Ozone Layer. This agreement was not without its detractors however, as CFC manufacturers downplayed the dangers of their products. The global market for CFCs was approximately $2 billion in 1974 when their ozone depleting effects were first discovered [4]; adjusting for inflation this is still less than 1% of the global market in coal, oil, and natural gas today. Innovation has a role to play in solving anthropogenic climate change, but will not be effective alone without broad coordinating policies to mandate emissions reductions and direct innovation, investment, and

operations towards a more sustainable direction.

1.2 The Economic Principle of Externalities

Since the 18th century, the idea of an *invisible hand* has been a mainstay of economic theory. This concept, introduced by Adam Smith in *The Theory of Moral Sentiments* and *The Wealth of Nations*, holds that a collection of individuals each acting in their own self-interest will converge upon a utilization of labor, capital, and natural resources which yield production quantities and prices that maximize overall *social welfare*. Social welfare refers to the overall value that society has gained from the economic exchange: how much all consumers value their consumption, minus the cost born by all producers. The concept of social welfare also extends beyond the instantaneous economic exchange to consider value that will be reaped by future generations, as a result of decisions which are made at present day.

However, self-interested economic behavior when using exhaustible common-pool resources is different than when using private resources. One of the first documentations of this effect was by William Forster Lloyd in 1833, discussing the use of pasture to raise cattle [5]. Beyond a saturation point of a private pasture, a farmer will add no more cattle, since the grass eaten by an additional cow is subtracted from the grass that the rest of their cows can eat. However, in a 'common' (a shared field), a farmer still has an incentive to add more cows to the field, since the grass eaten by each new cow is subtracted partially from that of the farmer's existing cows but mostly from the grass which would be eaten by other farmers' cows. Without proper management of the common, more work will be done raising more cows, though no more beef will be harvested.

The overuse of natural resources, due to marginal private benefit despite greater marginal damage to society, was further described by utilitarian philospher Henry Sidgwick in the late 1800s [6]. Interestingly, one of Sidgwick's examples was of the quality of the climate, the most common good of all (see the note at the start of this chapter). This marginal damage to society is today referred to as a negative *externality*–contrasted with a positive externality (e.g. improvements in local climate from planting trees).

> Take, for instance, the case of certain fisheries, where it is clearly for the general interest that the fish should not be caught at certain times, or in certain places, or with certain instruments; because the increase of actual supply obtained by such captures is much overbalanced by the detriment it causes to prospective supply. Here,–however clear the common interest might be–it would be palpably rash to trust voluntary association for the observance of the required rules of abstinence; since the larger the number that thus voluntarily abstain, the stronger becomes the inducement offered to those who remain outside the association to pursue their fishing in the objectionable times, places, and ways, so long as they are not prevented by legal coercion. (Sidgwick 1887, Page 410)

This idea is reinforced by Alfred Marshall in 1890 in his influential *Principles of Economics* [7], and further developed in 1920 by Arthur Cecil Pigou [8], who proposes taxes by the State to correct for these misaligned incentives. Pigovian theory says that after the application of appropriate tax rates, the market will converge to the optimal prices and production quantities for maximum social welfare (absent other market failures). Even the conservative economist Milton Friedman, who argued for less governmental intervention in markets, endorsed taxation as a means of controlling pollution and mitigating its deleterious effects [9].

> Much remains to be done, by a careful collection of the statistics of demand and supply, and a scientific interpretation of their results, in order to discover what are the limits of the work that society can with advantage do towards turning the economic actions of individuals into those channels in which they will add the most to the sum total of happiness. (Marshall 1890, Pages 454-455)

> It is plain that divergences between trade and social net product of the kinds we have so far been considering cannot ... be mitigated by a modification of the contractual relation between any two contracting parties, because the divergence arises out of a service or disservice rendered to persons other than the contracting parties. It is, however, possible for the State, if it so chooses, to remove the divergence in any field by "extraordinary encouragements" or "extraordinary restraints" upon investments in that field. The most obvious forms, which these encouragements and restraints may assume, are, of course, those of bounties and taxes. (Pigou 1920, Page 168)

> Most economists agree that a far better way to control pollution than the present method of specific regulation and supervision is to introduce market discipline by imposing effluent charges. (Friedman 1980, Page 217)

Pigovian approaches to negative externalities are not without their criticisms, however. One of the most well-known is that of Coase [10], which argues that if transaction costs are low enough (via effective judicial enforcement of property rights and a small number of involved parties), then the problem of externalities is better handled by private bargaining between the affected parties than by governmental intervention. However, this approach is not applicable to the problem of global climate, since the number of affected parties is in the billions–to say nothing of the number of polluters–so transaction costs are prohibitively high. The Paris Climate Accords can be seen as an example of successful bargaining at the international level, showing that cooperation to reduce GHG emissions is possible; however, neither the pledges made nor the policies currently enacted and scheduled are strong enough to avoid temperature rises which may destabilize the climate.

Other market failures besides externalities include market power [7], macroeconomic effects [11], bounded rationality [12], imperfect information [13, 14, 15], and non-convexities [16]. Therefore it is reasonable to conclude that 'the invisible hand' does not always provide for maximum social welfare. Although governmental intervention does not always lead to maximum social welfare (see: public choice theory), any unintended consequences can be weighed against demonstrated benefits in order to assess whether the intervention is a net positive.

1.3 Emissions Pricing Strategies

With a nod to Pigou, the levying of a tax on producers of a given pollution, to internalize the negative marginal social cost of the externality, is often known as a *Pigovian tax*. However, the true value of the marginal social cost of a ton of CO_2 (the *social cost of carbon*) may be hard to determine, especially in the case where many people are impacted both geographically and temporally. Additionally, the marginal social cost of a given pollutant may change with respect to the quantity emitted. In this case, knowing the marginal social cost of a pollutant is not sufficient to set the tax rate resulting in a socially-optimal quantity of emissions. Instead, the supply and demand curves for the particular good(s) being produced (which have

pollution as a side effect) must be known, and the curve of marginal social cost of emissions (as a function of pollution quantity) must be considered alongside with the supply and demand curves for each good in order to determine the socially-optimal emissions quantity, and therefore the tax rate which should be applied such that emissions are not expected to exceed this quantity. If precise data on these curves cannot be obtained, another approach is to periodically update the tax rate based on updated estimates of of marginal cost as the quantity of emissions changes [17].

As an alternative to setting a price on emissions, a government may set a jurisdiction-wide emissions limit, and mandate that all polluters must obtain emissions allowances (of which the government creates a set quantity), proportional to their pollution. These emissions allowances can be traded, therefore allowing the market to determine their socially optimal allocation. This approach is often known as *cap-and-trade* or an *emissions trading scheme*, and has its origins in the late 1960s with computer simulations showing that such an approach provides more cost-effective outcomes than traditional command-and-control regulation [18]. The emissions trading approach was first put into policy in the Clean Air Act of 1977, drawing on trading practices applied to the Los Angeles basin in 1974 as a result of the Clean Air Act of 1970; the first nationwide cap-and-trade program was introduced in the Clean Air Act of 1990 in order to mitigate the incidence of acid rain caused by emissions of sulfur dioxide.

Both a carbon tax and a cap-and-trade system create a price for carbon emissions, which will reverberate through the economy so that GHG emissions are a component of the prices of goods and services proportional to their carbon footprint. A carbon tax creates an explicit price with the reaction of the broader market (e.g. producers, consumers, investors, technology development) determining ultimate emissions, while a cap-and-trade system sets an explicit emissions reduction and the broader market determines a price. Worldwide, there are 57 emissions pricing programs either implemented or scheduled for implementation, which today cover approximately 15% of global emissions. This will rise to approximately 20% once the China national emissions trading program is implemented in 2020 [19]. However, the vast

majority of these prices are well below current estimates of the social cost of carbon (discussed further in 1.5), so marginal emissions for which the social cost outweighs the private gain are still likely.

Pricing of carbon in either approach can lead to carbon 'leakage', *i.e.* the increased cost of producing goods in a jurisdiction with a carbon tax can lead to a shift in production toward jurisdictions with lower rates, or no tax at all [20]. One approach to avoiding this leakage is a tariff on the embedded carbon in imported goods; however, this approach is only feasible for jurisdictions with the ability to set their own tariffs, precluding use by e.g. sub-national entities or national entities bound by trade agreements.

Electricity generation represents approximately one quarter of worldwide GHG emissions [1], and that share is expected to grow in the future as energy used for heating and transportation are transitioned from fossil fuels towards electricity, a process known as *electrification*. On a life-cycle basis, transitioning this energy consumption from fossil fuels to electricity is expected to lower overall GHG emissions, due to efficiencies of scale in large modern power plants and the introduction of larger shares of carbon-free energy in power systems. Electricity also has the benefit of relatively efficient, near-instantaneous transportation, and in a standardized form independent of primary energy sources. In more-developed countries where electricity access is ubiquitous (i.e. where the majority of GHG emissions originate), a single conversion on the consumption side from fossil fuels to electricity allows the energy network to gradually decarbonize through multiple phases of fuel-switching on a smaller number of generation-side assets.

1.4 Emissions Policy Design as Game Theory

Game theory is the study of building mathematical models which represent the actions of a collection of rational actors. The application to economics is immediately apparent. Although the roots of game theory can be traced back to the early 19th century work of Antoine Augustin Cournot [21], it blossomed as a field in the early-mid 20th century with the work of John von Neumann [22] and John Nash [23].

In market economies, the ultimate provisioning of goods and services is determined by very large quantities of people making an even larger quantity of decisions, which are typically modeled as rational (based on the information available to each actor, which may be incomplete). Since these actions can result in sub-optimal social welfare in the case of externalities, there is a rationale for a socially-minded entity (*e.g.* a government) to intervene in the marketplace in order to guide the collection of decisions to a solution with greater social welfare (see Section 1.2).

The form of this intervention and the market response to this intervention can be thought of as a game theory problem, a *leader-follower* problem. These sorts of problems were first described by Heinrich Freiherr von Stackelberg [24]. Similar game theory problems within power systems have been explored in the past in non-emissions contexts [25].

In the context of climate policy, the government (or an alternative socially-minded organization) acts as the leader, who must decide their action first, knowing that the market participants (followers) will decide their actions with respect to their own objectives and with full knowledge of the leader's action. The question therefore becomes: what is the best policy to pursue, such that emissions targets are likely to be met with a given level of certainty?

1.5 Literature Review: Balancing Power System Emissions and Costs

Research to include emissions into generator dispatch began in the early 1970s with the concepts of minimum emissions dispatch [26], pricing of emissions to include their impact in economic dispatch [27], and varying emissions prices to investigate the tradeoffs between fuel costs and emissions [28]. These studies focused on local effects of NO_x and SO_x, the most recognized pollutants from power system operations in the 1970s. A survey of developments in environmental/economic dispatch over the following two decades is given in [29].

Coordination of power system operations based on fuel quantity constraints was explored in the 1990s by Fred N. Lee and others via the use of 'pseudo fuel prices' [30], adaptation of these prices for longer-term fuel consumption constraints (e.g. based on annual fuel purchase contracts) as realizations of uncertain variables differ from projections [31], and a survey

of similar long-term resource allocation methods [32]. These longer-term approaches are more suitable for GHG emissions, since their impact is neither local nor short-lived. This is highlighted in a review of resource planning models by Benjamin Hobbs in 1995 [33], which featured a tradeoff curve between annual costs and annual CO_2 emissions.

The trend towards deregulation of electricity in the 1990s (e.g. the Energy Policy Act of 1992, FERC Orders 888, 889, & 2000) changed the model for power systems planning; commitment and dispatch became more the domain of independent system operators (ISOs) or regional transmission organizations (RTOs), while investment in new generation capacity became more the domain of independent power producers. This arrangement is more amenable to market-based solutions to emissions problems (i.e. a carbon tax or cap-and-trade) rather than command-and-control regulation. Although market signals cannot incentivize all cost-effective changes, they are nevertheless powerful tools to effect change in a market environment (see [34] for examples of market barriers from the energy efficiency context).

Pricing of CO_2 emissions began with a few European countries in the 1990s, but a significant amount of emissions were covered for the first time with the enactment of the European Union's emissions trading scheme in 2005. This has led to a greater focus on emissions within power systems literature regarding policies and planning. For example: considering CO_2 emissions in generation expansion planning models [35], comparing changes in wind capacity, load reductions, and dispatch rules on system emissions [36], and considering variable carbon prices in transmission expansion planning [37]. Still, of the literature which presents itself as about decarbonization of power systems, the largest share focuses on particular materials and technologies, rather than on the dynamics of power systems operation, investment, or policy [38].

In the United States, direct control or pricing of power systems carbon emissions has been the exception, rather than the rule. A far more popular policy approach has been Renewable Portfolio Standards (RPSs), in which states mandate that utility companies source some percentage of their delivered energy from renewable generation (or in some cases, a certain absolute quantity). Though the first RPS was enacted in Iowa in 1983, the bulk of state RPS

implementation happened in two waves: one in the late 1990s and one in the mid 2000s. Many states have subsequently increased their RPS targets, some several times [39]. By mandating the purchase of energy from renewable sources, RPSs increase the demand for renewable energy and therefore incentivize construction of new renewable generation. This is effectively an indirect subsidy for renewable generation, in recognition of the fact that there are unpriced negative externalities associated with fossil fuel generation. Direct federal subsidies of renewable electricity production were enacted as part of the Energy Policy Act of 1992, with several expansions and extensions since then.

Although federal subsidies and RPSs have been instrumental in the rollout of significant penetration of renewable capacity, they are a less economically efficient decarbonization policy than one that targets GHG emissions directly (at least in the short term). For example, the installation of an additional MWh of wind or solar generation count equally towards a renewable portfolio standard, irrespective of which fossil fuel generation sources they displace. However, depending on the domain and the emissions target, this efficiency gap may be small (as in [40]).

Renewable generation and fossil fuel generation are both effectively subsidized (renewables subsidized by ratepayers in RPS jurisdictions and by taxpayers for federal subsidies, fossil fuel by being allowed to pollute the atmosphere for free), while nuclear and hydroelectric power often do not count towards renewable goals, despite emitting no GHGs. Accounting requirements for RPSs typically involve renewable energy credits (RECs)–potentially several types, as some RPSs have carve-outs and/or multipliers for certain types of energy and/or for distributed generation–which require rule-setting and compliance monitoring for the trading, banking, and retirement of allowances. Finally, the negative price bidding by renewable sources (since with RECs and tax credits the effective marginal cost of generation can be negative) can in some circumstances increase power system emissions [41].

On the other hand, the technological progress in producing renewable generation technologies (e.g. developments in cost, efficiency, and durability) as a side effect to RPS mandates of scale can be viewed as a positive externality; the benefits of this knowledge flow to all pro-

ducers, not just the individual firm which originally produced a technological breakthrough. Therefore, an argument can be made that the effective subsidization of renewable generation installation can be warranted. Case studies on the emissions effects of various RPS targets have estimated that the cost per ton of carbon reduced can still be well below estimates of the social cost of carbon [42]. There is a growing trend towards transitioning from Renewable Portfolio Standards to Clean Electricity Standards (CESs), which include contributions from nuclear and hydro generation. When factoring in co-benefits such as reductions in NO_x and SO_x emissions, RPS/CES policies can be clearly beneficial to social welfare, even if they are not as efficient as policies explicitly based on GHG reductions.

At a whole-economy scale, integrated assessment models (IAMs) estimate the interactions between between the climate and the economy in order to derive estimates for the social cost of carbon, and can be used to model the relative costs of various GHG mitigation strategies. Well-developed IAMs include Hope's PAGE [43, 44, 45], FUND by Anthoff and Tol [46], and Nordhaus's DICE/RICE [47]. However, these models have their limitations when it comes to decision-making for low-carbon power systems. The modeling of energy networks is necessarily very high-level, and therefore is unable to compare the impact of policy and planning decisions for power systems specifically. Additionally, the estimates for the social cost of carbon have a considerable degree of uncertainty, due to uncertainty in projections of economic parameters and climate impacts, and use of a social cost of carbon alone to price carbon emissions ignores the differences between countries in their historical contributions to climate change and their present capacity to invest in lower-carbon energy systems.

A similar modeling effort is the Energy Policy Simulator developed by Energy Innovation [48]. The simulator is an interface for estimating how given policy instruments affect the trajectory of overall US GHG emissions. Many policy options specific to the electricity sector are available, although spatial and temporal constraints of power systems are not modeled in detail. Accompanying policy design considerations are given in a book by the same authors [49].

Further academic work on energy policy is also conducted at the following institutions:

- The Center on Global Energy Policy, Columbia University
- The Energy Policy Institute, University of Chicago
- The Kleinmann Center for Energy Policy, University of Pennsylvania

1.6 Contributions

How should we plan and operate power systems, when the true social cost of carbon emissions from fossil fuels is unknown? One approach is to look at what policies can be implemented in order to reach a given emissions goal, where this goal is determined via cooperation from climate scientists (*how much carbon can be emitted worldwide?*), international representatives (*how much of that carbon should each country be allowed to emit?*), and social planners (*how much of each country's emissions budget should be devoted to power systems?*). In the context of this dissertation, 'policy' is a broad umbrella for any planning decisions or operational rules which relate to power systems and decarbonization.

These policies can be mandates of emissions limits in operational and planning decisions, or policies of setting a price to induce economic actors to reduce their induced emissions. Alternatively, power systems can be planned and operated in adaptation to changing usage of the power system, due to decarbonization efforts outside the electricity sector. For example, electrification of transportation increases energy consumption from power systems while reducing overall GHG emissions; planning for this new electricity demand involves decarbonization policy that includes power systems, even though power system carbon emissions are not directly targeted. For the purpose of categorization, these three policy options are referred to as *carbon constraints*, *carbon pricing*, and *adaptation to external changes*, respectively.

Another categorization of policies and plans for low-carbon power systems is the domain over which they operate: do we need to model the policy impacts on the wholesale generation and transmission of electricity, the flow of electricity through the distribution grid, the use of electricity by consumers, or a combination of these domains?

For any combination of policy option and domain, there is a commonality, which is the theme of this dissertation. **In market environments, detailed models anticipating the economic reactions of independent stakeholders to a given emissions policy are necessary in order to reach emissions targets at lowest overall social cost.** This dissertation describes in detail several policy and planning approaches for power systems decarbonization. Each approach is mapped onto the two aforementioned categories in Figure 1.2. In addition, there are several proposed approaches worthy of future study, which are briefly described in Chapter 6.

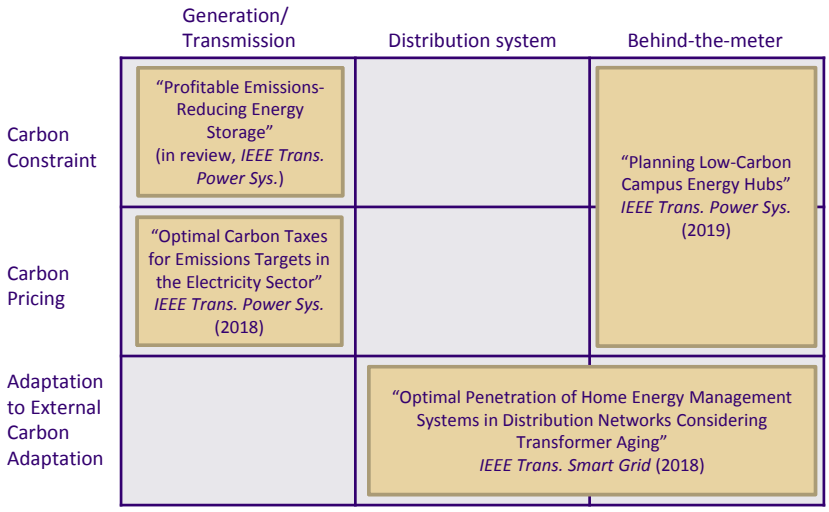

Figure 1.2: Low-carbon power system design models, organized by method and point(s) of application

There are several important aspects of power systems decarbonization policy that are outside the scope of this work:

- **What to do with revenue collected from carbon pricing?** Adding a price on

carbon makes electricity generated from lower-carbon sources more competitive with electricity generated from carbon-intensive sources. However, increasing taxation is politically sensitive and must often be offset with investment in public goods or reduction of taxes in other sectors in order to be politically palatable. Where to spend collected revenue is a distinct policy question which can be decided separately from what the price should be.

- **What technology developments would change carbon emissions trajectories?** Energy is an integral part of the world economy, and research and development in new technologies is a rich field. Although there will undoubtedly be new energy technologies which emerge in the future, there are a multitude of potential technologies and extreme uncertainty about whether any particularly technology will reach commercialization. The techniques presented in this dissertation can be applied to an arbitrary set of potential futures with different sets of commercial technologies, given estimations of their relative likelihood.

- **What spillovers effects will these policies have outside of power systems?** Any significant energy policy will have secondary effects on other sectors, both positive (e.g. increased employment in new lower-carbon energy industries, co-benefits from improved local air quality) and negative (e.g. decreased employment in carbon-intensive industries, utility ratepayer responsibility for prematurely-closed energy infrastructure). Inclusion of these factors would render detailed optimization of power systems policy intractable; integrated assessment models are better tools for these sorts of economy-wide analyses, where sector-specific details must necessarily be reduced in order to produce results in a reasonable amount of time.

- **What technical changes are needed for 100% carbon-free power systems?**. The technical considerations for transitioning power systems from business-as-usual to low-carbon systems are very different than those from transitioning a low-carbon

system to a carbon-free system. Transitioning to a carbon-free system will likely require sweeping changes in both grid control strategies and power markets, and will depend on the particular trajectory towards a lower-carbon system [50, 51].

- **How can political will be built for the policies needed for significant carbon reductions?** Economists have consistently agreed that pricing of externalities prioritizes the most-cost effective emissions reductions (in the general case); however, carbon pricing is one of the least popular policies in many jurisdictions, and public preference leans toward alternate policies such as Renewable Portfolio Standards or Clean Energy Standards which are more expensive per ton of CO_2 reduced. Political viability of more efficient policies will be dependent on messaging strategies and outreach to the general public.

- **How can the global transition to low-carbon power systems be conducted equitably?** Policies to achieve low-carbon power systems will have wide-ranging effects on the cost and availability of energy, which has distributional effects both within countries and internationally. Determining which complementary policies to implement to ensure that this transition is conducted 'fairly' will be a significant endeavor.

1.7 Organization

The following four chapters detail four models for planning various aspects of low-carbon power systems, either published or in review:

- Chapter 2: **Optimal Penetration of Home Energy Management Systems in Distribution Networks Considering Transformer Aging** [52] answers the question *How should we plan for increased penetration of electric vehicles and home energy management systems and their impacts on the distribution system?*

- Chapter 3: **Optimal Carbon Taxes for Emissions Targets in the Electricity**

Sector [53] answers the question *How can we determine what tax rate to apply to power systems emissions such that emissions are reduced below a given target?*

- Chapter 4: **Planning Low-Carbon Campus Energy Hubs** [54] answers the question *What is the relative efficiency of infrastructure design policies aimed at reducing induced emissions from large-scale greenfield developments?*

- Chapter 5: **Profitable Emissions-Reducing Energy Storage**, currently under revision for resubmission to *IEEE Transactions on Power Systems* [55], answers the question *How does an emissions-neutrality constraint applied to energy storage operation impact the quantity of storage economically installed and the resulting power system emissions?*

Chapter 6 details four additional models for planning low-carbon power systems, in preliminary stages of development but intended to round out the preceding publications:

- Emissions-Aware Tariff Design
- Operation of a Closed-Loop Carbon Cycle Power System
- Planning Low-Carbon District Energy Systems
- Comparing a Carbon Tax with Emissions Trading in Power Systems Operation

Finally, Chapter 7 concludes.

1.8 Optimization Notation

Optimization for power systems often takes the form of a series of equations similar to (1.1)-(1.3).

$$\min_{\boldsymbol{x},\boldsymbol{y}} f(\boldsymbol{x},\boldsymbol{y}) \tag{1.1}$$

subject to:

$$g_i(\boldsymbol{x},\boldsymbol{y}) \leq 0 \qquad \forall i \in I \tag{1.2}$$

$$h_j(\boldsymbol{x},\boldsymbol{y}) = 0 \qquad \forall j \in J \tag{1.3}$$

$$\boldsymbol{x} \in \mathbb{R}, \qquad \boldsymbol{y} \in \mathbb{I}$$

Traditionally, power system operators have a mandate to serve all connected load at minimum cost, subject to technical constraints and reliability requirements. In this paradigm, minimization of system cost $f(\boldsymbol{x},\boldsymbol{y})$ is equivalent maximization of overall social welfare. In some formulations, there is the ability to not serve a segment of the load demand, but only at extremely high cost (this is equivalent to a cap on the maximum price at which electricity can be sold). This penalty is known as the *value of lost load*. At a very high value of lost load, the solution maximizing social welfare approaches the solution found by minimizing the cost of satisfying all load.

Often, a subset of the decision variables are constrained to take only discrete values, represented by $\boldsymbol{y}$ in the formulation above (this is often referred to as *integer programming*). The constraints on the decision variables, $g_i(\boldsymbol{x},\boldsymbol{y})$ and $h_j(\boldsymbol{x},\boldsymbol{y})$, are typically technical constraints, but may also be constraints related to mathematical transformations to improve tractability or to represent the actions of followers in multi-level models (see Section 1.4).

When optimization problems with integer variables are solved, they are often not solved to the absolute best solution due to the computational effort required. Candidate solutions are typically evaluated until the solver can guarantee that the best solution can be no more than a given percentage better than the current best candidate (this percentage is known as the *optimality gap*, at which time the candidate solution is returned as 'the solution'). Although there may not be a large difference between the returned solution and the true optimum, there may be significant differences in terms of the decision variables, and therefore

important results such as prices and participant revenue [56]. Therefore, sensitivity analyses and/or Monte Carlo simulations are important, in order to be able to filter general trends out of a set of results which may have significant noise.

Chapter 2

OPTIMAL PENETRATION OF HOME ENERGY MANAGEMENT SYSTEMS IN DISTRIBUTION NETWORKS CONSIDERING TRANSFORMER AGING

Published as:

Olsen, D. J., Sarker, M. R., & Ortega-Vazquez, M. A. (2018). Optimal penetration of home energy management systems in distribution networks considering transformer aging. *IEEE Transactions on Smart Grid*, 9(4), 3330-3340.

2.1 Introduction

In the smart grid framework, real-time pricing (RTP) schemes have been proposed in order to better reflect the utilization of the generation and transmission assets at the retail level. These pricing schemes, together with the rapidly falling cost of communications and controls, will result in large volumes of customers featuring high degrees of demand flexibility [57]. In this context, customers will strive to minimize their electricity costs by reducing their consumption during high-price periods (traditionally correlated with peak demand periods), in favor of greater consumption in lower-price periods. In effect, this should reduce the traditional demand peaks (which can be in the early morning, the afternoon, or the evening, depending on the region and the customer mix) and fill in the valleys, while lowering the overall cost of procuring energy [58].

To take advantage of this pricing scheme, some residential customers are likely to install home energy management systems (HEMSs) to control their large appliances and electric vehicles (EVs). These systems can lower overall electricity bills while ensuring that occupants' needs are met [57, 58, 59, 60, 61, 62]. However, if a high enough percentage of residential

customers are optimizing their electricity use for the same tariff (e.g., RTP), large demand spikes may occur in the lowest-priced time periods, whose magnitudes may eclipse those of the traditional peaks [63].

High demand causes temperatures to rise in the pole-top transformers that these residential customers are connected to, leading to accelerated breakdown of the transformer insulation [64]. This is known as "accelerated aging". These new demand peaks can cause greater aging than the case without HEMS installations. However, a mixture of residences with and without HEMSs can result in lower overall demand peaks and consequently less transformer aging. This is the case because the peak consumption of the two groups (i.e., with and without HEMSs) is non-coincident.

In a 2006 survey of distribution utility capacity enhancement projects, new transformer installations represented the largest share of total costs [65]. Clearly, the maintenance of these sunk cost assets should be a priority, in order to avoid the cost of premature replacement. In this case, distribution system operators (DSOs) would like to be able to influence the rollout of HEMSs in their networks, in order to manage the aging of their transformers. One approach to do this is through the use of incentives, which have a long history of use in controlling customer loads through demand response [66] and energy efficiency programs [67, 68].

Other studies have investigated the impact of other emerging technologies on distribution transformer aging: uncontrolled EV charging in [69, 70, 71], controlled EV charging in [72, 73, 74], residential solar generation in [75], harmonics from solid state electronics in [76]. Operating strategies to manage this aging using demand response [77], EVs [72, 78], energy storage [79], and increased penetration of distributed generation [80] have been developed, but so far no work has been done to optimize the rollout of these emerging technologies with regard to transformer aging.

This study presents an approach for determining the optimal rollout of HEMSs in a distribution network, measured by the total cost of transformer aging, under several different rollout management strategies. Centrally optimizing the operation of this growing population

of smart devices would require the collection, transmission, and processing of large volumes of customer data (e.g. appliance characteristics, schedules, real-time temperatures), but optimizing the rollout of independent HEMSs on the network is a more tractable problem that can reduce the aging of transformers, potentially even below the baseline (pre-HEMS) case.

The main contributions of this study are:

- An approach for assessing the cumulative damage cost of a feeder (i.e. transformer aging) populated by mixed group of residential customers with and without HEMSs,
- A simplified formulation for determining the optimal combination of HEMS customers on a feeder, and
- A demonstration of these methods using representative data on feeder topology, customer appliances, and relevant external factors (e.g., outdoor air temperature and electricity tariff).

These contributions will provide DSOs with the ability to evaluate both the impact of a growing population of HEMS devices on their networks as well as their ability to mitigate the associated damages.

The rest of this chapter is organized as follows: Section 2.2 describes the model components, Section 2.3 provides a case study, Section 2.4 presents the results, Section 2.5 discusses considerations for implementation, and Section 2.6 concludes. A nomenclature section follows at the end of the chapter.

2.2 Proposed Approach

A distribution system, including distribution transformers and residential load profiles for both the HEMS and no-HEMS case, is modeled to study the impact of HEMS penetration on transformer damage costs. This approach has three major components: i) the modeling of the transformer damages, ii) the modeling of the rollout of HEMS in the distribution network, and iii) the modeling of HEMS load profiles. Though each of the components

operates independently, the modeling of HEMS load profiles is needed in order to model the transformer damages given a combination of HEMS and no-HEMS customers, which are used to model the HEMS rollout and management strategies. The relationship between the models is shown in Fig. 2.1. The following subsections describe each of these components.

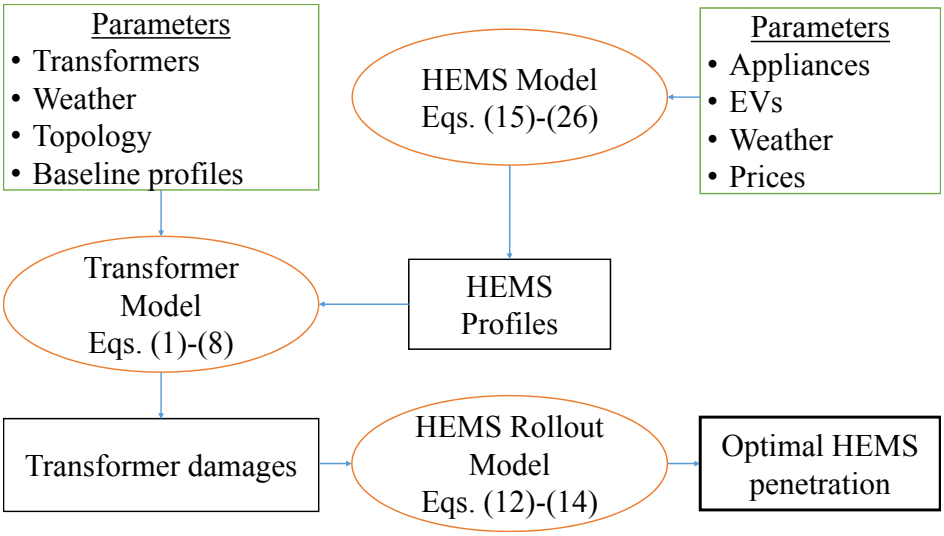

Figure 2.1: The relationship between model components

2.2.1 Transformer model

The loading $k_{j,t}$ of the transformer j at time t for a combination of HEMS and no-HEMS customers can be calculated as in Equation (2.1),

$$k_{j,t} = \frac{\sum_{i \in N} a_{ij} \cdot \left[d_{i,t}^{\text{no-HEMS}} \cdot (1 - p_i) + d_{i,t}^{\text{HEMS}} \cdot p_i \right]}{\alpha_j} \quad \forall t \in T, j \in M \tag{2.1}$$

This time-varying load, $k_{j,t}$, is used to estimate the accelerated aging of the transformer, using IEEE Standard C57.91-2011 [64], as described in Equations (2.2)-(2.8). Alternate estimation methods using genetic programs [81] and more complicated thermodynamic models [82] have also been proposed. A method of estimating the transformer parameters used in Equations (2.2)-(2.8) is given in [78].

$$FAA_{j,t} = \exp\left(\frac{15000}{383} - \frac{15000}{\Theta^{\mathrm{HS}}_{j,t} + 273}\right) \quad \forall j \in M, t \in T \tag{2.2}$$

$$LoL_j = \frac{\Delta t \sum_{t=1}^{T} FAA_{j,t}}{\beta_j} \quad \forall j \in M \tag{2.3}$$

$$\Theta^{\mathrm{HS}}_{j,t} = \Theta^{A}_{t} + \Delta\Theta^{\mathrm{TO}}_{j,t} + \Delta\Theta^{\mathrm{HS}}_{j,t} \quad \forall j \in M, t \in T \tag{2.4}$$

$$\Delta\Theta^{\mathrm{TO}}_{j,t} = (\Delta\Theta^{\mathrm{TO,U}}_{t} - \Delta\Theta^{\mathrm{TO}}_{t-1})\left(1 - \exp\left(-\frac{\Delta t}{\tau^{\mathrm{TO}}_{j}}\right)\right) + \Delta\Theta^{\mathrm{TO}}_{t-1} \quad \forall j \in M, t \in T \tag{2.5}$$

$$\Delta\Theta^{\mathrm{TO,U}}_{j,t} = \Delta\Theta^{\mathrm{TO,R}}_{j} \cdot \left[\frac{(k_{j,t})^2 \cdot R_j + 1}{R_j + 1}\right]^{n_j} \quad \forall j \in M, t \in T \tag{2.6}$$

$$\Delta\Theta^{\mathrm{HS}}_{j,t} = (\Delta\Theta^{\mathrm{HS,U}}_{j,t} - \Delta\Theta^{\mathrm{HS}}_{j,t-1})\left(1 - \exp\left(-\frac{\Delta t}{\tau^{\mathrm{HS}}_{j}}\right)\right) + \Delta\Theta^{\mathrm{HS}}_{t-1} \quad \forall j \in M, t \in T \tag{2.7}$$

$$\Delta\Theta^{\mathrm{HS,U}}_{j,t} = \Delta\Theta^{\mathrm{HS,R}}_{j} \cdot (k_{j,t})^{2m_j} \quad \forall j \in M, t \in T \tag{2.8}$$

Equations (2.2)-(2.8) describe the impact of the transformer loading on the corresponding impact on loss-of-life. Briefly, a specified loading yields ultimate top-oil (6) and hot-spot (8) temperature rises; the realized temperature rises are governed by the ultimate rises, previous rises, and thermal time constants (5,7); the absolute hot-spot temperature is based on the ambient temperature and these rises (4); and the cumulative loss-of-life is based on the absolute hot-spot temperature in each period (2,3). For more information, the reader is advised to refer to IEEE standard C57.91-2011 [64].

It is important to note that higher peak loading does not necessarily translate into greater transformer damage. This is because the transformer aging factor is related non-linearly to the transformer hot-spot temperature, which does not respond instantaneously to transformer loading due to the thermal time constants of the top-oil and winding hot-spot. As an example, Fig. 2.2 shows two of the load profiles that were constructed from the Pecan Street data (as described in III.B), and their resulting transformer aging when connected to identical transformers. In (a), the loading factor always remains under 1.3, and the cumulative aging of the transformer is 1.1 days. In (b), the loading factor reaches a peak of 1.47, but the cumulative aging of the transformer is only 0.5 days. This shows the importance of

optimizing for transformer damage directly.

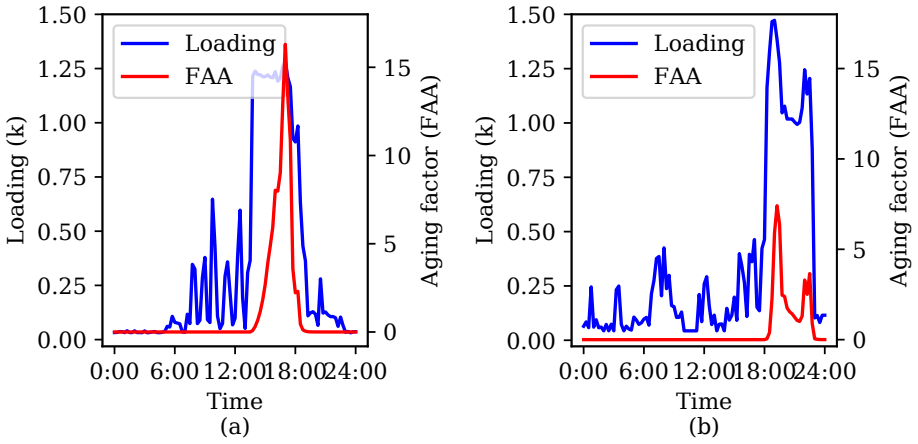

Figure 2.2: Illustration of potential differences between peak loading and transformer aging. In (a), a load profile with a lower peak loading but high transformer aging. In (b), a load profile with a higher peak loading but lower transformer aging.

2.2.2 Transition Strategies

Residential customers may have several reasons to install a HEMS. If they are exposed to TOU or RTP schemes [83, 84], a HEMS may help them save money on their electricity bills by scheduling loads. Even without TOU/RTP, some HEMSs may intelligently control appliances in order to facilitate integration of renewable energy [85], or for energy efficiency purposes. If customers live in areas that are prone to high demand or constrained supply during extreme weather events, they could contribute to grid reliability, and thus ensure their own continuity of supply. Other customers may desire remote control and automation over their home appliances. Regardless of the motivations, customers must balance their desire for a HEMS with the up-front cost and inconvenience of purchasing, installing, and configuring one. The interested reader is encouraged to refer to [86] for a discussion of motivations for HEMS installation.

In situations where the costs of HEMSs outweigh the perceived benefits, the DSO has the

ability to use techniques such as marketing materials, up-front incentives, or recurring bill credits to motivate customers. If the uptake of HEMSs can reduce the operating costs of the distribution system via reduced transformer aging then there may be a mutual benefit in the DSO offering an incentive to the customer in exchange for HEMS adoption. However, this mutual benefit may not exist over all HEMS penetration levels, so the DSO must manage the HEMS rollout to minimize costs.

Four strategies for managing the HEMS rollout are investigated. The first three strategies as heuristic strategies, and the last is an optimized strategy.

Heuristic Strategies

- Random Strategy: Residences are transitioned from no-HEMS to HEMS randomly. This could be the case where a distribution system operator (DSO) incentivizes HEMSs without any pre-defined targeting.

- Even Strategy: The residence targeting order (i.e. to transition to HEMS) to is based on the transformer with the lowest HEMS penetration at any given time. If there is a tie in lowest penetration, priority goes to the transformer with the highest number of residences, so that the increase in penetration is smallest. The residence to be transitioned is randomly chosen out of all of the residences at the transformer. This could be the case where the DSO incentivizes HEMSs by targeting residences at transformers which currently have low penetrations of HEMSs.

- Greedy Strategy: Residences are transitioned using a greedy algorithm. For each decision about the next residence to target, under each transformer the impact of transitioning one randomly chosen residence is calculated, and the transformer whose transition offers maximum benefit (or minimum loss) is chosen to be transitioned. This could be the case where a DSO incentivizes HEMS adoption by targeting residences at transformers which experience frequent high loading and therefore accumulate damage

rapidly.

Optimized Strategy

In the optimized strategy, a DSO selects the combination of HEMS residences with the minimum total transformer damage cost.

The problem of finding the optimal set of residences to transition is described in the objective function (2.9), where $k_{j,t}$ is calculated using Equation (2.1) and is related to LoL using Equations (2.2)-(2.8).

$$\min_{p} \sum_{j \in M} \alpha_j \cdot LoL(k_{j,t}) \tag{2.9}$$

subject to:

$$\text{Equations (2.1)-(2.8)} \tag{2.10}$$

$$\sum_{i \in N} p_i \leq c \tag{2.11}$$

For a case where there is a limit on how many residences can be transitioned (e.g., when the distribution company only has a certain budget) another constraint can be added, as shown in (2.11).

The complexity of this formulation, however, grows exponentially with the numbers of residences, $|N|$, since there are $2^{|N|}$ possible values of p_i, each with their own non-linear calculation of the total transformer damage cost, as shown in Equations (2.1)-(2.8). Even if a lookup table is created of the damage costs at each transformer, for each combination of HEMS and no-HEMS residences, there are still $\sum_{j \in M} 2^{r_j}$ damage costs which must be pre-calculated and loaded into an optimization problem, or estimated within the optimization process using a piecewise linearization technique such as special ordered sets of type 2 (SOS2) [87].

Fortunately, the problem can be simplified to a formulation where there are only $\prod_{j \in M} r_j$ candidate solutions, by using the following method:

- For each transformer, calculate the damage for each combination of no-HEMS and HEMS residences. For instance, a transformer that supplies three residences, where one has a HEMS, another has no HEMS, and the last has a HEMS can be represented as $(1, 0, 1)$.

- Group the combinations by the number of residences with HEMSs. For instance, $(0, 1, 1)$, $(1, 0, 1)$, and $(1, 1, 0)$ would be grouped based on each having two residences with HEMSs.

- For each group, discard all combinations except for the least damaging one. This damage cost represents the damage cost of that number of HEMS residences.

- Reformulate the decision of which residences to transition at the transformer (r_j binary decisions) to how many residences to transition (one integer decision in [0, r_j]).

- The discarded combinations are provably sub-optimal for the transformer in question, and since there is no interaction with any other transformers, the discarded combinations are also provably sub-optimal for the problem as a whole.

Therefore, the problem is reduced in complexity: the number of damage costs per transformer is thus reduced by a factor of $2^{r_j}/(r_j + 1)$, which in the $r_j = 20$ case is nearly 50,000. The problem is transformed from the formulation in Equations (2.9)-(2.11) to the optimization problem below:

$$\min_{v} \sum_{j \in M} \alpha_j \cdot LoL(k_{j,t}) \tag{2.12}$$

subject to:

$$\text{Equations (2.1)-(2.8)} \tag{2.13}$$

$$\sum_{j \in M} v_j = c \tag{2.14}$$

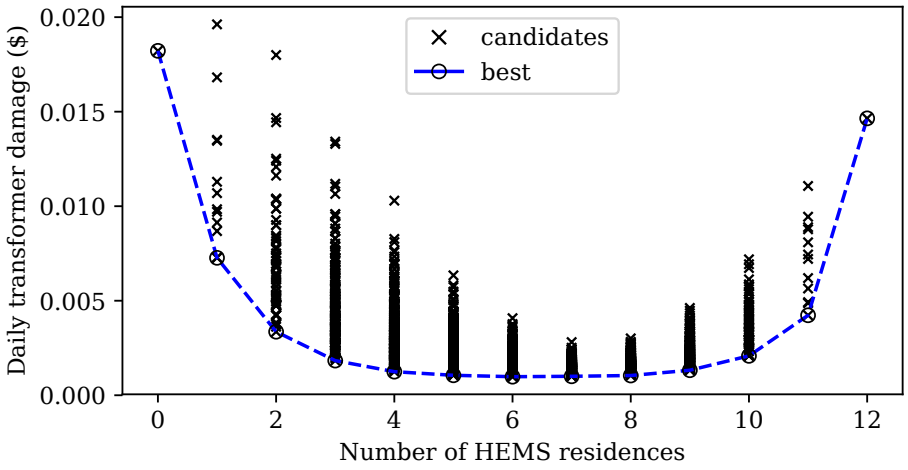

Figure 2.3: Elimination of sub-optimal candidate solutions

This process is illustrated in Fig. 2.3, representing a transformer connected to 12 residences. The transformer damage resulting from each combination of HEMS and no-HEMS customers is marked by the symbol '×', and the least-damaging combination for each number of is marked by the symbol '∘'. In this way, the 12 binary variables representing 2^{12} (4,096) potential solutions are reduced to an integer variable on [0,12], representing 13 potential solutions. Because the elimination of sub-optimal candidates solutions is conducted on a per-transformer basis, the level of computation involved in the elimination stage scales linearly with the total number of customers and the eliminations can be conducted in parallel to speed up computation.

Since the HEMS load profiles $d_{i,t}^{\text{HEMS}}$ are needed to calculate the time-varying transformer loading as described in Equation (2.1), a model for estimating the HEMS load profiles is needed. The model described in [59] is used, and is described in Section II.C.

2.2.3 HEMS Model

The load profiles for residences equipped with HEMS are constructed using an optimization formulation, where each residence minimizes their electricity costs while maintaining

constraints on indoor temperature, EV battery state-of-charge (SoC), and other appliance operations within acceptable bounds, as described in equations (2.15)-(2.26) [59]. Considered appliances are water heaters (WH), heating ventilation and air-conditioning (HVAC) systems, EVs, dishwashers, washers, and dryers. This problem is mathematically formulated as follows:

$$\min \Delta t \sum_{t \in T} \pi_t \left[P_t^{\text{base}} + \sum_{a \in A} P_a \frac{\delta_{a,t}}{L_a} + P_t^{\text{EV}} \right] \tag{2.15}$$

subject to:

$$\delta_{a,t} \leq V_{a,t} \quad \forall t \in T, a \in A \tag{2.16}$$

$$\sum_{t \in T} \delta_{a,t} = D_a \quad \forall a \in A \tag{2.17}$$

$$\sum_{h=t}^{t+D_a-1} \delta_{a,h} \geq D_a \cdot (\delta_{a,t} - \delta_{a,t-1}) \quad \forall t \in T, a \in A \tag{2.18}$$

$$\sum_{h=0}^{t-1} \delta_{\text{washer},h} \geq D_{\text{washer}} \cdot \delta_{\text{dryer},t} \quad \forall t \in T \tag{2.19}$$

$$0 \leq P_t^{\text{EV}} \leq \overline{P^{\text{EV}}} \cdot \alpha_t \quad \forall t \in T \tag{2.20}$$

$$SoC_{t+1} = SoC_t + \Delta t \cdot P_t^{\text{EV}} \cdot \eta - \xi \frac{M_t}{\sum_{t \in T} M_t} \quad \forall t \in T \tag{2.21}$$

$$\underline{SoC} \leq SoC_t \leq \overline{SoC} \quad \forall t \in T \tag{2.22}$$

$$\underline{\Theta_a} \leq \Theta_{a,t} \leq \overline{\Theta_a} \quad \forall a \in \{\text{WH}, \text{HVAC}\}, t \in T \tag{2.23}$$

$$\Theta_t^{\text{room}} = \exp\left(\frac{\Delta t}{\tau_{\text{HVAC}}}\right) \Theta_{t-1}^{\text{room}} + \left(1 - \exp\left(\frac{\Delta t}{\tau_{\text{HVAC}}}\right)\right) \left(\Theta_t^{\text{A}} + \frac{\delta_{\text{HVAC},t}}{L_{\text{HVAC}}} Q_{\text{HVAC}} P_{\text{HVAC}}\right) \quad \forall t \in T \tag{2.24}$$

$$\Theta_t^{\text{water}} = \exp\left(\frac{\Delta t}{\tau_{\text{WH}}}\right) \Theta_{t-1}^{\text{water}} + \left(1 - \exp\left(\frac{\Delta t}{\tau_{\text{WH}}}\right)\right) \left(\Theta_t^{\text{tank}} + \frac{\delta_{\text{WH},t}}{L_{\text{WH}}} Q_{\text{WH}} P_{\text{WH}}\right) \quad \forall t \in T \tag{2.25}$$

$$\Theta_t^{\text{tank}} = \Theta_t^{\text{water}} - H_t \Theta_t^{\text{out}} \quad \forall t \in T \tag{2.26}$$

Equation (2.15) is the objective function, which consists of minimizing the cost of procur-

ing energy as a function of the energy prices and the power consumption of base loads, controllable loads, and EV charging. The constraints are:

- Dishwashers, washers, and dryers can only operate during certain hours for noise reasons (2.16), must be on for their duration time (2.17), and must stay on for their full duration once activated (2.18). Additionally, the washing machine must finish running before the dryer can be run (2.19).

- Electric vehicles' charging power is limited to the chargers' rated power and can only be non-zero when the vehicle is plugged in (2.20). The battery state-of-charge follows conservation of energy when considering charging power and required transportation energy (2.21), and the state-of-charge stays within operational limits (2.22).

- Temperatures controlled by each thermal appliance $\Theta_{a,t}$ remain within acceptable ranges (2.23).

- Appliance controlled temperatures maintain conservation of energy considering the appliance power, heat loss to the environment, (2.24)-(2.25), and hot water consumption patterns (2.26).

To model the diversity of residential demands for the HEMS model, the optimization is run for many different parameter sets. Equipment parameters that can be varied include appliance power ratings and capacities. Operational parameters that can be varied include temperature setpoints for thermostatically controlled appliances and availability ranges for non-thermal appliances. Initial conditions that can be varied include the EV SoC upon arrival and the starting temperature of thermostatically controlled appliances.

2.3 Case Study

To test the effect of increasing HEMS penetration on a distribution network, a representative distribution feeder is populated with two sets of representative residential load profiles, one

representing the no-HEMS case and one representing the HEMS case (i.e., appliance demand is optimized based on Equations (2.15)-(2.26). Several penetration levels of HEMSs are tested using the transition strategies described in Section II.B and II.C. For each HEMS penetration level, the LoL for each transformer is calculated and converted to a damage cost using a cost of transformer replacement of 166.1 $/kVA [65], and summed to yield the total damage cost for that penetration level.

Ten trials are run, in which the residential load profiles are randomly assigned to locations in the feeder, in order to reduce the impact of anomalous load profile groupings and observe the variance in total transformer damage costs.

The case study was run on a desktop computer with a quad-core 3.10 GHz processor and 16 GB of RAM, and was completed in approximately 17 hours. The majority of this time (14 hours) was consumed by the sub-optimal candidate elimination stage (as described in Section II.B.2 and demonstrated in Figure 3). Since the calculation time for this stage scales linearly with the number of customers and is parallelizable, the authors believe that this approach is suitable for larger case studies, especially since this is a planning model and not an operating one.

2.3.1 Feeder

A Taxonomy Test Feeder developed by the Pacific Northwest National Laboratory (PNNL), specifically R1-12-47-1 [88], is used as a representative feeder. This feeder is rated at 12.47 kV and classified as a "moderate suburban and rural" topology. As this feeder is described in the GridLAB-D .glm file, each triplex load is served by an individual pole-top transformer (598 transformers in total), several of which are connected to a single node in the distribution system. In the context of the GridLAB-D feeder model, "triplex" refers to a service drop to a single residence, providing split phase 120/240V power over a three-wire bundle. The sizes for the transformers ranged from 5 to 62.5 kVA, with an average of 18.6 kVA. The demands for each triplex load ranged from 0 to 66 kVA, with an average of 10.2 kVA. Further information about the distribution is shown in Table 2.1. Only a single demand for each load was given,

this demand is assumed to be the value of the daily peak.

Table 2.1: Characteristics of residential load distribution (kVA)

Minimum	Maximum	Mean	Median	Mode	Mode Freq.
0.027	66.0	10.2	5.83	2.59	27.8%

To convert this topology into one that is more representative of a typical suburban feeder, where several residences are connected to a single distribution transformer [89], the transformers connected to a single node in the topology were merged into a single transformer. Note that the capacity rating of this single transformer is the sum of the individual transformer ratings. This process results in 426 new transformers, with ratings ranging from 5 to 75 kVA, with an average of 26.8 kVA. The number of residences for each of these new transformers is determined by summing the demand of each triplex load connected to the node in the original topology, and dividing this total demand by the demand of the most common load in the network (2.6 kVA, assumed to represent a single residence). This resulted in 2,153 residences for the feeder, with the number of residences at each transformer ranging from 1 to 19. An illustration of this process is shown in Fig. 2.4, and the results for this case study are shown in Fig. 2.5. Forty-four percent of the transformers on the feeder were consolidated, and four transformers were split for tractability purposes, but as can be seen, the distribution of transformer sizes and demands remains similar (pre-consolidation $\mu = 0.53$, $\sigma = 0.24$; post consolidation $\mu = 0.54$, $\sigma = 0.28$). The vast majority of transformer ratings still fall in the 10-50 kVA range. Transformer parameters n_j, m_j, R_j, and β_j are taken from IEEE Standard C57.91-2011 [64].

2.3.2 Baseline Load Profiles

Baseline residential load profiles are sampled from the Pecan Street database [90]. The profiles are scaled so their peak is equal to the typical residential demand from the Taxonomy Test

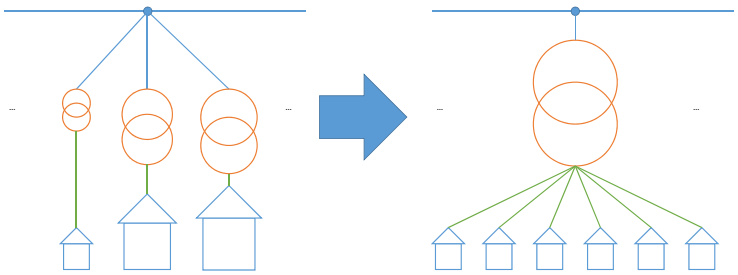

Figure 2.4: Consolidation and standardization of residential customers.

Feeder (i.e. 2.6 kVA), and finally summed with an electric vehicle (EV) charging profile. This EV charging profile is modeled using NHTS data [91] to estimate the distribution of arrival times and charge statuses for electric vehicles. Scale factors for the baseline load profiles had an average of 0.62, with a standard deviation of 0.20.

2.3.3 HEMS Load Profiles

The parameters used to generated the HEMS profiles are summarized in Table 2.2. The model is run for 24 hours using a timestep of 15 minutes (Δt). Prices are obtained from ERCOT [92] and temperatures from NOAA records for Austin, TX, USA [93] for July 1st, 2014; both the prices and temperatures are representative of weekdays in July. EVs are assumed to have a maximum charge rate of 3.3 kW and an energy capacity of 24 kWh [59]. The initial state of charge for electric vehicles varied from 21-67%, with an average of 42% and a standard deviation of 13%. The optimization problems are formulated as a mixed integer linear program (MILP), implemented using GAMS [94], and solved using CPLEX

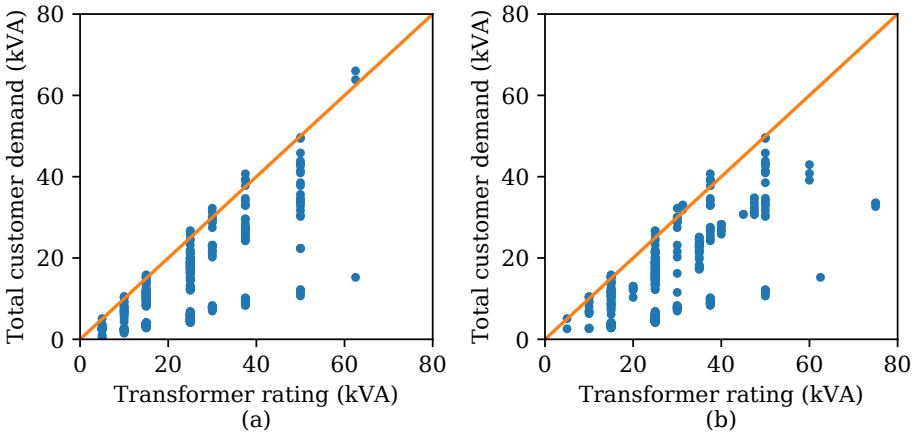

Figure 2.5: Results of transformer consolidation: (a) Pre-consolidation, and (b) Post consolidation.

[95]. Finally, the HEMS load profiles were scaled to match the total daily energy of the baseline load profiles, on a customer-by-customer basis. Scale factors for the HEMS load profiles had an average of 0.77, with a standard deviation of 0.21.

Average load profiles for both cases are shown in Fig. 2.6. As can be seen, the HEMS optimization results in increased power consumption during relatively low-priced periods and decreased power consumption in the higher-price periods. This is enabled by the presence of deferrable loads (i.e., washing machines, dryers, dishwashers, EV charging) and loads with integrated thermal energy storage (i.e., water heaters, HVAC).

2.4 Results

The results from the trials are shown in Figs. 2.7 and 2.8 and Table 2.3. Fig. 2.7 shows the range of daily transformer damage costs (over 10 trials) for varying HEMS penetration (0 to 100% in steps of 10%) under the randomized (a), even (b), greedy (c), and optimal (d) strategies. Fig. 2.8 shows the mean damage for each strategy for varying HEMS penetration (0 to 100% in steps of 1%). As can be seen in Fig. 2.8, at 0% HEMS penetration, the mean daily transformer damage cost is approximately $8.21. By managing the rollout using the

Table 2.2: Parameters used to generate HEMS load profiles

Appliance	Max. Power	Power Levels	Availability	Duration
Water Heater	3.5-5.5 kW	2	None	None
HVAC	2-4 kW	2	None	None
EV	3.3 kW	Continuous	Varied	None
Dishwasher	1 kW	1	6:00-22:00	1 h
Washer	1 kW	1	6:00-22:00	1 h
Dryer	1 kW	1	6:00-22:00	1 h
Appliance	Low Setpoint	High Setpoint	Initial	Capacity
Water Heater	45-51 °C	51-58 °C	45-56 °C	20-105 g
HVAC	16-21 °C	20-30 °C	16-28 °C	N/A

optimal strategy, the average daily transformer cost can be reduced to $1.00 by less than 5% HEMS penetration, and can be reduced to $0.30 by 20% HEMS penetration. This is because even a relatively small penetration of HEMSs reduces peak loading, which is responsible for most transformer damage. Conversely, as HEMS penetration increases from 80% to 100%, total transformer damage is greatly increased, since the clustering of demand in a few low-priced periods creates new peaks of loading. The mean daily transformer damage cost in the 100% HEMS case is $403.69.

As can be seen in Figs. 2.7 and 2.8, the strategies are consistent with where they identify the range of HEMS penetrations with minimum total transformer damage cost: typically between 20 and 60%. Of the three heuristic strategies, the greedy strategy is typically the best, followed by the even penetration, with the random transition typically the worst. From Table 2.3 transformer damages found by these three strategies are on average 211%, 216%, and 535% higher than optimal for the greedy, even, and random strategies, respectively. The difference in damages between the greedy and the optimal strategy are due to the specificity of transition targeting; the optimal strategy targets transitions by residence, while the greedy

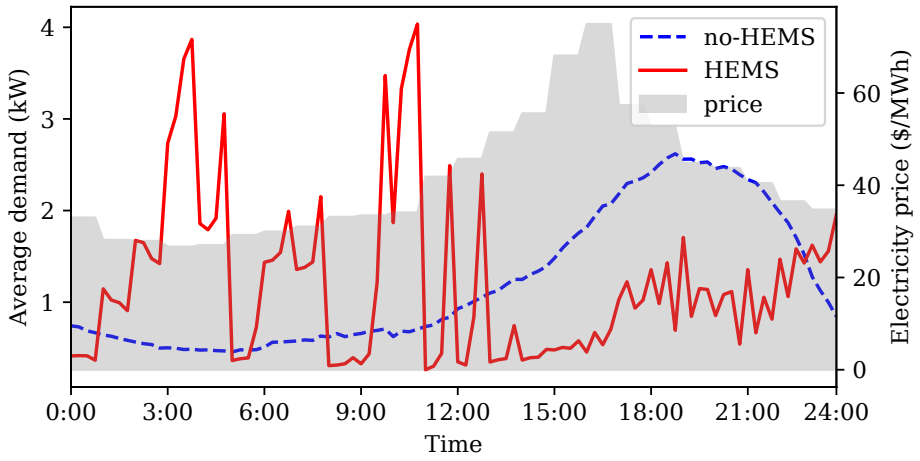

Figure 2.6: Average load profile for the base and HEMS case, along with the electrical tariff π_t.

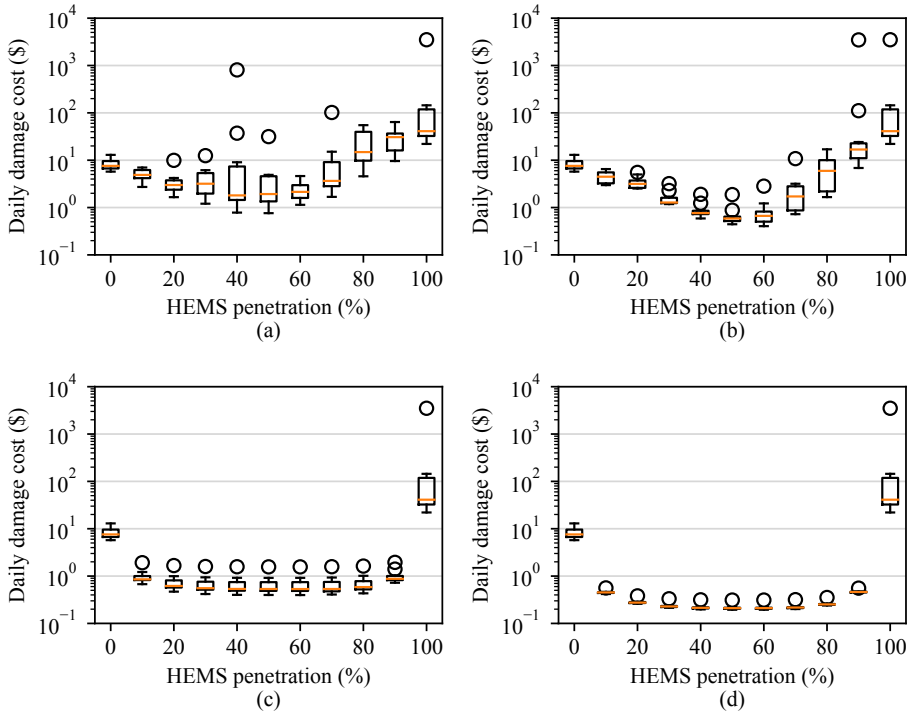

Figure 2.7: Distribution of transformer damage costs for 10 trials. (a) Distribution for random transitions, (b) Distribution for even transition strategy, (c) Distribution for greedy transition strategy, and (d) Distribution for optimal transition strategy.

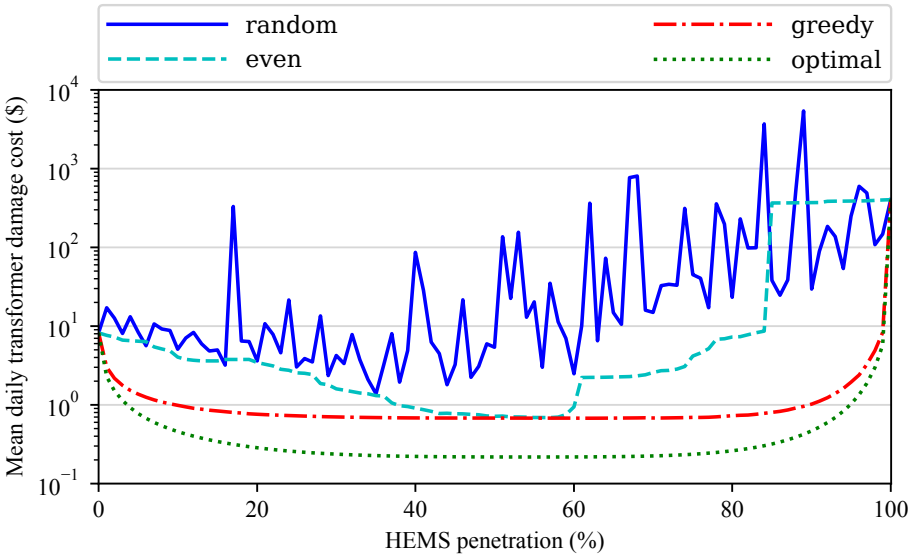

Figure 2.8: Mean transformer damage costs for 10 trials

Table 2.3: Average results from the various transition strategies

Strategy	Minimum-Cost Penetration	Minimum Damage ($/day)	Penetrations within 10% of Minimum Damage
Random	35%	$1.38	35%
Even	57%	$0.69	47-59%
Greedy	62%	$0.68	23-82%
Optimal	55%	$0.22	29-75%

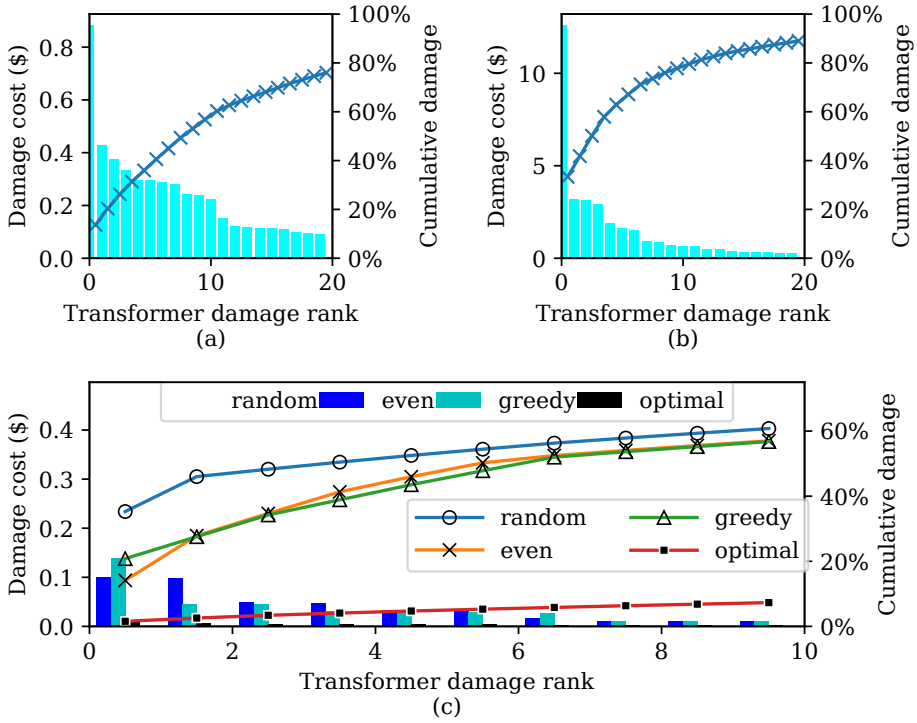

Figure 2.9: Distribution of transformer damages for a single trial: (a) 0% HEMS penetration, (b) 100% HEMS penetration, and (c) Least cost penetration for each strategy. Bars represent the individual damage cost form the most-damaged transformers, while lines represent the cumulative damage. In each subfigure, bars represent the individual damage cost form the most-damaged transformers, while lines represent the cumulative damage.

strategy targets transitions by transformer, with a random residence at that transformer chosen for transition.

Fig. 2.7 shows that the variance of transformer damages costs across trials is highest in the random strategy, and low in the greedy and optimal strategies. As shown in Table 2.3, the greedy and optimal strategies also identify a wider range of penetration levels whose damages are within 10% of the strategy's optimum: 59% and 46% for the greedy and optimal strategies, respectively. This is because those strategies are better at targeting high-impact transitions, so the transitions near the minimum damage are relatively low-impact.

Fig. 2.9 shows the distribution of damage costs for the 20 most damaged transformers

in the network for: (a) the 0% HEMS penetration case, (b) the 100% HEMS penetration case, and (c) the HEMS penetration with minimum total damage for each of the strategies. In this particular system, the majority of the total transformer damage cost comes from a small number of transformers, 10 transformers for the case with 0% HEMS penetration case and 3 transformers in the 100% HEMS penetration case, as seen in Fig. 2.9(a) and Fig. 2.9(b). Fig. 2.9(c) shows that at the HEMS penetration with minimal damage cost for each strategy, the damages are more evenly distributed for the even strategy and the greedy strategy, but still skewed for the random strategy, since there is no targeting of residences by transformer. In the minimum cost solution found by the random strategy, as with the 0% and 100% penetration cases, a large share of the total transformer damage is derived from one highly-damaged transformer. This sort of analysis can used by a DSO to identify transformers which would benefit from up-sizing.

Since the HEMS optimization changes the schedule of residential loads, it also affects losses in the network. This effect can be observed by looking at losses in the triplex lines connecting each residence to the distribution transformer. In the test feeder, all of these lines are specified as 30 feet long. In the baseline case, the losses in these lines add 0.20% (508 kWh) to the daily total energy demand from the homes. In the HEMS case, these losses are increased to 0.26% (662 kWh). Since these losses are small compared to the overall energy consumption (251 MWh), they are not considered in the HEMS rollout model.

In order to convince residential customers to transition to the use of a HEMS, a DSO will likely have to provide monetary incentives, educational materials, outreach, or similar, which will incur a cost. Therefore, the DSO needs to balance the objectives of minimizing transformer damage costs and minimizing acquisition costs. One such approach involves calculating the present cost of continued transformer damage in order to estimate a total value of combining acquisition and damage.

Fig. 2.10 illustrates the impact of including these acquisition costs in the determining the penetration level with total minimum cost. Fig. 2.10(a) shows the impact of varying acquisition costs on the net-present cost (i.e. damage and acquisition) for each penetration level,

given the optimal customer selection, and Fig. 2.10(b) shows the impact of the acquisition costs on the net-present value of transitioning the residences to the optimum HEMS penetration level. Net-present value of perpetual damage is calculated using a 5% discount rate as described in [96]. For the sake of simplicity, it is assumed that there is a single average acquisition cost, which incorporates the outreach and incentive payment given to customers who accept it as well as the cost of outreach to customers who do not accept the incentive.

As shown by Fig. 2.10(b), even a modest acquisition cost drastically alters the HEMS penetration with minimum total cost: an acquisition cost of \$10 reduces the optimal penetration from 55% to 11%, and an acquisition cost of \$50 further reduces it to 4%. However, even a high acquisition cost provides for some cost savings, as long as only a few residences are transitioned and they are carefully selected. For example, at an acquisition cost of \$1,000 per residence, it is still beneficial to transition 1% of residences to HEMS operation, and the net-present value is greater than \$20,000. On the other hand, if the penetration of HEMS is high, and further penetration will increase operating costs, the DSO may offer residences an incentive to *not* install a HEMS device. This is one option a DSO could take in order to avoid the cost of reinforcing their network (other potential options are discussed in Section V). In this case, the optimal penetration is higher than in the case where no incentives are present. At an anti-HEMS incentive of \$50 per residence, the optimal penetration is increased from 55% to 94%.

Of course, some residential customers may not be responsive to the desires of the DSO in minimizing their transformer damage. They may install a HEMS despite its negative impact on the distribution network, and they may not install a HEMS despite the positive impact it would have. To model these customers, a share of the residences on the feeder can be designated as 'unresponsive' residences which will ignore the desires of the DSO. The impact of varying shares of these unresponsive residences is demonstrated in Fig. 2.11. With optimal control the minimum damage cost is \$0.22/day, with 10% unresponsive the minimum cost is \$0.33, with 25% unresponsive the minimum cost is \$0.50, and with 50% unresponsive the minimum cost is \$0.88.

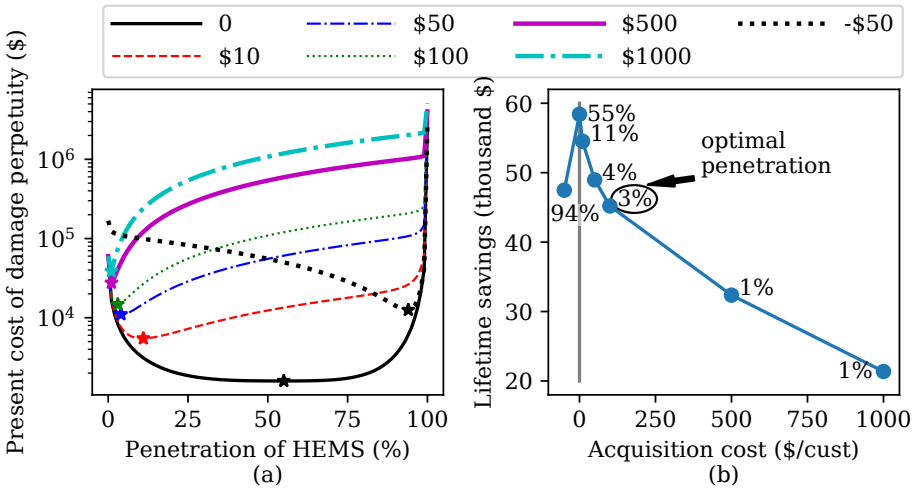

Figure 2.10: Optimal penetration of HEMS given varying acquisition costs. (a) The impact of acquisition costs on optimal penetration of HEMS. Optimal penetration levels for each curve are shown by a star, and (b) The impact of acquisition costs on lifetime savings from optimal HEMS rollout.

2.5 Considerations for Implementation

The random and even penetration algorithms are simple to implement, and can be solved in $\mathcal{O}(n)$ time, where n is the number of residences in the system. The greedy algorithm is more complex, and requires $\mathcal{O}(n \cdot m)$ time, where m is the number of transformers in the system. The optimal algorithm has the highest complexity, requiring $\mathcal{O}(2^{r^{\max}})$ time, where $r^{\max}$ is the maximum number of residences connected to a single transformer. The time required by the optimal algorithm is dominated by the transformers with the highest number of residential customers. However, the strategies with increased complexity yield substantial costs savings when compared to the random strategy. As can be seen in Table 2.3, the greedy and optimal strategies yield cost savings of 51% and 84%, respectively. A real-life implementation of such methodologies by a DSO would require weighing the benefits of complicated strategies against their additional benefits. Additionally, accurate modeling of customer load profiles in the HEMS and no-HEMS cases control is crucial to generating meaningful results. The

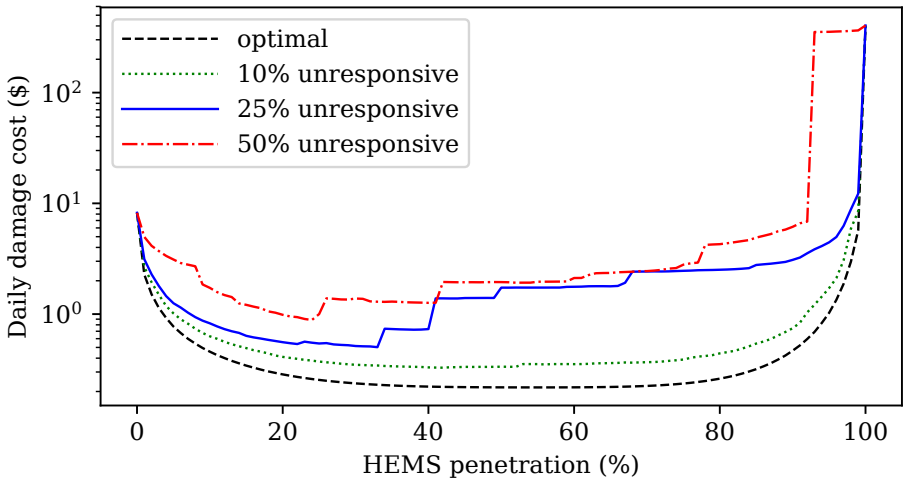

Figure 2.11: The impact of unresponsive residences on the transformer damage cost

population of HEMS customers may also have a variety of HEMS algorithms, which could make modeling more difficult.

For example: algorithms may minimize total electricity costs [59], total energy consumption, peak load, demand limit violations [60], or load during certain time periods [62], may maximize occupant comfort, or may consist of a multiobjective formulation balancing several objectives [57, 58]. For a multiobjective formulation, several options are possible, such as allowing customers to dynamically adjust individual objective weightings or controlling the weightings of the separate objectives automatically using occupancy detection and supervised learning of occupant preferences.

Though this paper focuses on the control of HEMS penetration by incentivizing customers to install a HEMS, these strategies can only reduce costs when the penetration of HEMS is below the value with minimum cost. If instead the penetration of HEMS is already above the minimum-cost value, then alternate strategies must be implemented. For example, a HEMS algorithm that considers both transformer aging and energy costs could be deployed, as described in [74], the transformer could be replaced with a larger one to improve its lifetime, the DSO could incorporate a real-time distribution charge [97], or the customers

could be given an incentive payment by the DSO in exchange for not using a HEMS. The latter approach is shown in Fig. 2.10(a).

2.6 Conclusion

An approach is developed and tested to determine the optimal penetration of HEMS in a distribution system, and the cost savings available from this transition, using several methods of managing HEMS rollout. If all residences are equipped with HEMSs, transformer damage costs are estimated to be 1-2 orders of magnitude higher (in our case study, 49 times higher) than they would be in the no-HEMS case. In this case, a centralized HEMS management scheme may be beneficial. However, if the adoption of HEMS is managed using a heuristic or optimal strategy, then transformer damage costs are reduced below their values in the no-HEMS case by 1-2 orders of magnitude (in our case study, 38 times lower). These results are however, highly system dependent.

The optimal penetration of HEMSs is highly dependent on the cost of incentivizing residences to adopt HEMSs. Without incentive costs, the optimal penetration in the case study was found to be 55%, but when incentivization costs are \$50 per residence, the optimal penetration drops to 4%. Conversely, a \$50 cost to incentivize a residence to forgo HEMS operation increases the optimal penetration to 94%. Substantial cost savings are also possible even if not all customers are responsive to the desires of the DSO. Potential cost savings are shown to persist even with high HEMS incentivization costs, as long as the residences to incentivize are carefully targeted. This is because a majority of the total transformer damages comes from a small number of overloaded transformers.

Nomenclature

Sets

M	the set of transformers, indexed by j
N	the set of residences, indexed by i

T the set of time periods, indexed by t

A the set of residential appliances, indexed by a

Transformer Model

Parameters

$\mathbf{A}$ a binary matrix, where $a_{ij} = 1$ if residence i is connected to transformer j, and 0 otherwise

$d_{i,t}^{\text{no-HEMS}}$ the demand of residence i at time t if residence i does not have a HEMS (kW)

$d_{i,t}^{\text{HEMS}}$ the demand of residence i at time t if residence i has a HEMS (kW)

r_j the number of residences at transformer j

n_j top-oil thermal parameter for transformer j (unitless)

m_j hot-spot thermal parameter for transformer j (unitless)

R_j ratio of losses at rated load to losses at no load for transformer j (unitless)

α_j the nameplate rating of transformer j (kVA)

β_j rated lifetime of transformer j (hours)

τ_j^{TO} top-oil temperature time constant for transformer j (hours)

τ_j^{HS} hot-spot temperature time constant for transformer j (hours)

$\Delta\Theta_j^{\text{TO,R}}$ ultimate top-oil rise over ambient temperature of transformer j at rated load ($^{\text{o}}$C)

$\Delta\Theta_j^{\text{HS,R}}$ ultimate hot-spot rise over top-oil temperature of transformer j at rated load ($^{\text{o}}$C)

Variables

$FAA_{j,t}$ the accelerated aging factor of transformer j at time t (unitless)

$k_{j,t}$ the loading ratio of transformer j at time t (unitless)

LoL_j the cumulative loss-of-life for transformer j (%)

$\Theta_{j,t}^{HS}$ winding hot-spot temperature of transformer j at time t (°C)

$\Delta\Theta_{j,t}^{\mathrm{TO}}$ top-oil rise over ambient temperature of transformer j at time t (°C)

$\Delta\Theta_{j,t}^{\mathrm{TO,U}}$ ultimate top-oil rise over ambient temperature of transformer j at time t (°C)

$\Delta\Theta_{j,t}^{\mathrm{HS}}$ hot-spot rise over top-oil temperature of transformer j at time t (°C)

$\Delta\Theta_{j,t}^{\mathrm{HS,U}}$ ultimate hot-spot rise over top-oil temperature of transformer j at time t (°C)

p a vector of binary variables where $p_i = 1$ if customer i has a HEMS, and 0 otherwise

v_j the number of residences at transformer j with HEMSs

HEMS Model

Parameters

π_t electricity price for time period t ($/MWh)

P_t^{base} base load power consumption at time t (kW)

P_a rated power of appliance a (kW)

L_a number of power levels for appliance a (for discrete-power appliances only)

$V_{a,t}$ availability of appliance a at time t (binary)

D_a duration parameter for appliance a (number of periods)

$\overline{P^{\mathrm{EV}}}$ maximum charging power for electric vehicle (kW)

$\underline{SoC}$ minimum state-of-charge for electric vehicle battery (kWh)

$\overline{SoC}$	maximum state-of-charge for electric vehicle battery (kWh)
η	electric vehicle battery charging efficiency (unitless)
ξ	electric vehicle daily energy requirement (kWh)
M_t	electric vehicle motion schedule at time t (binary)
$\underline{\Theta_a}$	minimum temperature for thermal appliance a (°C)
$\overline{\Theta_a}$	maximum temperature for thermal appliance a (°C)
Q_a	coefficients of performance for thermal appliance a (°C/kW)
τ_{HVAC}	HVAC thermal time constant (hours)
τ_{WH}	water heater thermal time constant (hours)
H_t	fraction of heated water withdrawn at time t (unitless)

Variables

$\delta_{a,t}$	status of appliance a at time t (for discrete-power appliances only)
P_t^{EV}	power consumption of electric vehicle charging at time t (kW)
SoC_t	state-of-charge for electric vehicle battery at time t (kWh)
Θ_t^{room}	temperature of HVAC-conditioned space at time t (°C)
Θ_t^{tank}	temperature of water heater tank at time t (°C)
Θ_t^{water}	temperature of heated water at time t (°C)

Shared Parameters

Θ_t^{A}	ambient temperature at time t (°C)
Δt	the time interval length (hours)

Chapter 3

OPTIMAL CARBON TAXES FOR EMISSIONS TARGETS IN THE ELECTRICITY SECTOR

Published as:

Olsen, D. J., Dvorkin, Y., Fernández-Blanco, R., & Ortega-Vazquez, M. A. (2018). Optimal carbon taxes for emissions targets in the electricity sector. *IEEE Transactions on Power Systems*, 33(6), 5892-5901.

3.1 Introduction

3.1.1 Background

The risks posed by anthropogenic climate change are dire, and organized effort is required in order to mitigate and eliminate, when possible, the effects [1]. Pricing the emissions of greenhouse gases (GHGs) is a well-established approach to internalizing these negative externalities and should result in shifting the supply-demand equilibrium to a socially optimal point [8]. Since the true costs from climate change are uncertain and hard to quantify with any precision (though attempts have been made, as in [98]), one approach to create a price for emissions is to design policies that aim to reduce emissions to a level that is generally accepted to avoid the worst effects. Unlike renewable portfolio standards or tax credits for renewable energy investment or production, this approach is directly targeted toward reducing GHG emissions. As noted in [41], subsidies for production of renewable energy can lead to negative bids by renewable generators, which may result in higher costs and emissions than if they bid zero-cost. According to a 2019 study by the World Bank [19], there are 57 regional, national, and sub-national carbon pricing schemes implemented or scheduled for implementation, ranging from \$1-127/tCO_2e and covering 15% of global emissions (soon to

be approximately 20% once China's pricing scheme becomes active in 2020).

The two main approaches to pricing emissions are a tax on GHG emissions (*i.e.* a carbon tax) [99] and a cap-and-trade system [100]. A carbon tax sets a price directly with the goal of implicitly reducing emissions, while a cap-and-trade system sets emissions reductions explicitly, implicitly creating a price. Each system has pros and cons: a cap-and-trade system can be more precise about the level of emissions reductions achieved, but requires complex rules regarding distributing, auctioning, and trading of allowances. A carbon tax is simpler and may be easier to implement, but impact on emissions is less certain [101], as the reactions to such a tax by the broader market (*e.g.* generation and transmission investors, electricity consumers, and generation manufacturers) are difficult to model.

Secondary policy considerations are similar between the two: entities may purchase carbon offsets to reduce net emissions, tariffs can maintain competitiveness with jurisdictions without carbon pricing, and policies can be designed to be revenue-neutral. Such policy design considerations for a carbon tax are discussed in [102, 103]. Additionally, pricing of carbon in either approach can lead to carbon 'leakage', *i.e.* the increased cost of producing goods in a jurisdiction with a carbon tax can lead to a shift in production toward jurisdictions with lower rates, or no tax at all [20].

The impact of carbon taxes on the economy and the environment have been widely studied, using various tax rates: the Brookings Institute in 2012 studied a tax which would begin at \$15/tCO_2e with an annual escalator [104], the Congressional Budget Office in 2013 evaluated various rates between \$15-29/tCO_2e [105], and the Energy Information Agency in 2014 investigated rates of \$10 & \$25/tCO_2e [106]. However, these studies do not address at what rate carbon should be taxed.

This paper approaches the topic from a different angle. Instead of studying the impact of a certain tax rate, we set a tax rate to achieve a certain environmental impact (*e.g.* pledges from the Paris Agreement [107]) at minimal tax rate. Specifically, we present an approach for setting the *optimal carbon tax* for a given power system such that the resulting minimum-cost generator commitment and dispatch yields emissions that are at or below a specified target.

The consequence of a tax rate that is too low is failure to meet emissions targets, and the consequence of a rate too high is undue economic burden. Minimizing the tax rate also has practical motivations: lower tax rates are often more politically palatable (*i.e.* more likely to be enacted, less likely to be repealed), and generally reduce rates of tax evasion [108].

Some carbon taxing systems are designed to 'recycle' the revenue received, either by investing in clean generation technologies or by reducing tax rates on other sectors of the economy to achieve revenue 'neutrality'. However, care must be taken to account for the uncertainty in future carbon consumption, especially as carbon pricing tends to reduce consumption.

3.1.2 Literature Survey

Work including emissions into generator dispatch began in the 1970s with the concepts of minimum emissions dispatch [26], pricing of emissions to include their impact in economic dispatch [27], and varying emissions prices to investigate the tradeoffs between fuel costs and emissions [28]. However, these studies focused on local effects of NO_x and SO_x.

The concepts of 'pseudo fuel prices' and algorithms for setting them are explored in [30], and expanded in [31] to include periodic price adaptation in order to meet long-term fuel consumption targets as realizations differ from projections. Similar algorithms are used to set weights based on emissions targets in [109] for economic dispatch problems. Several methods for coordinating long-term targets for emissions and short-term operations are discussed in [32, 110], but explicit emission pricing is absent, to the best of the authors' knowledge.

Explicit GHG pricing and its impact on optimal power flow problems are discussed in [111]. [112] presents a bi-level approach for setting a tax rate to achieve a GHG emissions target with minimal tax burden, but intertemporal constraints (*e.g.* ramp rates, start-ups) are ignored. Without considering these constraints, the determined tax rate may not meet the desired target. 'Optimal' tradeoffs between GHG emissions and cost according to a Nash bargaining process are developed in [113, 114].

All of the above approaches contain deficiencies when it comes to setting a carbon tax

rate with an eye on scheduling algorithms (*i.e.* unit commitment models). In short, one or more of the following is missing:

1. Intertemporal variables and constraints (*e.g.* ramp rate limitations, minimum up- and down-times).

2. Explicit carbon pricing in dispatch/commitment.

3. A method for setting an optimal carbon price.

By contrast, in this work we propose a Weighted Sum Bisection (WSB) method, a computationally efficient approach, to set the minimal carbon tax rate that results in a power system meeting emissions targets while incorporating unit commitment, ramp rate limitations, and system flexibility and contingency reserve requirements.

3.1.3 Contributions

This work makes the following contributions:

1. A bi-level planning model including unit commitment based on cyclic representative days, avoiding the need for assumptions about initial conditions.

2. An efficient method for determining the minimal carbon tax rate which achieves emissions reductions targets.

3. A demonstration of the computational efficiency of the proposed method and of the reciprocal relationship between tax rates for emissions targets and investment decisions.

The rest of this chapter is organized as follows: Section 3.2 describes the problem formulation, Section 3.3 discusses potential solution techniques, Section 3.4 describes a case study, Section 3.5 presents the results, and Section 3.6 concludes. A nomenclature section follows at the end of the chapter.

3.2 Problem Formulation

The problem is formulated as a bi-level planning problem, with the regulator's tax rate ($P^{\mathrm{CO_2}}$) optimization in the upper level (3.1)-(3.2) and the system operator's unit commitment with carbon tax (UCCT), over a set of representative days, in the lower level (3.3)-(3.21). The UCCT includes the dc power flow approximation of the system power flows, penalties for shedding load and renewable generation, and reserve and ramping adequacy requirements. We assume an electricity market based on a unit commitment in which bids represent true fuel and tax costs.

$$\min P^{\mathrm{CO_2}} \tag{3.1}$$

subject to:

$$E^{\mathrm{total}} \leq E^{\max} \tag{3.2}$$

$$E^{\mathrm{total}} \in \arg\min \Big\{ C^{\mathrm{shed}} + C^{\mathrm{gen}} + P^{\mathrm{CO_2}} E^{\mathrm{total}} \tag{3.3}$$

$$C^{\mathrm{shed}} := \sum_{a\in A} \pi_a \sum_{t\in T} \sum_{b\in B} \Big(P^{\mathrm{load}} s^{\mathrm{load}}_{b,t,a} + \sum_{i\in R} P^{\mathrm{ren}} s^{\mathrm{ren}}_{i,t,a} \Big) \tag{3.4}$$

$$C^{\mathrm{gen}} := \sum_{a\in A} \pi_a \sum_{t\in T} \sum_{i\in I} \Big(C^{\min}_i u_{i,t,a} + C^{\mathrm{su}}_i v_{i,t,a} + \sum_{s\in S} b_{i,s} g_{i,s,t,a} \Big) \tag{3.5}$$

$$E^{\mathrm{total}} := \sum_{a\in A} \pi_a \sum_{i\in I} \sum_{t\in T} \Big(E^{\min}_i u_{i,t,a} + E^{\mathrm{su}}_i v_{i,t,a} + \sum_{s\in S} h_{i,s} g_{i,s,t,a} \Big) \tag{3.6}$$

subject to:

$$g_{i,t,a} = g^{\min}_i u_{i,t,a} + \sum_{s\in S} g_{i,s,t,a} \,;\, \forall i \in I, t \in T, a \in A \tag{3.7}$$

$$0 \leq g_{i,s,t,a} \leq g^{\max}_{i,s} u_{i,t,a} \quad \forall i \in I, s \in S, t \in T, a \in A \tag{3.8}$$

$$v_{i,t,a} + z_{i,t,a} \leq 1 \,;\, \forall i \in I, t \in T, a \in A \tag{3.9}$$

$$v_{i,t,a} - z_{i,t,a} = u_{i,t,a} - u_{i,t-1,a} \,;\, \forall i \in I, t \in T, a \in A \tag{3.10}$$

$$\sum_{\tau=t-\mathrm{g}^{\mathrm{up}}_i+1}^{t} v_{i,\tau,a} \leq u_{i,t,a} \,;\, \forall t \in T, i \in I, a \in A \tag{3.11}$$

$$\sum_{\tau=t-\mathrm{g}_i^{\mathrm{down}}+1}^{t} z_{i,\tau,a} \leq 1 - u_{i,t,a}\,;\, \forall t \in T, i \in I, a \in A \tag{3.12}$$

$$-r_i^{\mathrm{down}} \leq g_{i,t,a} - g_{i,t-1,a} \leq r_i^{\mathrm{up}}\,;\, \forall t \in T, i \in I, a \in A \tag{3.13}$$

$$\sum_{i \in I} m_{i,b}^{\mathrm{unit}} g_{i,t,a} - \sum_{l \in L} m_{l,b}^{\mathrm{line}} f_{l,t,a} - s_{b,t,a}^{\mathrm{ren}} = d_{b,t,a} - s_{b,t,a}^{\mathrm{load}}\,;\, \forall b \in B, t \in T, a \in A \tag{3.14}$$

$$-f_l^{\max} \leq f_{l,t,a} \leq f_l^{\max}\,;\, \forall l \in L, t \in T, a \in A \tag{3.15}$$

$$f_{l,t,a} = \frac{1}{x_l} \sum_{b \in B} m_{l,b}^{\mathrm{line}} \theta_{b,t,a},\,;\, \forall l \in L, t \in T, a \in A \tag{3.16}$$

$$\sum_{i \in I \setminus R} u_{i,t,a}(g_i^{\max} - g_{i,t,a}) \geq 3\% \sum_{b \in B} d_{b,t,a} + 5\% \sum_{i \in R} g_{i,t,a} + \max_{i \in I} g_i^{\max}\,;\ \forall t \in T, a \in A \tag{3.17}$$

$$\sum_{i \in I} \min\left(r_i^{\mathrm{up}} u_{i,t,a}, (g_i^{\max} - g_{i,t,a})\right) \geq w_{t,a}^{\mathrm{up}} + d_{t,a}^{\mathrm{ramp}}\,;\forall t \in T, a \in A \tag{3.18}$$

$$\sum_{i \in I} \min\left(r_i^{\mathrm{down}} u_{i,t,a}, g_{i,t,a} - g_i^{\min} u_{i,t,a}\right) \geq w_{t,a}^{\mathrm{down}} + d_{t,a}^{\mathrm{ramp}}\,;\forall t \in T, a \in A \tag{3.19}$$

$$0 \leq s_{b,t,a}^{\mathrm{load}} \leq d_{b,t,a}\,;\ \forall b \in B, t \in T, a \in A \tag{3.20}$$

$$0 \leq s_{b,t,a}^{\mathrm{ren}} \leq \sum_{i \in R} m_{i,b}^{\mathrm{unit}} g_{i,t,a}\,;\ \forall b \in B, t \in T, a \in A \Bigg\} \tag{3.21}$$

The regulator's objective is given in (3.1), and constrained by the emission limit (3.2) and the lower-level problem (3.3)-(3.21). The system operator's objective is given in (3.3)-(3.6). Generator costs curves are piecewise linear (3.7)-(3.8). Binary commitment variables are defined in (3.9)-(3.10) and generator minimum up- and down-times are constrained using (3.11)-(3.12). Generator ramp rate constraints are given in (3.13). Power balance is given by (3.14). Line flow limits are given by (3.15)-(3.16). Operating reserve requirements based on the 3+5% and N-1 policies are ensured using (3.17) with flexibility requirements ensured in (3.18)-(3.19). Load and renewable generation shedding is constrained by physical limits in (3.20)-(3.21).

For the intertemporal constraints (3.10)-(3.13), time periods before the first are treated cyclically. For instance, $t = 24$ is substituted for $t = 0$, and $t = 23$ for $t = -1$. This ensures that end-of-day commitments are feasible and that initial conditions are representative,

assuming that the days surrounding the representative day are substantially similar. Considering constraints (3.17)-(3.19), the ideal quantity of regulation and load-following reserves is an active research topic [115, 116]; for simplicity, we use the heuristic 3+5% rule originally proposed in [117]. This formulation assumes a perfectly competitive market; otherwise, the impact of the carbon tax on emissions may vary, as shown in [118].

3.3 Solution Techniques

One approach to finding the optimal tax rate would be to solve a standard unit commitment over the set of representative days, with a constraint on total emissions, and to take the marginal value of the emissions constraint as the tax rate:

$$\min C^{\text{gen}} + C^{\text{shed}} \tag{3.22}$$

$$\text{Equations (3.4)-(3.21)} \tag{3.23}$$

$$E^{\text{total}} \leq E^{\max} : \lambda \tag{3.24}$$

where λ denotes the marginal value of the constraint.

We call such an approach "Constrained Emission Marginal Value (CEMV)" method. However, due to the non-convexity of the UCCT problem (due to binary variables), this approach is liable to produce sub-optimal solutions. Varying $E^{\max}$ will find solutions on the Pareto frontier of the feasible cost/emissions space, but the resulting λ, when used as P^{CO_2} in the UCCT, may find different solutions. This is because concave portions of the Pareto frontier may not be found by the linearly weighted UCCT formulation, since the optima only exist on the convex hull of the Pareto frontier [119]. This undesirable outcome is illustrated in Fig. 3.1 and demonstrated for the test system in Section 3.5. Depending on where in the convex region $E^{\max}$ falls, the value of λ (*i.e.* the slope of the curve) when input as P^{CO_2} into the UCCT problem may find: a) a solution with emissions which are greater than the target (A $\rightarrow$ A' in the figure), b) a solution in which emissions are lower than the target, but the production cost is higher than necessary (B $\rightarrow$ B'), c) the optimal cost/emissions point,

but at a P^{CO_2} that is larger than necessary, or d) the minimum P^{CO_2} which results in the optimal cost/emissions point. Therefore, it should not be assumed that the CEMV method can find (d) reliably.

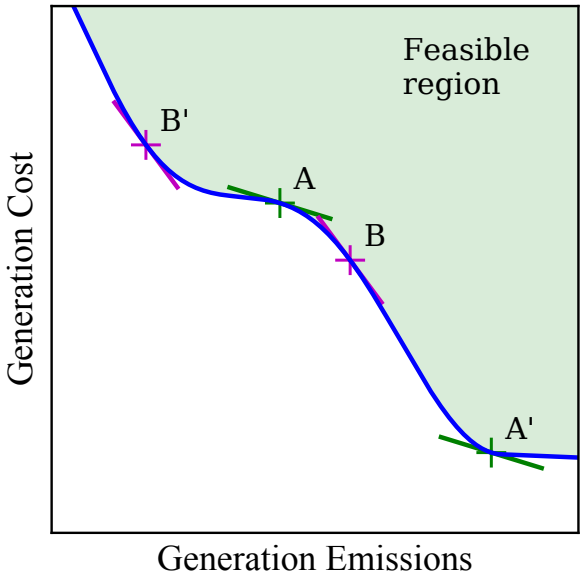

Figure 3.1: The marginal values at points {A,B}, when used as tax rates, result in the solutions at {A',B'}.

By contrast, the WSB method finds the optimal tax rate by iteratively guessing a P^{CO_2} value, solving the UCCT problem, and tuning P^{CO_2} using the bisection method. Briefly, if a zero of a continuous function is known to be in a certain interval, it can be reliably found by repeatedly bisecting the interval and selecting the sub-interval in which the root must lie, based on the sign of the function value at the midpoint. Since the goal is to find the tax rate resulting in emissions at or below a certain target, the function is $f(P^{CO_2}) = E^{\text{total}}(P^{CO_2}) - E^{\max}$, and its zero-crossing is at the value of the optimal tax rate, where $E^{\text{total}}(P^{CO_2})$ is found for a given value of P^{CO_2} by solving the UCCT. For a given value of P^{CO_2}, the UCCT can be solved independently for each representative day, aiding computation. For a non-convex Pareto frontier such as ours, the values of the individual objectives as a function

of the weighting factor are noncontinuous but monotonic. Therefore, the WSB method is guaranteed to find the smallest tax rate resulting in emissions at or below the target, if this target is feasible. A very high tax rate (e.g. \$1,000/ton) can be used to estimate the maximum feasible emissions reduction and set the upper bound of the tax range. Since precision is doubled with each iteration, convergence is linear [120]. This approach is shown in Fig. 3.2.

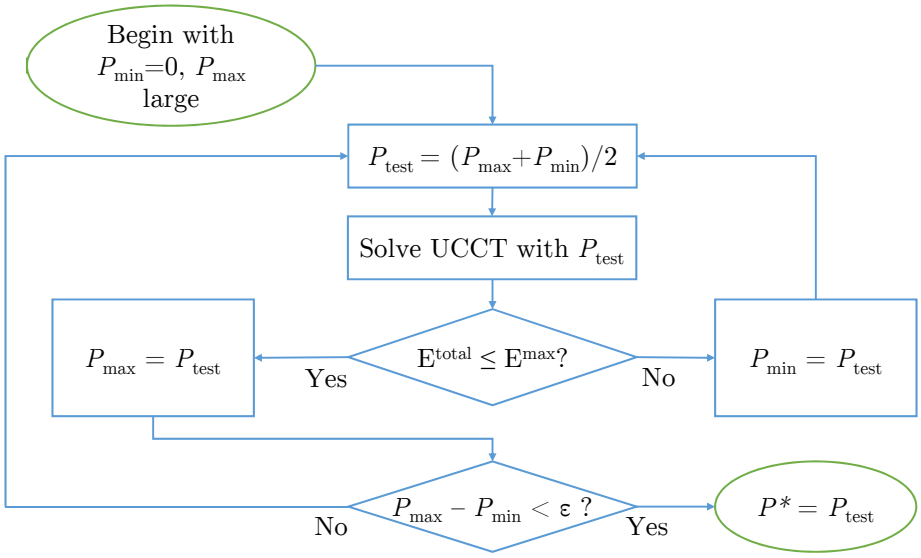

Figure 3.2: Flowchart for finding optimal P^{CO_2} using the Weighted Sum Bisection method.

3.4 Case Study

The electrical system for this case study is a modified ISO New England (NE) test system [121]. Data from the Energy Information Administration (EIA) are used for fuel prices [122] and for per-MMBTu CO_2e emissions by fuel [123]. Though variability from renewable generation can induce additional CO_2 emissions from thermal generators [124], this effect was not modeled in the case study. Five representative days are chosen using a hierarchical clustering algorithm [125] and run at a one-hour time resolution. The load shed penalty is set

at $10,000/MWh and the renewable spillage penalty is $20/MWh. Ramping requirements are set such that the system has the capacity to react to 1%/hour load ramps and all wind farms ramping their production ± 20% over one hour, based on analysis of Bonneville Power Administration wind power production data in [126]. This case study was implemented using GAMS v24.0 and solved using CPLEX v12.5 with a 0.1% optimality gap on an Intel Xenon 2.55 GHz processor with at least 32 GB RAM.

3.5 Results

3.5.1 System Characteristics

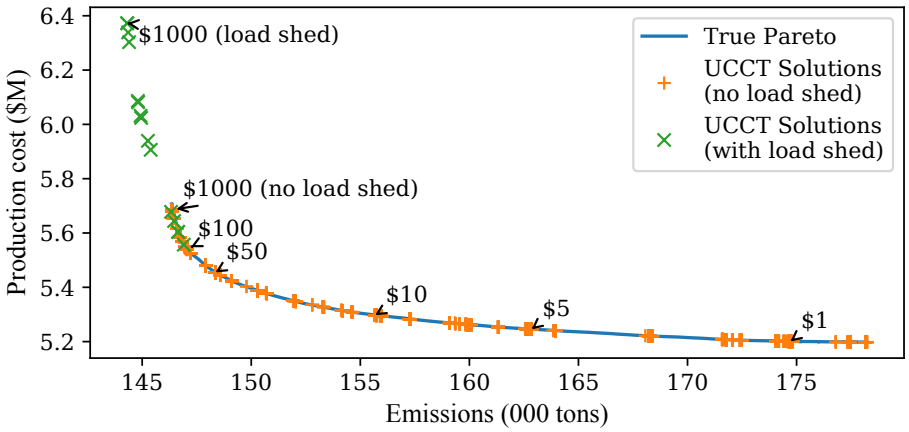

Figure 3.3: The cost/emissions Pareto frontier. The line is points found by constraining emissions, the crosses are points found by varying P^{CO_2}.

Fig. 3.3 shows the Pareto frontier of the trade-off between emissions and production costs (*i.e.* fuel and shed costs). The full Pareto frontier is sampled at 100 equally-spaced points by constraining emissions and varying E^{max}, and the convex hull of the cost/emissions space is sampled by using the UCCT and varying P^{CO_2}, with and without load-shedding. Load shedding is only economically justified under very high tax rates and results in very high costs, so load-shedding solutions are omitted in all following figures for the sake of clarity.

Though the Pareto frontier may at first glance appear convex, there are many small concave regions. This can be seen by plotting the marginal value at the sample points, as shown in Fig. 3.4; since the marginal values do not increase monotonically, the frontier must be non-convex [127].

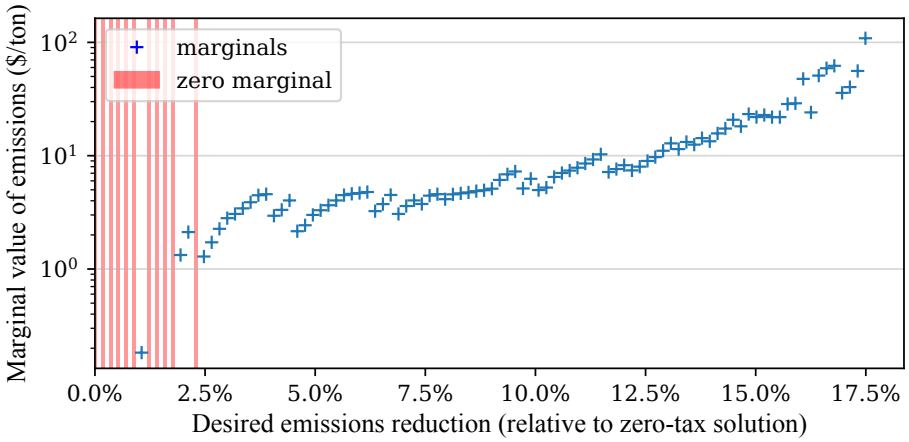

Figure 3.4: Marginal value found at 100 sample points on the Pareto frontier.

3.5.2 Determining a Tax Rate to Meet Policy Goals

If the CEMV method were used to set a tax rate, there is no guarantee that the solution to the UCCT problem would meet the desired emissions reduction. This is illustrated in Fig. 3.5, which uses the same set of sample points as Figs. 3.3 and 3.4. As shown, values of P^{CO_2} derived from the CEMV method do not reliably meet their desired emissions reductions when used in the UCCT. By comparison, the WSB method is guaranteed to meet or exceed the emissions reduction target. Convergence of the WSB method to its final values is shown in Fig. 3.6 for a target emissions reduction of 15%. The WSB method, given an emissions target, reliably converges to an optimal tax rate within 1¢ from an initial range of \$0-\$100/ton in 14 iterations of the UCCT problem. Though the tax rate which is converged upon may not be the true optimum, it can be shown that the solution exceeds the true optimum by no more

than a specified tolerance, and this tolerance can be halved with each additional iteration of the UCCT problem. By comparison, naively finding the tax rate by solving for each possible rate in 1¢ increments would require 10,000 solves. The wider the range of potential solutions, and the greater the desired accuracy, the more efficiently the WSB performs.

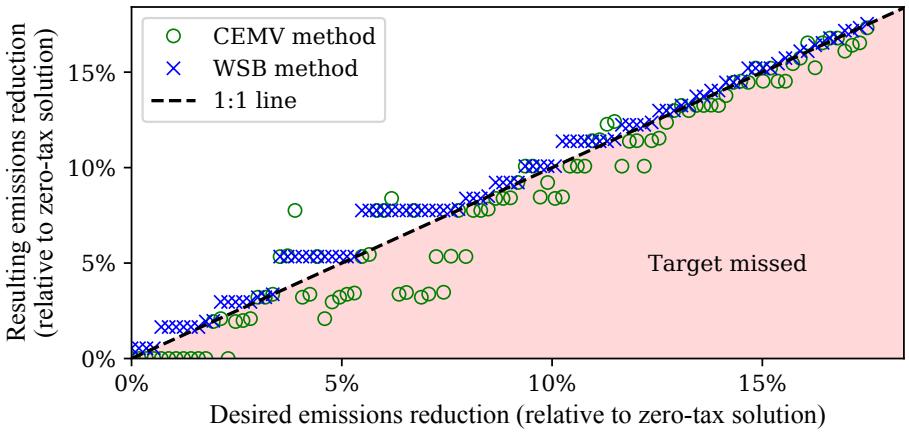

Figure 3.5: Comparison of results using the CEMV method and the WSB method.

The importance of including binary variables is illustrated in Fig. 3.7. For this figure, the UCCT formulation is transformed into a transmission-constrained economic dispatch (TCED) problem by ignoring intertemporal constraints (3.10)-(3.13) and setting $\{g_i^{\min}, C_i^{\min}, E_i^{\min}\} = 0$ for all generators. By using the WSB method to find the required tax rate for a given desired emissions reduction for the TCED problem, and inputting that resulting tax rate into the UCCT problem, it can be seen that the realized emissions reductions fail to meet the targets. Factors which can contribute to this outcome include: the requirement to burn fuel to synchronize generators on start-up, and the requirement to commit additional generators to prepare for large ramps in net load, which occur more commonly and with greater magnitude with the introduction of large quantities of renewables.

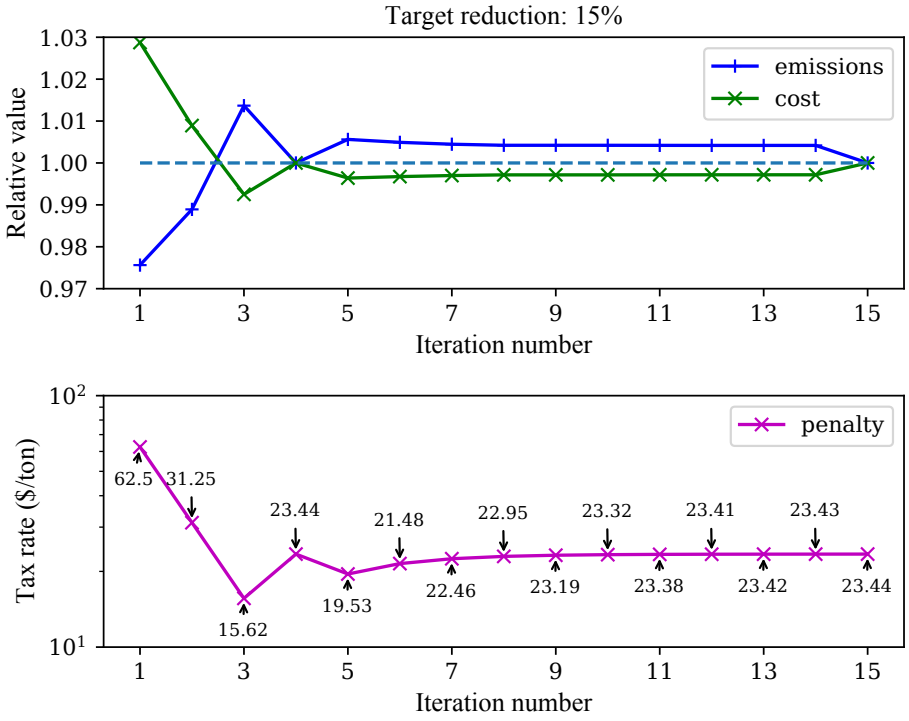

Figure 3.6: Convergence of WSB method to final value.

3.5.3 Handling Uncertainty

Since this formulation requires estimating the distribution of representative days in a future year, there is some uncertainty in the actual realization. The variance in annual realized emissions, based on this sampling probability, is given by (3.25). If policy-makers desire to achieve emissions reductions with a specified level of certainty, tax rates can be set such that the likelihood of achieving such reduction happens with the desired probability using (3.26) due to the Central Limit Theorem [128].

$$\text{Var}[E^{\text{total}}] = \sigma_E^2 = 365 \sum_{a \in A} \pi_a (E_a - E^{\text{total}})^2 \tag{3.25}$$

$$\text{Prob}[E^{\text{total}} \leq E^{\max}] = \Phi \left(\frac{E^{\max} - E^{\text{total}}}{\sigma_{E^{\text{total}}}} \right) \tag{3.26}$$

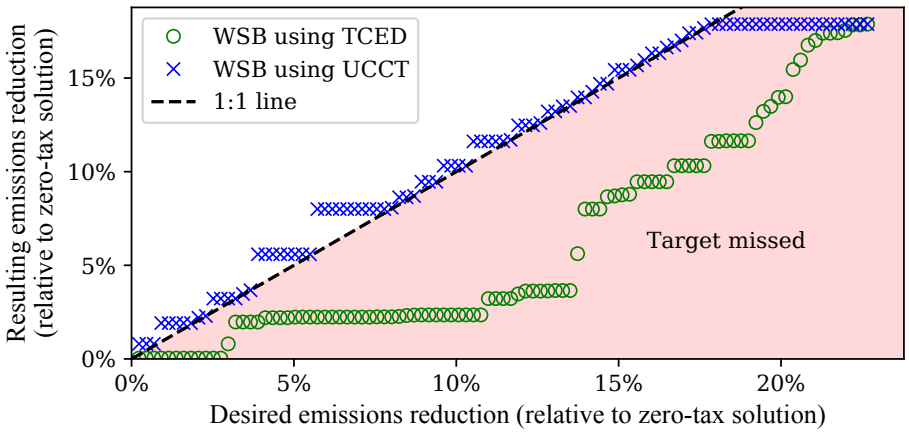

Figure 3.7: Comparison of WSB results when ignoring binary variables and intertemporal constraints (TCED problem) vs. including them (UCCT method).

where $\Phi(\cdot)$ is the cumulative distribution function of the standard normal distribution.

The choice of increasing or decreasing the tax rate in the WSB method is then based on whether this likelihood meets the desired level of certainty. Fig. 3.8 illustrates the uncertainty range around the expected cost and emissions, and Fig. 3.9 illustrates the tax rate required to achieve a desired emissions reduction for various values of certainty. As shown, the required tax rate to meet a given emissions target increases with the level of certainty required, and some emissions reductions targets which are achievable on average are not able to be met with much certainty, no matter the tax rate.

A similar process can be used in order to handle the uncertainty of fuel prices. Currently in the United States, abundant shale gas makes gas-fired power plants more competitive, but these low prices may not persist. If there is a desire to set a tax rate to be robust to fluctuations in the price of natural gas, the tax-setting process can be run using the highest gas price that can be reasonably expected.

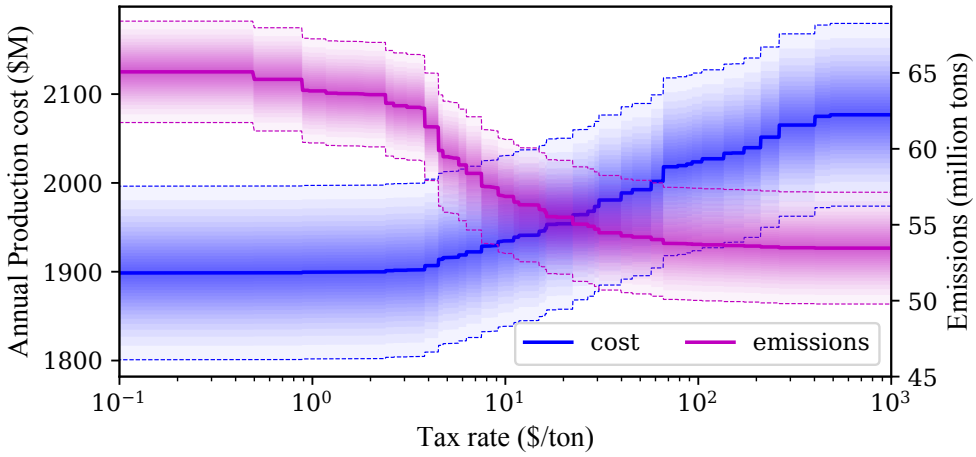

Figure 3.8: Fuel cost and emissions as a function of tax rate, incorporating weather uncertainty. Bands represent 95% certainty range.

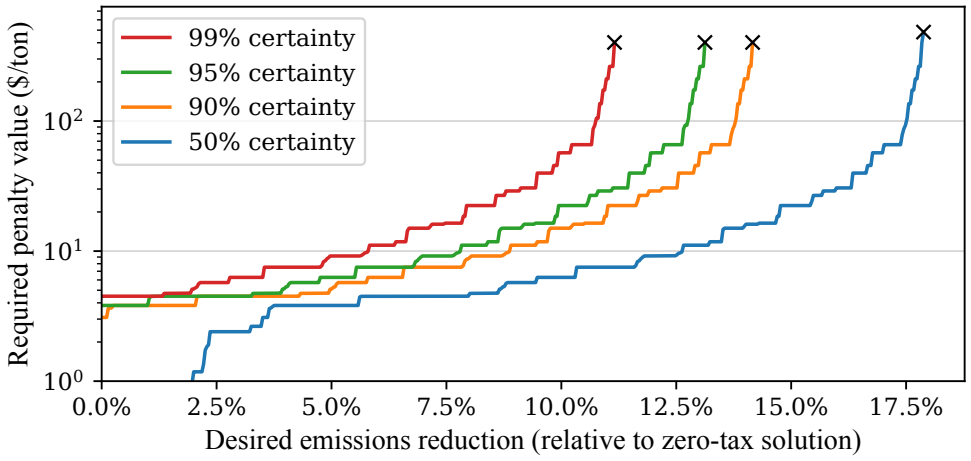

Figure 3.9: Tax rate required to achieve emissions reductions, based on weather uncertainty.

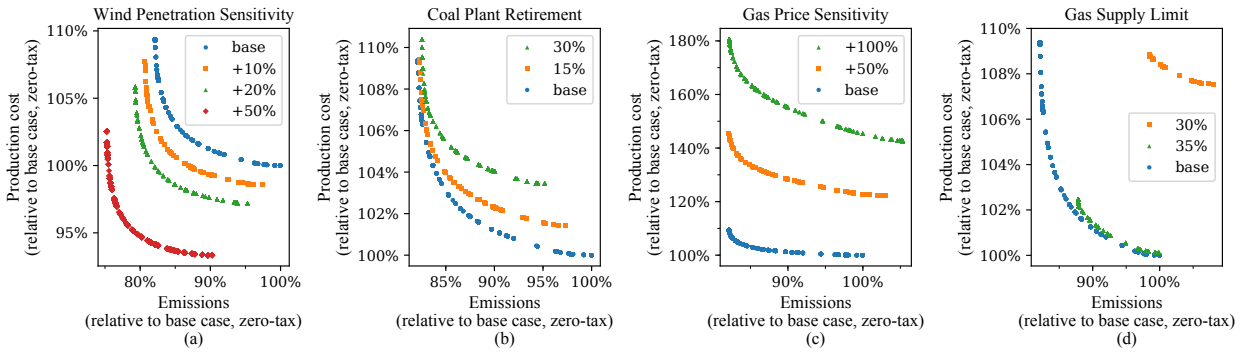

Figure 3.10: Sensitivities of Pareto frontier to (a) wind penetration, (b) coal plant retirement, (c) natural gas price, and (d) gas supply limit.

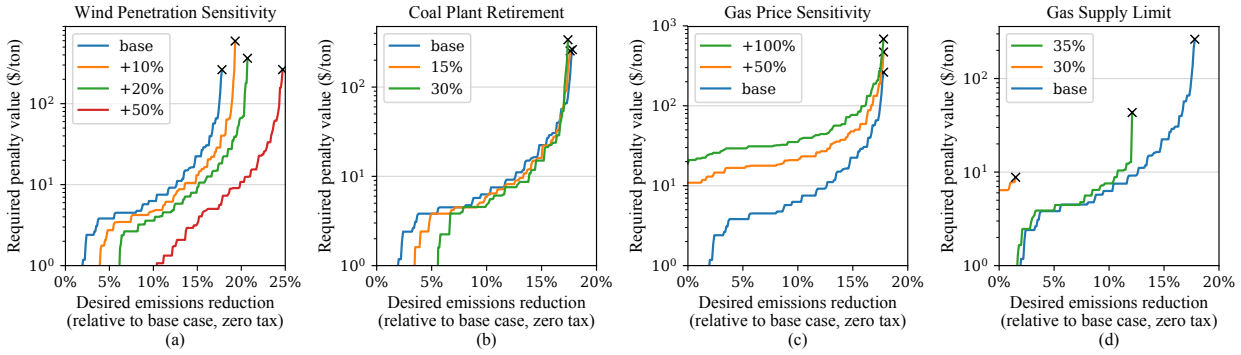

Figure 3.11: Sensitivities of required tax rate to (a) wind penetration, (b) coal plant retirement, (c) natural gas price, and (d) gas supply limit.

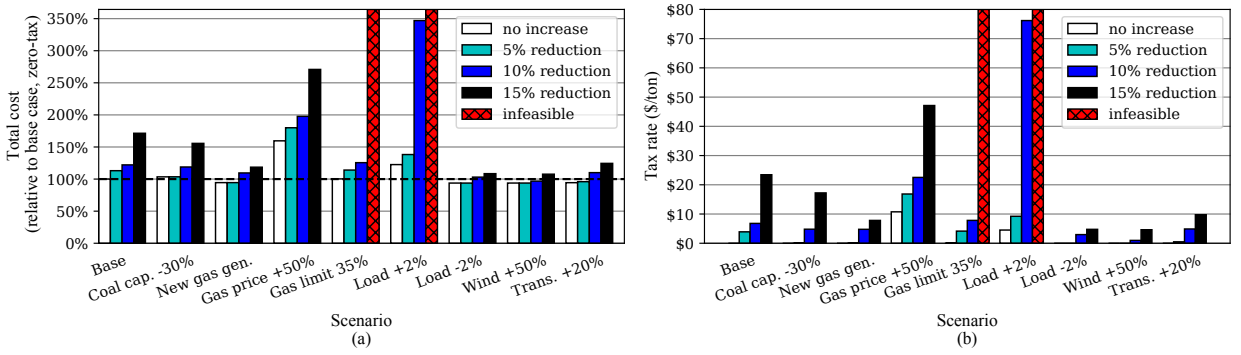

Figure 3.12: Results of selected scenarios for specified emission reduction targets, (a) total cost, (b) required tax rate.

3.5.4 Sensitivity Analyses

Sensitivity analyses to changes in the system's wind penetration, coal plant retirement, gas prices, and gas supply limitations on UCCT solutions are shown in Figs. 3.10(a)-(d), respectively, and the impact on the tax rates required to achieve desired emissions reductions are shown in Figs. 3.11(a)-(d). Additional scenarios are also run for specific emissions reductions targets and shown in Fig. 3.12:

- **Wind Penetration**: Wind penetration, initially at 8% of total energy, is increased by 10, 20, or 50%.

- **Coal Retirement**: Coal generation is retired, either one or two highest-cost generators (15% or 30% of the coal-generating capacity), consistent with estimates in [129].

- **New Gas Generator**: One new 250 MW gas generator is added at the bus with highest average locational marginal price (LMP), bus 8, increasing the gas capacity by 2.4%.

- **Gas Price**: The price of natural gas generation is increased by either 50 or 100%.

- **Gas Limit**: For each day, gas generators are limited in the amount of energy that they can supply, at either 30 or 35% of daily total energy. This is intended to simulate constraints in gas availability due to increased demand from gas generators as a result of carbon pricing [130] or regional gas shortages such as those experienced in New England [131] and Southern California [132] in 2014.

- **Load Increase/Decrease**: The demand for electricity at each hour is scaled up or down by 2%.

- **Transmission Capacity**: The capacity of all transmission corridors is increased by 20%.

Several of these scenarios have similar effects: increases in wind penetration, gas generation capacity, or transmission capacity, or decreases in load. For all of these scenarios, the zero-tax solutions have lower costs and emissions than the base case, a given emissions target can be met with a lower tax rate, and the maximum emissions reduction is increased. These effects can be seen in Figs. 3.10(a) and 3.11(a) for the wind penetration case and in Fig 3.12 for the other cases.

Other scenarios have differing effects. For the coal plant retirement case, the zero-tax solution has lower emissions than the base case but is more expensive, since the retired coal generation is replaced by more-expensive gas generation. However, despite the higher zero-tax cost, a desired emissions reduction can be met with a lower tax rate, as shown in Figs. 3.10(b) and 3.11(b), and some targets can be met at a lower total cost. For example, a 15% GHG reduction target in the base case requires a tax rate of \$23/ton and a total cost of increase of 71%, but the same target can be met with a \$17/ton tax rate and 56% cost increase in the 30% coal retirement case, as shown in Fig. 3.12. For the gas price increase cases, the zero-tax solution is both more expensive and higher-emitting than the base case, and a desired emissions reduction requires a higher tax rate, but the range of possible emissions reductions is not affected, as shown in Figs. 3.10(c) and 3.11(c). For the case where there are limitations on the energy supplied by gas generators, the effect is highly dependent on the limit values and emissions targets, as shown in Figs. 3.10(d) and 3.11(d). When gas generators are limited to providing no more than 35% of total energy, there is minimal impact for emissions reductions less than 10%, but past this point there is limited ability to reduce emissions, and reductions require a higher tax rate. At a limit of 30%, the zero-tax solution is 7.6% more expensive and emits 7.6% more GHGs when compared to the base case, and only a very modest reduction in emissions (1.5%) is possible. This illustrates the impact that gas system constraints can have on emission reductions goals.

The impact of relaxing the system flexibility constraints (3.18)-(3.19) is also investigated. For this system, the greatest impact is seen at lower tax rates, where relaxing the ramping capability requirement results in slightly higher emissions at slightly lower production cost, as

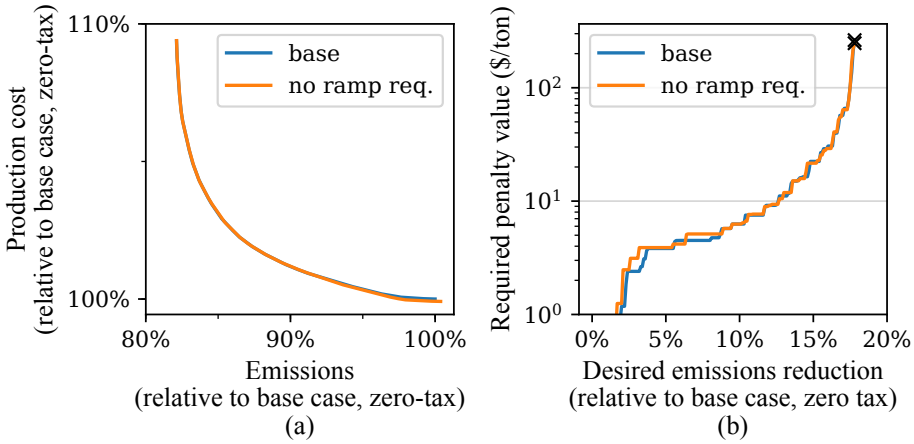

Figure 3.13: Impact of relaxing system ramp requirement constraint on (a) cost/emissions Pareto frontier, and (b) tax rate required to achieve emissions reductions.

shown in Fig. 3.13(a). At zero tax rate, emissions are 0.4% higher and production cost is 0.1% lower as compared to the base case. The impact on the tax rate required for a given emission reduction is similar, as shown in Fig. 3.13(b): greater impact at low emissions reductions targets, with differences diminishing at more aggressive emissions reductions targets. The converse is true when observing the impact on profit by generation technology: low tax rates have minimal impact, while higher tax rates have more significant impacts. At tax rates of \$0-10/ton, the average impact on profit is within 1.5% for all generation technologies, while for tax rates of \$10-100/ton, relaxing the flexibility constraints results in profits on average 102% higher for coal generators, and 5-6% lower for all other generation technologies.

3.5.5 Impact on Investment Decisions

As can be seen in Fig. 3.14(a), larger emissions reduction targets lead to higher average LMPs, which translates to a better value proposition for investing in new non-coal generation (as shown in Fig. 3.14(b), the carbon tax reduces profit by coal generators). For example, at a target emissions reduction of 5%, the profit for wind generators is 17% higher as compared to the zero-tax solution; at a target of 10%, the profit is 33% higher. In the New Gas Generator

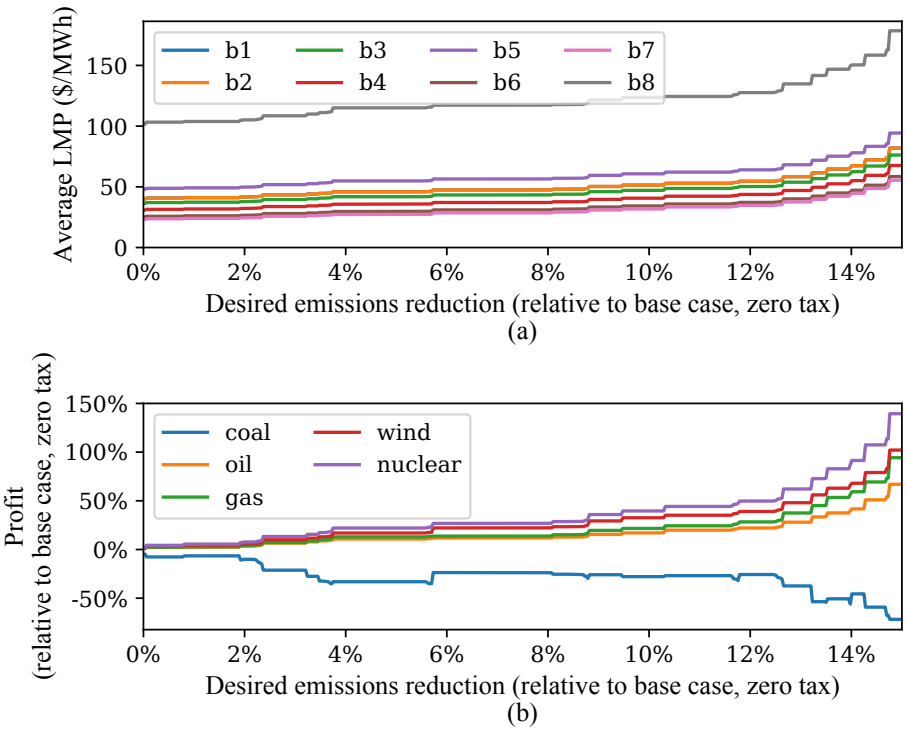

Figure 3.14: (a) Average LMPs for buses b1-b8 as a function of desired emissions reduction, and (b) Profit by fuel as a function of desired emissions reduction.

scenario, the new generator makes 12% more profit at an emissions reduction target of 10%; at a target reduction of 5%, no tax is required.

Along with higher LMPs, emission reduction targets also result in increased congestion surplus, improving the value proposition for investments in new transmission. At a target GHG reduction of 5%, the congestion surplus is increased by 9.5%; at a 10% target the surplus is increased by 16.1%. Congestion surplus as a share of total cost remains relatively constant, however: 20.6% in the zero-tax case, 20.4% in the 5% target case, and 19.6% in the 10% target case.

In addition to higher average LMPs, there is also an increase in the variability of LMPs, which improves the value proposition for grid-scale energy storage devices, consistent with findings in [133]. At a 5% emissions reduction target, the average LMP for each bus is 35-

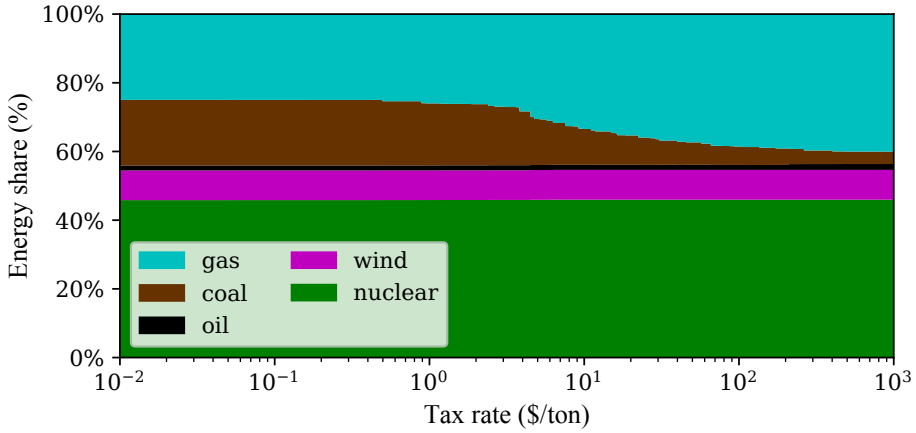

Figure 3.15: Energy by fuel as a function of tax rate.

60% higher (average of 46%), while the standard deviation of LMPs for each bus is 101-113% higher. However, while investments in wind and gas generation tend to reduce emissions (and therefore the tax rate required to meet emissions targets), the impact of energy storage is much less clear [134].

3.5.6 Coal Generators and Market Share

As would be expected, as the desired emissions reduction and the tax rate required to achieve this reduction both increase, the share of energy which is provided by coal and the profit made by coal generators both decrease, as can be seen in Figs. 3.14(b) and 3.15. These reduced profits may lead to earlier coal generation retirement and reductions in coal mining employment [135]. However, strategic investments in new wind generation and transmission network expansion both allow emissions targets to be met with a lower tax rate compared to the base case, and increase the profit of coal-powered generators, as shown in Table 3.1. Additionally, emissions taxes which are set based on emissions targets increase the incentive for owners of coal-powered generation to invest in renewable generation, since the increased profits for coal generators caused by a lower tax rate provides an 'extra' revenue stream.

Table 3.1: Coal profit dependence on investments, 5% reduction target, given increases in wind penetration or transmission capacity

Scenario	Additional Coal Profit ($)	Additional Wind Profit ($)	% Increase (coal/wind)
+10% Wind	24,212	77,336	31.3%
+20% Wind	62,170	140,276	44.3%
+10% Trans.	22,835	N/A	N/A
+20% Trans.	131,112	N/A	N/A

3.6 Conclusion

The Weighted Sum Bisection method can be efficiently applied to the problem of determining the optimal tax rate to meet a given emissions target, and has been shown to be compatible with uncertainty in weather, demand, fuel prices, and generation fleet. In addition to changing short-term generator commitment and dispatch, pricing carbon for emissions targets is also associated with several longer-term effects.

Higher prices for electricity reduce overall demand and increase the value proposition for investment in new cleaner generation, transmission, and grid-scale energy storage, as well as technologies which generate or consume electricity more efficiently. Carbon capture and sequestration projects also become more attractive. Conversely, investment in these resources reduces the tax rate required to achieve certain emissions targets.

In addition, carbon pricing collects revenue which can be used to invest in projects to reduce GHG emissions, adapt to climate change, and/or provide economic relief to communities which are negatively impacted by taxation of carbon, such as those heavily reliant on coal-mining. This revenue stream could also be used to offset tax reductions elsewhere to obtain revenue neutrality.

3.7 Subsequent Work

Subsequent work which has built on the approach presented in this chapter includes:

- Milyani and Kirschen [136], that extends the tax-setting methods in this chapter to include both a tax rate and targeted subsidies; this paper shows that the revenue-neutral combination of taxes and subsidies can achieve given emissions reductions at drastically lower tax rates, compared to tax rates alone.

- Pereira et al. [137], that extends the tax setting methods in this chapter to include tax rate trajectories and generation and transmission expansion planning; this paper shows that near-term tax rates improve the capacity of power systems to operate with lower emissions in future years, by incentivizing the construction of additional lower-emissions equipment.

Nomenclature

Sets and Indices

A Set of representative days, indexed by a.

B Set of transmission network buses, indexed by b.

I Set of generating units, indexed by i.

L Set of transmission lines, indexed by l.

R Subset of renewable generators ($R \subset I$).

S Set of generator power output blocks, indexed by s.

T Set of time intervals, indexed by t or τ.

Parameters

$b_{i,s}$ Marginal cost of block s of generator i (\$/MWh).

$C_i^{\min}$ Minimum cost of generator i (\$/h).

C_i^{su} Start-up cost of generator i (\$).

$d_{b,t,a}$ Demand at bus b, time t, day a (MW).

$d_{t,a}^{\text{ramp}}$ Load ramp requirement at time t, day a (MW/h).

$E^{\max}$ Regulator's GHG emission target (tons).

$E_i^{\min}$ Minimum GHG emissions of generator i (tons/h).

E_i^{su} Start-up GHG emissions of generator i (tons).

$f_l^{\max}$ Capacity of transmission line l (MW).

$g_i^{\max}$ Maximum power output of generator i (MW).

$g_i^{\min}$ Minimum power output of generator i (MW).

$g_{i,s}^{\max}$ Maximum power output of block s, generator i (MW).

g_i^{down} Minimum down-time of generator i (h).

g_i^{up} Minimum up-time of generator i (h).

$h_{i,s}$ Marginal GHG emissions of block s, generator i (tons/MWh).

$m_{l,b}^{\text{line}}$ Line connection map. $m_{lb}^{\text{line}} = 1$ if line l starts at bus b, $= -1$ if line l ends in bus b, 0 otherwise.

$m_{i,b}^{\text{unit}}$ Unit map. $m_{i,b}^{\text{unit}} = 1$ if generator i is located at bus b, 0 otherwise.

P^{CO_2} GHG emissions tax rate (\$/ton-CO_2e).

P^{load} Load shed penalty (\$/MWh).

P^{ren} Renewable generation shed penalty (\$/MWh).

r_i^{down} Maximum down-ramp rate of generator i (MW/h).

r_i^{up} Maximum up-ramp rate of generator i (MW/h).

$w_{t,a}^{\text{down}}$ Wind down-ramp requirements at time t, day a (MW/h).

$w_{t,a}^{\text{up}}$ Wind up-ramp requirements at time t, day a (MW/h).

x_l Reactance of line l (Ω).

π_a Probability of day a.

Variables

C^{gen} System operator's generation cost ($).

C^{shed} System operator's shed cost ($).

E_a GHG Emissions for day a (tons).

E^{total} Total GHG emissions (tons).

$f_{l,t,a}$ Power flow on line l, time t, day a (MW).

$g_{i,t,a}$ Power output of generator i, time t, day a (MW).

$g_{i,s,t,a}$ Power output of generator i, block s, time t, day a (MW).

$s_{b,t,a}^{\text{load}}$ Load shed at bus b, time t, day a (MWh).

$s_{b,t,a}^{\text{ren}}$ Renewable generation shed at bus b, time t, day a (MWh).

$u_{i,t,a}$ Binary variable for the commitment status of generator i, time t, day a.

$v_{i,t,a}$ Binary variable for the start-up of generator i, time t, day a.

$z_{i,t,a}$ Binary variable for the shut-down of generator i, time t, day a.

$\theta_{b,t,a}$ Voltage phase angle of bus b, time t, day a (rad).

Chapter 4

PLANNING LOW-CARBON CAMPUS ENERGY HUBS

Published as:

Olsen, D. J., Zhang, N., Kang, C., Ortega-Vazquez, M. A., & Kirschen, D. S. (2018). Planning Low-Carbon Campus Energy Hubs. *IEEE Transactions on Power Systems*, 34(3), 1895-1907.

4.1 Introduction

Buildings and their occupants require several forms of energy (e.g. electrical, thermal, kinetic), each of which can often be supplied via several means. For example, thermal energy can be delivered via district heating or via conversion from electricity or natural gas. By considering all energy requirements and equipment of a multiple-energy system simultaneously, overall operation can be improved; this modeling approach is often referred to as using *energy hubs* [138], which create algebraic representations of energy flows into, out of, and within a system for the purpose of optimization. Operational improvements can be measured in terms of cost, reliability, environmental impact, or other metrics. For example, an energy hub may have electricity and natural gas as inputs, require electricity and heat as output, and have a heat pump and a combined-heat-and-power (CHP) unit as energy conversion equipment. An optimization for cost may result in sourcing heat primarily from natural gas via the CHP unit, while an optimization for local air-quality may result sourcing heat primarily form electricity via the heat pump. Optimization of energy hub scheduling considering the Pareto frontier of cost/emissions tradeoffs is presented in [139].

Because energy flows in an energy hub are constrained by planning and construction decisions as well as the selection of equipment type and capacity, these decisions have a long-lasting impact. The design of an entirely new multiple-energy system is sometimes known

as *greenfield* design. Energy hub models for the optimization of planning and operation of multiple-energy systems have been developed at the building [140, 141, 142, 143], district [144, 145, 146], and regional [147] scales. An energy hub framework which incorporates building equipment and plug-in hybrid electric vehicle charging to respond to frequency control is presented in [148]. A review of energy hub models and other related modeling frameworks (*e.g.* microgrids) can be found in [149].

Several papers have investigated simultaneous optimization of planning and operation in energy hubs while considering carbon emissions. Considering carbon emissions as an additional objective to be minimized creates a Pareto frontier of solutions which trade off emissions reductions for cost increases, and vice versa. The full Pareto frontier of cost and emissions can be sampled using the ϵ-constraint method [142, 144, 145], or if the set of potential technologies is small, the results for all combinations can be explicitly calculated [143]. Evins [141] presents a multi-level model where building and energy hub variables are optimized in the upper-level while operation variables (including binary variables for fuel cell status) are optimized in the lower level. Solutions are found using a non-dominated sorting genetic algorithm in order to trace out the Pareto frontier.

Another approach to sampling the Pareto frontier is a linear weighting factor, which can find points on the convex hull of the frontier. In this context, the weighting factor is a price for carbon emissions. Regulatory imposition of a price on externalities improves overall social welfare [8], and is one approach to avoiding a 'tragedy of the commons' outcome where individually rational decisions result in a socially-suboptimal solution compared to a cooperative approach [150]. Carbon pricing is increasingly common [19], and can be implemented via a real price (a tax or an emissions-trading scheme) or a mandate to consider the *social cost of carbon* (SCoC) in planning decisions [151, 152, 153].

The motivation for this paper is to bridge perceived gaps in the existing literature: a), a mixed-inter linear program (MILP) model for planning and incentivizing low-carbon energy hubs, considering an independent operator that may not share the low-carbon goals of planners, and b) incentivization of low-carbon goals via an optimized price for carbon.

Picard and Helsen [143] evaluate only a limited number of possible equipment combinations in order to be able to evaluate all of their costs and emissions. Several authors [142, 144, 145] build MILP models, but without an independent operator. Therefore the derived solutions *could* satisfy the emissions constraints, but may not in practice. Evins [141] incorporates an independent, emissions-indifferent operator, but their approach utilizes an external building simulation (EnergyPlus) and candidate solutions are found via a genetic algorithm, so the quality of the best currently-found solution relative to the true optimum is unknown.

This paper extends the analysis of low-carbon energy hub design to include two strategic considerations. The first makes investment decisions while accounting for a hub operator that may ignore emissions-reduction goals, and the second decides carbon prices to induce lower-emission investment and operation decisions. The underlying greenfield energy hub model is also enhanced. Specifically, this paper makes the following contributions:

- The formulation of four different frameworks for optimizing low-carbon energy hub investment and operation, to account for differences in policy and market structures: Single Builder-Operator, Bi-level Regulator/Builder-Operator, Bi-level Builder/Operator, and Tri-level Regulator/Builder/Operator.

- An expanded investment optimization problem, including on-site renewable generation, grid capacity costs, and storage for each energy type.

- A new formulation of the greenfield energy hub operation model using the concept of *energy buses*. This formulation simplifies the investment optimization problem without loss of accuracy.

The rest of this chapter is organized as follows: Section 4.2 describes the various optimization perspectives present in each framework, Section 4.3 describes the formulation of the energy hub model, Section 4.4 describes the techniques used to reformulate the multi-level frameworks into more tractable forms, Section 4.5 describes a case study, Section 4.6 presents

results, Section 4.7 discusses implications, and Section 4.8 concludes. A nomenclature section follows at the end of the chapter.

4.2 Low-Carbon Design Frameworks

A strategy for controlling operational carbon emissions when planning equipment investments for a greenfield energy hub depends on the answers to two fundamental questions:

1. Does the hub operator share the hub builder's goal to reduce carbon emissions?

2. Are carbon emissions controlled via an explicit constraint or a carbon price set to meet a given target?

The answers to these questions determine the four possible frameworks defined below and illustrated in Fig. 4.1.

- **Framework 1: Single Builder-Operator, Emission-Constrained**: A single entity designs and operates the hub at or below a given emissions target.

- **Framework 2: Bi-Level Regulator/Builder-Operator, Carbon Tax**: A regulatory agency sets a carbon tax rate, such that a builder-operator's minimum-cost investment and operation solution results in emissions at or below a given emissions target.

- **Framework 3: Bi-Level Builder/Operator, Emission Constrained**: A builder makes hub investment decisions, considering the overall cost of constructing and operating the hub, such that the minimum-cost operation results in emissions at or below a given emissions target.

- **Framework 4: Tri-Level Regulator/Builder/Operator, Social Cost of Carbon**: A regulatory agency sets a Social Cost of Carbon (SCoC) rate, to reduce emissions to or below a certain target. The builder makes hub investment decisions considering

the overall cost of constructing and operating the hub as well as the social cost of carbon emissions. The hub is independently operated based on a minimum cost-solution.

	builder & operator	
	singular	distinct
carbon constrained	Framework 1	Framework 3
carbon tax	Framework 2	Framework 4

Figure 4.1: Taxonomy of low-carbon investment and design frameworks

Each framework represents a different policy strategy that a regulator may have available for controlling carbon emissions. Each framework results in a distinct optimization formulation, with a distinct Pareto frontier of cost/emissions tradeoffs. Framework 1 represents the most efficient scenario, where a regulator can set an emissions limit and the builder and operator will work together to achieve it. Framework 2 represents the case where the regulator cannot dictate an emissions limit to the hub builder, but can set a carbon tax rate. Generally, higher tax rates are politically unpopular and increase the rate of tax evasion [108]. Therefore for the purposes of this framework, the regulator wants to minimize the tax rate (maximum likelihood of political feasibility), subject to the constraint that the chosen tax rate, if implemented, will result in meeting the emissions target. Framework 3 represents the case where the regulator sets an emissions limit and mandates that the builder chooses equipment such that the emissions constraint is robust to an operator that may decide to ignore emissions in favor of cost savings. Framework 4 is similar to Framework 3, except that the regulator cannot dictate an emissions limit to the hub operator, but can mandate that the builder consider a SCoC rate when deciding equipment investments. Each framework is further discussed in the following subsections.

4.2.1 Common Framework Definitions

Common between all framework formulations are the energy hub network constraints described in Section 4.3, as well as the definitions of the investment cost, operating cost, revenue, and emissions given in (4.1)-(4.4), respectively. Eq. (4.1) defines the total investment cost C^{invest} in terms of the investment quantity variables multiplied by each variable's per-unit cost. The annual operating cost C_y^{operate} depends on the grid power purchases and the fuel prices in each time period (4.2). The annual operating revenue R_y^{operate} depends on the grid power exports and the feed-in prices in each time period (4.3). Finally, the annual carbon emissions E_y^{operate} depend on the grid power purchases and the carbon intensity of each fuel in each time period (4.4).

$$C^{\text{invest}} := \sum_{m \in M} C_m^{\text{cap}} P_m^{\max} + \sum_{g \in G^{\text{C}}} C_g^{\text{unit}} I_g + \sum_{g \in G^{\text{S}}} \left(C_g^{\text{power}} D_g^{\max} + C_g^{\text{energy}} Q_g^{\max} \right) \tag{4.1}$$

$$C_y^{\text{operate}} := 365 \sum_{s \in S} \pi_s \sum_{t \in T} \sum_{m \in M} f_{m,s,t,y} P_{m,s,t,y} \Delta t \tag{4.2}$$

$$R_y^{\text{operate}} := 365 \sum_{s \in S} \pi_s \sum_{t \in T} \sum_{m \in M} h_{m,s,t,y} r_{m,s,t,y} \Delta t \tag{4.3}$$

$$E_y^{\text{operate}} := 365 \sum_{s \in S} \pi_s \sum_{t \in T} \sum_{m \in M} e_{m,s,t,y} P_{m,s,t,y} \Delta t \tag{4.4}$$

4.2.2 Framework 1: Single Builder-Operator

The single builder-operator model features builder-operator coordination and an explicit carbon constraint, as shown in Fig. 4.2(a). The objective function is the net-present cost of building and operating the hub (4.5); Eqs. (4.5)-(4.7) formalize this problem.

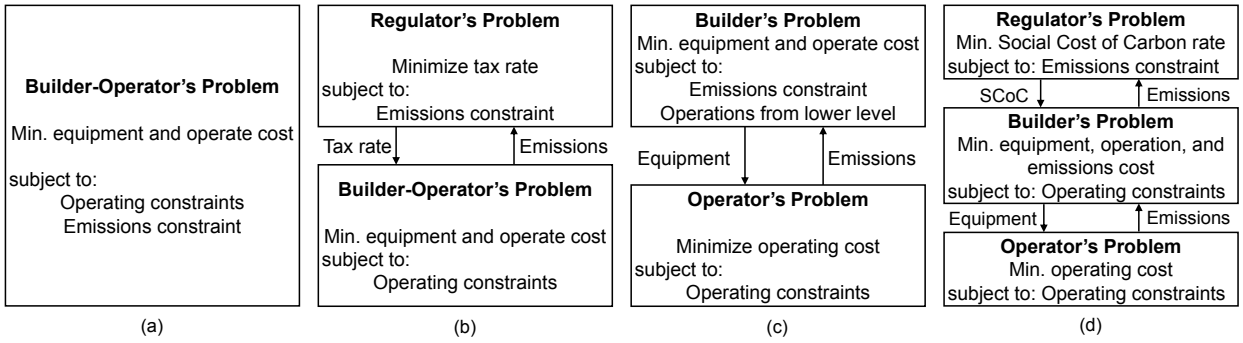

Figure 4.2: Low-carbon design frameworks: (a) Single Builder-Operator, (b) Bi-level Regulator/Builder-Operator, (c) Bi-level Builder/Operator, and (d) Tri-level Regulator/Builder/Operator.

$$\min C^{\text{invest}} + \sum_{y=1}^{Y} \frac{\left(C_y^{\text{operate}} - R_y^{\text{operate}}\right)}{\left(1+i\right)^y} \tag{4.5}$$

subject to:

$$\text{Network constraints: (4.22)-(4.30)} \tag{4.6}$$

$$E_y^{\text{operate}} \leq E^{\max} \quad \forall y \in Y \tag{4.7}$$

4.2.3 Framework 2: Bi-Level, Regulator/Builder-Operator

The bi-level regulator/builder-operator problem features builder-operator coordination and a carbon price set by an upper-level regulator, as shown in Fig. 4.2(b). Eqs. (4.8)-(4.12) formalize this problem. In this framework, the regulator's objective is to find the minimum tax-rate P^{CO_2} (4.8) such that emissions are at or below a target (4.9) when the builder-operator independently minimizes its net-present cost of building and operating the hub (4.10)-(4.12) based on the tax-rate.

$$\min P^{\mathrm{CO_2}} \tag{4.8}$$

subject to:

$$E_y^{\mathrm{operate}} \leq E^{\max} \quad \forall y \in Y \tag{4.9}$$

$$E_y^{\mathrm{operate}} \in \underset{\boldsymbol{I},\boldsymbol{P}^{\max},\boldsymbol{D}^{\max},\boldsymbol{Q}^{\max},\boldsymbol{V},\boldsymbol{Q},\boldsymbol{r}}{\arg\min} \Big\{ C^{\mathrm{invest}} + \sum_{y=1}^{Y} \frac{\left(C_y^{\mathrm{operate}} - R_y^{\mathrm{operate}} + T_y^{\mathrm{operate}}\right)}{\left(1+i\right)^y} \tag{4.10}$$

subject to:

$$T_y^{\mathrm{operate}} = \max\left(P^{\mathrm{CO_2}} E_y^{\mathrm{operate}}, 0\right) \quad \forall y \in Y \tag{4.11}$$

$$\text{Network constraints: (4.22)-(4.30)} \Big\} \tag{4.12}$$

The annual tax bill for carbon emissions T_y^{operate} is constrained to be non-negative in (4.11); otherwise, at high tax rates the lower-level problem can become unbounded. This can occur if there is at least one time period with negative marginal emissions of electricity, a condition that can be caused by transmission grid congestion.

4.2.4 Framework 3: Bi-Level, Builder/Operator

The bi-level builder/operator problem features no builder-operator coordination and an explicit carbon constraint, as shown in Fig. 4.2(c). Eqs. (4.13)-(4.16) formalize this problem. The builder's objective is to minimize the overall construction and operating cost (4.13) such that the emissions are at or below a target (4.14) when the operator independently minimizes its operating cost (4.15) subject to hub constraints (4.16).

$$\min_{\boldsymbol{I},\boldsymbol{P}^{\max},\boldsymbol{D}^{\max},\boldsymbol{Q}^{\max}} C^{\text{invest}} + \sum_{y=1}^{Y} \frac{\left(C_y^{\text{operate}} - R_y^{\text{operate}}\right)}{\left(1+i\right)^y} \tag{4.13}$$

subject to:

$$\sum_{s\in S} \pi_s E_{s,y}^{\text{operate}} \leq E^{\max} \quad \forall y \in Y \tag{4.14}$$

$$C_{s,y}^{\text{operate}}, E_{s,y}^{\text{operate}}, R_{s,y}^{\text{operate}} \in \arg\min_{\boldsymbol{V},\boldsymbol{Q},\boldsymbol{r}} \left\{ C_{s,y}^{\text{operate}} - R_{s,y}^{\text{operate}} \right. \tag{4.15}$$

subject to:

$$\text{Network constraints: (4.22)-(4.30)} \left. \right\} \quad \forall s \in S, y \in Y \tag{4.16}$$

4.2.5 Framework 4: Tri-Level, Regulator/Builder/Operator

The tri-level Regulator/Builder/Operator problem features no builder-operator coordination and a price to be set for the Social Cost of Carbon, $SCoC$ (¥/ton), as shown in Fig. 4.2(d). Eqs. (4.17)-(4.21) formalize this problem. The regulator's objective is to minimize the $SCoC$ (4.17) such that the builder, when minimizing the combined cost of investment, operation, and carbon (4.19), and the operator, minimizing its operating cost (4.20) subject to energy hub constraints (4.21), result in annual emissions below a given target (4.18). Note that the $SCoC$ is not a cost that necessarily needs to be paid, as long as it is considered in the builder's objective function.

$$\min SCoC \tag{4.17}$$

subject to:

$$\sum_{s\in S} \pi_s E_{s,y}^{\text{operate}} \leq E^{\max} \quad \forall y \in Y \tag{4.18}$$

$$E_{s,y}^{\text{operate}} \in \underset{\boldsymbol{I},\boldsymbol{P}^{\max},\boldsymbol{D}^{\max},\boldsymbol{Q}^{\max}}{\arg\min} \Bigg\{$$

$$C^{\text{invest}} + \sum_{y=1}^{Y} \left[\frac{\left(C_y^{\text{operate}} - R_y^{\text{operate}}\right)}{\left(1+i\right)^y} + SCoC \cdot E_y^{\text{operate}} \right] \tag{4.19}$$

subject to:

$$C_{s,y}^{\text{operate}}, E_{s,y}^{\text{operate}}, R_{s,y}^{\text{operate}} \in \underset{\boldsymbol{V},\boldsymbol{Q},\boldsymbol{r}}{\arg\min} \big\{ C_{s,y}^{\text{operate}} - R_{s,y}^{\text{operate}} \tag{4.20}$$

subject to:

$$\text{Network constraints: (4.22)-(4.30)} \big\} \quad \forall s \in S, y \in Y \Bigg\} \tag{4.21}$$

4.3 Energy Hub Model Formulation

The energy hub operational model assumes a greenfield design, where the topology of the network is not predefined [146], with enhancements to reduce dimensionality and include additional investment decisions. In the greenfield model in [146], there is a branch between every combination of device output port and device input port which handle the same energy type. For that formulation, the number of branch flow variables grows with the number of devices at a rate of $\mathcal{O}(n^2)$.

By contrast, this formulation introduces the concept of *energy buses*. Each energy bus is positioned such that any sources of this energy (i.e., from hub input ports and from converters and storage devices) flow directly into this bus, and any sinks of this energy (to hub output ports and to converters and storage devices) are fed directly from this bus. Therefore, the number of branch flow variables is reduced when compared to a formulation where every source can connect to every sink; $\mathcal{O}(n)$ vs. $\mathcal{O}(n^2)$. Fig. 4.3 shows the resulting network

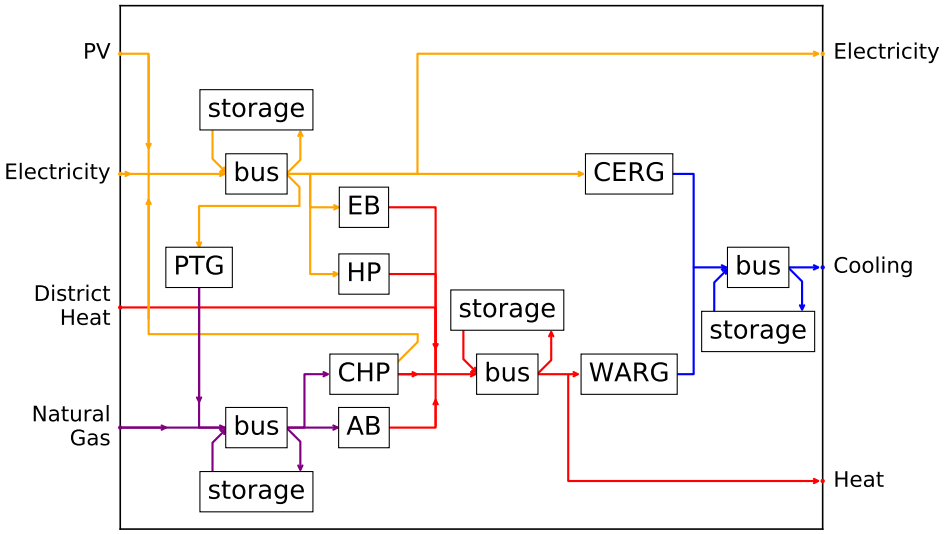

Figure 4.3: Network topology. Abbreviations: auxiliary boiler (AB), compression expansion refrigeration group (CERG), combined heat and power (CHP), electric boiler (EB), heat pump (HP), power-to-gas (PTG), water absorption refrigeration group (WARG).

topology.

In addition to the converters in [146], investment decisions include on-site distributed renewable generation, the provision of grid import/export capacity, storage for all energy types, and the inclusion of power-to-gas equipment [154]. Since CO_2 is an input to the power-to-gas process, gas which is created using this process and burned is CO_2-neutral, though the electricity used during the conversion process may not be. For the considered devices, connecting all compatible input and output ports for electricity flows would require 23 branches, while introducing energy buses enables the same functionality with only 10 branches.

For a given energy hub, the operating decision variables are the branch flows $\boldsymbol{V}_t$, the state of charge for the storage devices $\boldsymbol{Q}_t$, and the grid export $\boldsymbol{r}_t$. Eqs. (4.22)-(4.30) constrain the values of these decision variables. The dual variable associated with each constraint is shown in parentheses.

$$\boldsymbol{Z}\boldsymbol{V}_t = \mathbf{0} \quad \forall t \in T \quad (\alpha_{p,t}) \tag{4.22}$$

$$Q_{g,t} = Q_{g,t-1} - \boldsymbol{J}_g \boldsymbol{A}_g \boldsymbol{V}_t \Delta t \quad \forall g \in G^{\mathrm{S}}, t \in T \quad (\beta_{g,t}) \tag{4.23}$$

$$0 \leq Q_{g,t} \leq Q_g^{\max} \quad \forall g \in G^{\mathrm{S}}, t \in T \quad (\underline{\gamma}_{g,t}, \overline{\gamma}_{g,t}) \tag{4.24}$$

$$\boldsymbol{J}_g \boldsymbol{A}_g \boldsymbol{V}_t \leq D_g^{\max} I_g \quad \forall g \in G^{\mathrm{C}}, t \in T \quad (\zeta_{g,t}) \tag{4.25}$$

$$-D_g^{\max} \leq \boldsymbol{J}_g \boldsymbol{A}_g \boldsymbol{V}_t \leq D_g^{\max} \quad \forall g \in G^{\mathrm{S}}, t \in T \quad (\underline{\kappa}_{g,t}, \overline{\kappa}_{g,t}) \tag{4.26}$$

$$P_{m,t} := \boldsymbol{U}\boldsymbol{V}_t \leq B_{m,t} P_m^{\max} \quad \forall m \in M, t \in T \quad (\rho_{m,t}) \tag{4.27}$$

$$\boldsymbol{W}\boldsymbol{V}_t = L_{m,t} + r_{m,t} \quad \forall m \in M, t \in T \quad (\mu_{m,t}) \tag{4.28}$$

$$0 \leq r_{m,t} \leq P_m^{\max} \quad \forall m \in M, t \in T \quad (\underline{\phi}_{m,t}, \overline{\phi}_{m,t}) \tag{4.29}$$

$$0 \leq K_l V_{l,t} \quad \forall t \in T, l \in L \quad (\sigma_{l,t}) \tag{4.30}$$

$$\forall s \in S, y \in Y$$

Eq. (4.22) expresses the conservation of power in all converters, storage devices, and energy buses using a connection and efficiency matrix $\boldsymbol{Z}$ [146]. The state of charge for these storage devices is tracked in (4.23) and bounded by energy capacities in (4.24). Power flows through each converter are constrained by (4.25) and through each storage device by (4.26). Eq. (4.27) constrains hub input flows based on grid connection capacity and time-varying power availability, while (4.28) relates hub output flows to end-use power demand and power exports and (4.29) ensures that power exports do not exceed the grid connection capacity. Eq. (4.30) ensures that the directionality of branch flows is maintained, except for state of charge branches which are bi-directional.

Eqs. (4.22)-(4.30) apply for each representative day, during each year. Therefore an additional two dimensions (s and y) are added to variables $\boldsymbol{V}_t$, $\boldsymbol{Q}_t$, and $\boldsymbol{r}_t$ and to parameters $B_{m,t}$ and $L_{m,t}$; Eqs. (4.22)-(4.30) then apply $\forall s \in S, y \in Y$.

4.4 Multi-Level Reformulation Techniques

Two techniques are used to solve the multi-level optimization problems presented in Section 4.2. The first technique constructs a single-level equivalent MILP from the bi-level Builder/Operator problems of Frameworks 3 and 4. There are two steps to this technique: first a non-linear single-level equivalent is constructed (Section 4.4.1), and then it is approximated by a MILP formulation (Section 4.4.2).

The second technique solves the minimum carbon-price problem with an upper-level regulator and a lower-level non-convex builder-operator using the bisection method (Section 4.4.3). This technique is used in Framework 2 and Framework 4, after a single-level equivalent is constructed.

For each framework, since the operation problems for each day are independent, the problem can be decomposed using Benders' Decomposition [155]: the investment variables are solved in the master problem and each day's operational variables are solved in a subproblem.

4.4.1 Constructing a Single-Level Equivalent for the Distinct Builder and Operator Case

An independent cost-minimization problem for the operator must be solved for each representative day s of each representative year y. For investment problem formulations where the builder and the operator are distinct, the builder must anticipate the emissions resulting from these cost-minimization decisions to make its investment decisions; this ensures that the emissions constraints can be satisfied or the social cost of GHG emissions can be appropriately considered in the objective. Since the operator's cost minimization problem is linear and therefore convex, the strong duality theorem can be used to constrain the variables in the operator's problem (the most relevant of which are the resulting cost and emissions) to only the set of cost-minimizing values [127].

The dual problem is defined in terms of the dual variables of the constraints (4.22)-(4.30) and the parameters of the original primal problem. The dual objective is given in (4.31) with feasibility constraints corresponding to each primal variable given in (4.32) for $\boldsymbol{Q}_t$, (4.33) for

$\boldsymbol{r}_t$, and (4.34) for $\boldsymbol{V}_t$, with dual variable domains given in (4.35).

$$\max_{\alpha,\beta,\gamma,\zeta,\kappa,\rho,\mu,\phi,\sigma} \hat{C}^{\mathrm{DLL}} := \sum_{t\in T}\Bigg\{ \sum_{g\in G^{\mathrm{C}}} \Big(- D_g I_g \zeta_{g,t} \Big) + \sum_{g\in G^{\mathrm{S}}} \left(-Q_g^{\max}\overline{\gamma}_{g,t} - D_g^{\max}\left(\underline{\kappa}_{g,t} + \overline{\kappa}_{g,t}\right)\right) + \sum_{m\in M} \left(-L_{m,t}\mu_{m,t} - P_m^{\max}\left(B_{m,t}\rho_{m,t} + \overline{\phi}_{m,t}\right)\right) \Bigg\} \tag{4.31}$$

subject to:

$$\beta_{g,t} - \beta_{g,t+1} + \overline{\gamma}_{g,t} - \underline{\gamma}_{g,t} = 0 \quad \forall g \in G^{\mathrm{S}}, t \in T \tag{4.32}$$

$$\overline{\phi}_{m,t} - \underline{\phi}_{m,t} - h_{m,t}\Delta t - \mu_{m,t} = 0 \ \ \forall m \in M, t \in T \tag{4.33}$$

$$\sum_{m\in M}\Big[U_{m,l}\Big(f_{m,t}\Delta t + \rho_{m,t}\Big) + W_{m,l}\mu_{m,t}\Big] + \sum_{p\in P}\Bigg\{ \sum_{g\in G^{\mathrm{S}}}\Big[J_{g,p}A_{p,l}\big(\Delta t\beta_{g,t} + \overline{\kappa}_{g,t} - \underline{\kappa}_{g,t}\big)\Big] + \sum_{g\in G^{\mathrm{C}}} J_{g,p}A_{p,l}\zeta_{g,t}\Bigg\} + \sum_{p\in P^{\mathrm{out}}}\Big(Z_{l,p}\alpha_{p,t}\Big) - K_l\sigma_{l,t} = 0 \quad \forall l \in L, t \in T \tag{4.34}$$

$$\underline{\gamma}, \overline{\gamma}, \zeta, \underline{\kappa}, \overline{\kappa}, \rho, \underline{\phi}, \overline{\phi}, \sigma \geq 0 \tag{4.35}$$

Therefore, the power flows within the energy hub on a given day can be constrained to the values that would result from a hub operator's cost minimization using the primal feasibility constraints (4.36), the dual feasibility constraints (4.37), and the strong duality constraint (4.38), and the problem can simultaneously consider the upper-level objective and constraints of the regulator.

$$\text{Eqs. (4.22)-(4.30)} \qquad \text{(PLL feasibility)} \tag{4.36}$$

$$\text{Eqs. (4.32)-(4.35)} \qquad \text{(DLL feasibility)} \tag{4.37}$$

$$\hat{C}^{\mathrm{PLL}} := C^{\mathrm{operate}} - R^{\mathrm{operate}} = \hat{C}^{\mathrm{DLL}} \quad \text{(Strong duality)} \tag{4.38}$$

4.4.2 MILP Approximation of Non-Linear Strong Duality Constraint

Although the hub operator's cost-minimization problem, its dual problem, and the strong duality constraint are all linear in terms of the lower-level primal and dual variables, the strong duality constraints are non-linear when the equipment capacities are included as decision variables. To avoid the difficulty of solving a Mixed Integer Non-Linear Problem (MINLP), these equipment capacity variables can be discretized in order to convert the problem to a more tractable MILP version.

The continuous variables $P_g^{\max}$, $Q_g^{\max}$, $D_g^{\max}$, and the integer variables $I_g^{\max}$ are approximated by a series of binary variables using (4.39)-(4.42). Rather than having each binary variable represent a single unit of capacity, a binary counting approach is used, where each binary variable represents one digit of a binary representation of an integer number, as shown in Fig. 4.4. In this way, a relative step size of $1/2^n$ is possible with only n binary variables for each continuous variable (e.g., a step size of 0.1% for 10 binaries). This method implicitly creates bounds on the approximated continuous variables, since each approximated value can only range from the value represented by $\{0, 0, \ldots, 0\}$ to the value represented by $\{1, 1, \ldots, 1\}$. Therefore, the values of the step sizes must be chosen carefully.

$$P_g^{\max} \approx \sum_{n=0}^{N} 2^n x_{m,n}^{\mathrm{a}} \Delta P_g \quad \forall m \in M \tag{4.39}$$

$$Q_g^{\max} \approx \sum_{n=0}^{N} 2^n x_{g,n}^{\mathrm{b}} \Delta Q_g \quad \forall g \in G^{\mathrm{S}} \tag{4.40}$$

$$D_g^{\max} \approx \sum_{n=0}^{N} 2^n x_{g,n}^{\mathrm{c}} \Delta D_g \quad \forall g \in G^{\mathrm{S}} \tag{4.41}$$

$$I_g^{\max} \approx \sum_{n=0}^{N} 2^n x_{g,n}^{\mathrm{d}} \quad \forall g \in G^{\mathrm{C}} \tag{4.42}$$

Using (4.39)-(4.42), the non-linearity in the strong duality constraint is therefore reduced to only products of binary and continuous variables. These non-linear products are approximated using the big-M technique [156], resulting in strong duality constraints that are MILP

$681 =$	2^9	$+$	2^7	$+$	2^5	$+$	2^3		$+$	2^0
$=$	1	0	1	0	1	0	1	0	0	1

Figure 4.4: Binary representation of 681. 10 bits can represent 1024 values.

rather than MINLP. For computational performance, it is standard practice to choose the values of M such that they are as small as possible while still allowing for the full range of values for the continuous variables [95]. Since the dual variables for the network constraints are related to the price of input energy flows, scaling energy prices (and therefore big-M values) may improve performance.

4.4.3 Determining a Minimum Carbon Tax using the Bisection Method

Incorporating a carbon price in the lower-level builder-operator problem is an instance of using a linear weighting factor to optimize trade-offs between multiple competing objectives. In this case, these objectives are the operating emissions and the sum of investment and operating costs. By varying the carbon price ($P^{\mathrm{CO_2}}$ or $SCoC$), the Pareto frontier is sampled at points which lie on the convex hull of the cost/emissions solution space [119]. Since the lower-level builder-operator problem is non-convex due to the inclusion of binary variables, the minimum-carbon-price solution which satisfies an emissions constraint may result in a total investment and operating cost that is higher than could be found using an ϵ-constraint method (Frameworks 1 & 3). However, the resulting emissions would also be lower.

Since the upper-level price-setting problem minimizes a single continuous variable (the tax rate), and the resulting emissions from the lower-level problem are monotonically non-increasing with respect to an increasing tax rate, the problem can be solved to within a specified tolerance by the bisection method, as shown in [53].

4.4.4 Computational Complexity

Since the performance of MILP solvers depends on the number of variables and constraints in a model, the number of variables of each type are listen in Table 4.1, where set names are used to represent the number of elements in the set. These expressions can be used to balance the accuracy of different model elements when computation time and/or available memory are an issue.

Table 4.1: Computational Complexity

# of integer variables	$M + 2G^{\mathrm{S}} + G^{\mathrm{C}}$
# of binary variables	$N^{\mathrm{A}}M + G^{\mathrm{S}}\left(N^{\mathrm{B}} + N^{\mathrm{C}}\right) + N^{\mathrm{D}}G^{\mathrm{C}}$
# of continuous variables	$STY\big[2L + 6G^{\mathrm{S}} + 5M + P^{\mathrm{out}} + G^{\mathrm{C}}$ $+2MN^{\mathrm{A}} + 2G^{\mathrm{S}}\left(N^{\mathrm{B}} + N^{\mathrm{C}}\right) + G^{\mathrm{C}}N^{\mathrm{D}}\big]$
# of constraints	$STY\big[2L + 6G^{\mathrm{S}} + 5M + P^{\mathrm{out}} + G^{\mathrm{C}}$ $+6MN^{\mathrm{A}} + 6G^{\mathrm{S}}\left(N^{\mathrm{B}} + N^{\mathrm{C}}\right) + 3G^{\mathrm{C}}N^{\mathrm{D}}\big]$

4.5 Case Study

4.5.1 Parameters

This case study considers the construction of a new subsidiary administrative center in the Tongzhou region of Beijing. Fuel prices and converter parameters are taken from [146], with electricity being bought-back at 85% of the off-peak price. A power-to-gas converter is added, with an assumed capacity of 100 MW at a cost of 40 M¥ [157]. Increased prices of electricity during peak periods are in force from June 1st to September 31st. District heating is assumed to be available only from November 15th to March 15th each year. Heating, cooling, and electricity demand patterns as a function of outdoor temperature are adapted from [158]. Solar generation profiles and temperatures for Beijing are obtained from NREL's Typical Meteorological Year dataset [159]. The optimization horizon is 20 years, with fuel prices

increasing at 2% per year, energy demands at 4%, and a 10% discount rate. All investments are made at year zero.

Input capacity is assumed to cost 100 k¥/MW for each fuel, and PV capacity is assumed to cost 5 M¥/MW. Electricity storage capacity is assumed to cost \$1000/kW and \$50/kWh [160]. Thermal storage capacity is assumed to cost \$25/kW and \$25/kWh [161]. Bulk LNG storage capacity costs approximately \$250/MWh [162] and \$20,000/MW [163] (converted from tons, and tons/year). Since a campus-scale LNG facility is smaller than the export-scale facilities in [162, 163], specific costs are assumed to be greater by a factor of 10. All calculations are conducted in ¥, at a rate of 6.6 ¥/\$.

The carbon intensity of the district heating system is assumed to be 0.3 t/MWh [164]. The carbon intensity of natural gas is taken as 0.181 t/MWh, based on the chemical composition of methane. The carbon intensity of grid power is time-varying, based on the characteristics of the marginal generators [165]. For this case study, a range of marginal emission rates is obtained by running unit commitment problems for a modified ISO-NE test system [121], with wind generation providing 15% of the annual energy consumption.

Since solving the planning problem while modeling operations for each day of the year entails an excessively high amount of computation, a subset of representative days are selected using a modified k-means algorithm, where discrete variables are preserved and distances from clusters are evaluated based on the Z-score for each time-varying parameter. For this case study, a k value of 10 was chosen because it appears to balance computational complexity with descriptiveness, with at least one time period of negative marginal emissions. Short-term marginal emissions can be zero due to renewable spillage, or even negative due to transmission congestion.

4.5.2 Solution Methods

The model is implemented in GAMS 25.0 [94] and solved using CPLEX 12.8 [95] on machines with at least 16 cores, each running at at least 2 GHz, with at least 64 GB of RAM.

Using this combination of hardware and software, progress on closing the optimality

gap can be slow for the distinct builder/operator frameworks (Frameworks 3 and 4), as these problems are in general NP-hard [166]. Progress of branch and cut (B&C) solvers can generally be improved by providing the solver with a feasible warm start, to provide an upper limit for pruning branches and as a starting point for relaxation induced neighbor search heuristics [167]. A feasible solution for a problem with a given $E^{\max}$ can be used as a warm start for a problem with any greater value of $E^{\max}$ (a relatively relaxed problem).

Due to the binary representation of integer variables described in Section 4.4.2, solutions representing 'adjacent' integer values can be very different in terms of their binary components, and vice versa, which may hinder the effectiveness of neighbor-search heuristics built into B&C solvers. Therefore, a branch-and-cut-and-heuristic [168] process is implemented, in which incumbent solutions are periodically output to an accompanying heuristic which attempts to find a better feasible candidate to return to the B&C solver.

For a candidate solution with $E^{\text{operate}} < E^{\max}$, the set of adjacent solutions are first enumerated by perturbing the value of integer investment variables by one capacity step and then calculating the binary variable representation *a priori*. These candidate adjacent solutions ('neighbors') are then evaluated for network feasibility, emissions-constraint feasibility, and cost reduction by running the networks constraints (4.22)-(4.30) with investment variables fixed (an LP). If there are no adjacent solutions which meet the network feasibility constraint and emissions constraint at lower-cost, the heuristic halts. Otherwise, the feasible and lower-cost solutions are ranked in terms of their cost reduction per emissions-increase (neighbors with greater cost-reduction per emissions-increase are deemed 'better'). From this subset of neighbors, the 'best' candidate is chosen and the heuristic is repeated using that candidate as a starting point until a candidate is found for which there are no neighbors which meet the emissions and network feasibility constraints at lower cost. The lowest-cost emissions-feasible candidate is then returned to the B&C solver as a new incumbent solution.

The computational complexity of these neighbor searches depends on the definition of 'adjacent' solutions. If only one investment variable at a time is perturbed, the required number of LP solves will grow with $\mathcal{O}(n \cdot \Delta E)$, where n is the number of integer invest-

ment variables ($|M| + |G|$) and ΔE is the difference between the emissions at the current candidate and the emissions target. If instead, neighbors are enumerated by perturbing two investment variables simultaneously (*e.g.* the quantity of a particular type of converter is reduced while the capacity of a storage device is increased), the number of LP solves will grow with $\mathcal{O}(n^2 \cdot \Delta E)$; more neighbors are evaluated per heuristic iteration, providing potentially better performance per iteration at the expense of increased time per iteration.

4.5.3 Sampling the Pareto Frontier

In order to sample the Pareto frontier for the frameworks with direct emissions constraints (*i.e.* Frameworks 1 and 3), the minimum cost emissions-unconstrained solution can first be obtained to determine the baseline emissions, and then a set of emissions-limits can be calculated for a specified resolution (e.g. 100 points for 1% $E^{\max}$ resolution); these independent emissions-limit problems can then be solved in parallel.

Information from 'nearby' solutions can be used to improve knowledge about the optimality gap of the best known solution. For a given emissions target problem (A), if a solution for a tighter emissions-limit problem (B) is found with a lower cost than the currently best-known solution for problem (A), the cheaper solution from (B) be substituted for the currently best-known solution for (A), since a solution for a tighter problem (B) is always valid for a relaxed problem (A). Conversely, for a given emissions target problem (C), if a better lower bound is found for a more relaxed emissions-limit problem (D) is found, the lower bound from (D) can be substituted for the lower bound in (C), since the true optimum for a tightened problem (C) can only be greater than or equal to that of the relaxed problem (D).

In order to sample the Pareto frontier of the weighted-sum frameworks (*i.e.* Frameworks 2 and 4), the optimization problem can be solved for a range of carbon prices, *i.e.* the carbon tax rate in Framework 2 or the $SCoC$ rate for Framework 4. For a given carbon price, the best warm start from the set of previously found solutions can be evaluated by calculating the total cost (investment + operation + total carbon penalty) for the set of currently-known

solutions, and providing the solver with the lowest total cost solution as a warm start.

Several other solution techniques for bi-objective mixed-integer optimization problems also exist; [169] presents one based on the ϵ-*Tabu*-constraint method and also provides a review of several others.

4.5.4 Computational Performance

Frameworks 1 and 2 are solved to optimality for all emissions targets. When solving Framework 3, the performance of the MILP solver with the neighbor-search heuristic varies depends on the specified emissions target. For low emissions reductions targets, the problem can be solved to optimality; however, for moderate to aggressive targets CPLEX is found to stall in its progress in closing the optimality gap. For emissions reductions targets of up to 25%, CPLEX can solve to within 1% optimality gap. For emissions reductions targets of up to 50%, CPLEX can solve to within 6% optimality gap. The worst performance was found at an emissions reduction target of 72%: progress stalls with an optimality gap of 17%. Sample optimality gap trajectories are shown in Figure 4.5. Since the solution method for Framework 4 involves iterative solves of Framework 3, it suffers from the same computational challenges. To reduce the optimality gap further, the complexity of the case study must be reduced (see Table 4.1), more processing power must be applied to the model, or more time must be allowed for solver convergence (the latter two of which are typically available to policy makers).

4.6 Results

Fig. 4.6 shows the total costs of the optimal energy hubs chosen by Frameworks 1-4 as a function of emissions target. Framework 1 results in the cheapest operating costs for a given emissions target, because the investment and operational variables are optimized simultaneously and there is no cost for emissions. Framework 2 can be significantly more expensive than Framework 1 for mid-range emissions reduction targets, but at very high emissions reductions targets this gap approaches zero as the high tax rate incentivizes the lower-level

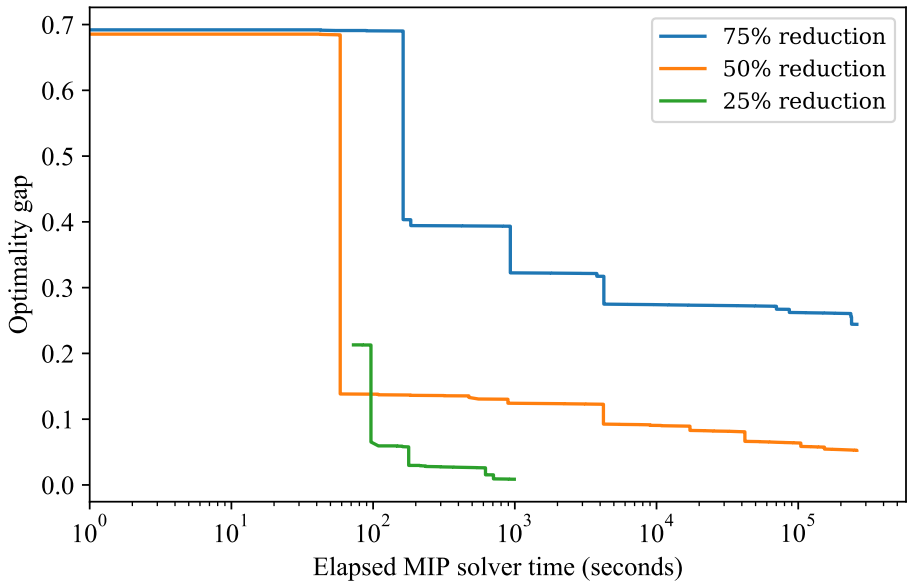

Figure 4.5: Optimality gap trajectories for selected emissions targets, Framework 3.

builder-operator to make investment and operating decisions with very low (or zero) carbon emissions. Framework 3 is not significantly more expensive than Framework 1 at modest emissions-reduction targets, but at aggressive emissions-reduction targets it is more expensive than both Framework 1 or Framework 2. In order to ensure that emissions decided by the lower-level operator do not exceed the target, the energy hub infrastructure must be 'overbuilt': built to be able to satisfy end-use demands while giving the operator few to no opportunities to use cheap but carbon-intensive energy sources. For a given emissions target, Framework 4 is as expensive or more expensive than Framework 3, since all of the constraints of the distinct Builder/Operator formulation still exist, but the upper-level regulator can only influence the investment decisions indirectly using the $SCoC$. This also creates large gaps between adjacent solutions. For example, no solutions are found with maximum annual emissions between 136 and 186 kilo-tons per year; any emissions target in this range must be met by imposing a high enough $SCoC$ to result in the (more expensive) 136 kilo-ton solution.

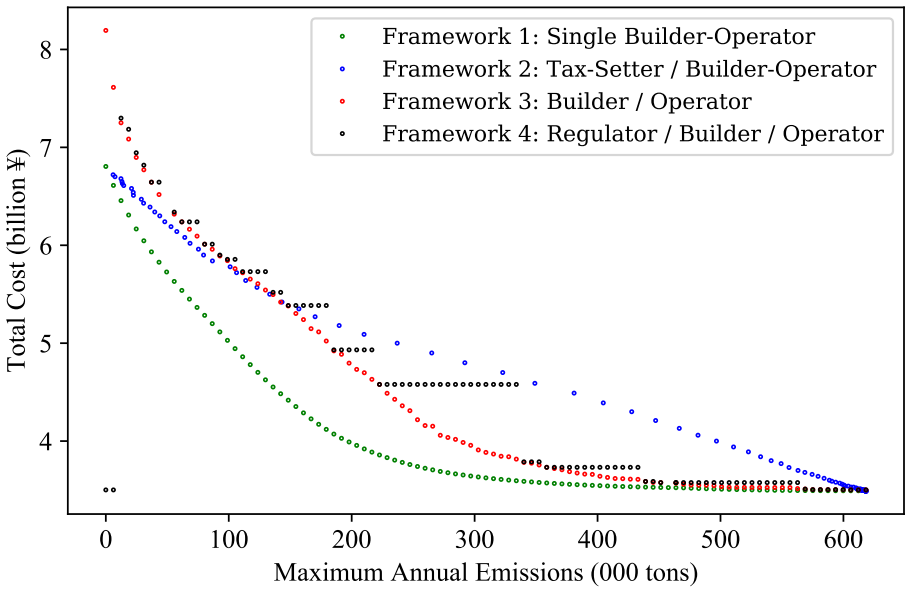

Figure 4.6: Comparison of cost/emissions Pareto frontiers for Frameworks 1-4.

4.6.1 Results for Framework 1: Single Builder-Operator

In the single builder-operator framework, the total cost of building and operating the hub grows from 3.49 B¥ when emissions are unconstrained (the 'base case') to 6.80 B¥ for a 100% emissions reduction target. Cost components for several milestone emissions targets are shown in Table 4.2. Much of the change in total cost occurs with aggressive emissions reductions targets, and consequently moderate emissions reductions targets are possible with only modest increases in total cost.

Fig. 4.7 shows the lifetime quantity of fuels flowing into the energy hub as a function of the emissions target. As the emission reduction target increases, the share of energy provided by electricity and district heat steadily declines. The changes in the costs components and in the fuel mix are significantly smaller in the 0% to 50% target range than in the 50% to 100% range. For moderate emissions reductions targets (up to approximately 65%) gas consumption increases. On the other hand, past this point gas consumption drops quickly, to virtually zero in the zero-net-emissions case. PV generation increases by only 23% between

Table 4.2: Framework 1: Costs of solutions as a function of emissions targets

Emissions reduction target	Total cost (B¥)	Investment cost (B¥)	Net operational cost (B¥)
None	3.49	1.64	1.85
25%	3.52	1.62	1.90
50%	3.62	2.13	1.50
75%	4.35	4.12	0.23
100%	6.80	8.39	-1.59

the base case and a 50% target reduction, but grows by 337% for a 100% target reduction.

Fig. 4.8 shows how the choice of equipment varies as a function of the emissions reduction target. No matter the desired emissions reduction target, the optimal investment decisions include at least one 40 MW compression-expansion refrigeration group (CERG), one 100 MW combined-heat-and-power unit (CHP), one 40 MW heat pump (HP), and two 20 MW water-absorption refrigeration groups (WARG). The investment in CHP peaks at 3 units at emission reduction targets of 55-65%, as the emissions created by burning gas are less than the emissions due to importing electricity and heat from the grid. Past this peak, the use of CHP declines and is replaced by electricity from PV generation and heat from heat pumps. The combination of HPs and WARGs is less efficient at converting electricity into cooling than CERGs, but the conversion to heat allows the use of intermediate thermal storage which is significantly cheaper than electricity storage. Storage allows end-use demands to be met with lower investments in input capacity and conversion equipment. Electric boilers are never chosen, and auxiliary boilers and power-to-gas units are only chosen for a few very aggressive emissions reduction targets.

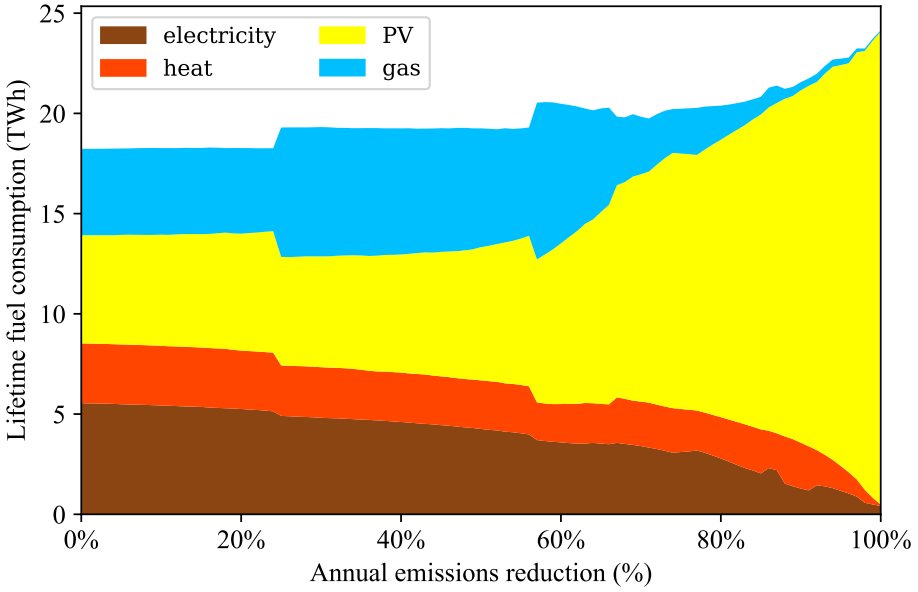

Figure 4.7: Fuel consumption as a function of emissions targets.

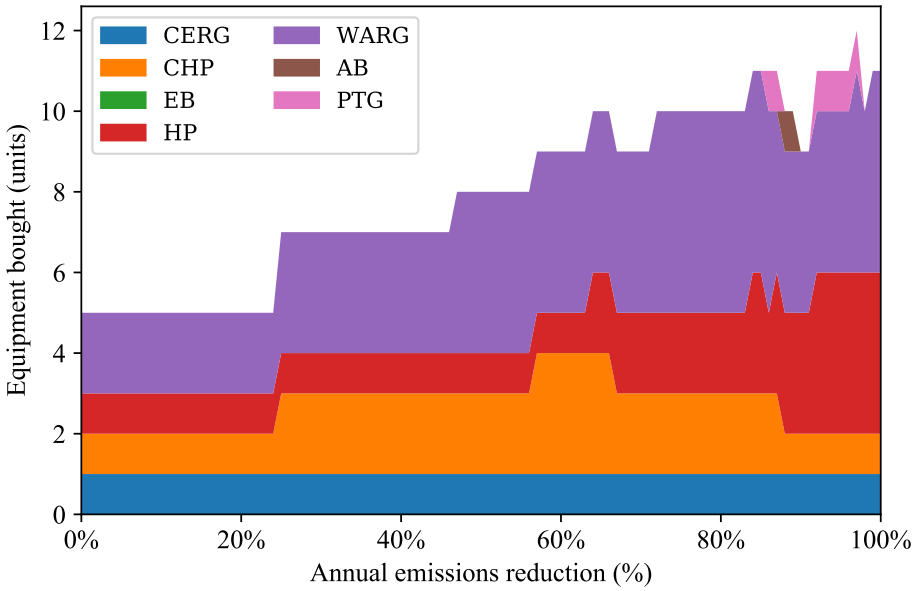

Figure 4.8: Equipment purchased as a function of desired emissions reduction. See Fig. 4.3 for abbreviations.

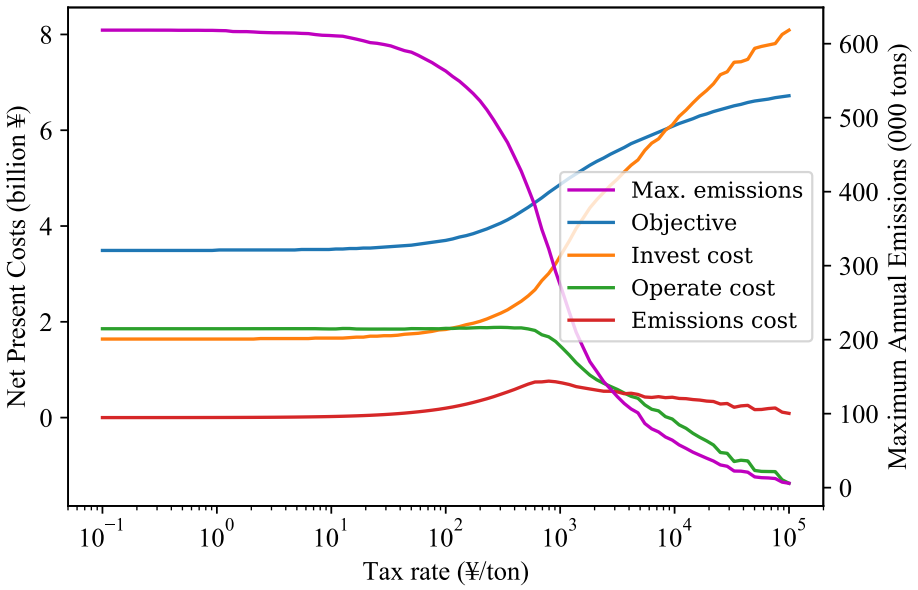

Figure 4.9: Costs and emissions as a function of carbon tax rate for Framework 2.

4.6.2 Results for Framework 2: Regulator / Builder-Operator

Fig. 4.9 shows the cost of each objective component and the resulting maximum emissions as a function of the carbon tax rate for the bi-level regulator/builder-operator framework. The majority of the emissions reductions are achieved at tax rates between 100 and 10,000 ¥/ton (15-1,500 $/ton). Table 4.3 indicates the tax rates required to achieve selected milestones.

4.6.3 Results for Framework 3: Builder / Operator

Fig. 4.6 and Table 4.4 show that when the hub operator cannot be trusted to cooperate to achieve emission reduction targets, the hub must be 'overbuilt' as compared to the cooperative scenario of Framework 1. For example, a target reduction of 50% in Framework 1 is achievable with a total cost of 3.62 B¥, of which 2.13 B¥ is for equipment purchases. On the other hand, when an operator who cares only about operating costs uses these equipment, the resulting emissions only decrease by 28.5%. To achieve the 50% reduction in Framework 3,

Table 4.3: Framework 2: Tax rates required to meet emissions goals

Emissions reduction target	Tax rate (¥/ton)	Total cost (B¥)	Investment cost (B¥)	Net operate cost (B¥)	Emissions cost (B¥)
None	N/A	3.49	1.64	1.85	0
5%	52	3.61	1.75	1.85	0.110
10%	112	3.73	1.87	1.86	0.217
25%	358	4.15	2.28	1.88	0.548
50%	842	4.74	3.10	1.64	0.753
75%	2,109	5.35	4.59	0.763	0.548
90%	9,988	6.10	6.21	-0.106	0.408

equipment costing 3.07 B¥ are needed, with a resulting total cost of 3.89 B¥. In effect, lack of cooperation between the builder and operator are responsible for an overall cost increase of 7% and an increase of 45% in construction costs.

4.6.4 Results for Framework 4: Regulator / Builder / Operator Framework

When an energy hub builder is forced to consider a social cost of carbon when designing an energy hub, more money is invested in more-expensive but less-polluting equipment. Table 4.5 shows the results for several emissions reductions benchmarks. When results from this emissions pricing framework are compared against results from the regulator/builder-operator framework (Table 4.3), it can be seen that emissions targets up to 50% can be realized at a lower total cost. This is due in part to the fact that the builder selects equipment as if emissions were taxed, but the operator doesn't actually have to pay the price for their emissions. At emissions reduction targets of 75% and higher, however, Framework 4 results in higher costs than Framework 2. Since the operator does not see the price of emissions, the hub must be 'overbuilt' to account for the operator's indifference toward emissions. The

Table 4.4: Comparing costs for equivalent targets in Frameworks 1 and 3

Emissions reduction target	Framework 1 cost (B¥)	Framework 3 cost (B¥)	Total cost increase	Investment cost increase
25%	3.52	3.57	1.3%	27.5%
50%	3.62	3.89	7.3%	44.6%
75%	4.35	5.30	21.8%	35.7%
100%	6.80	8.14	19.6%	33.8%

result is a hub with high PV capacity and no connection to the district heat or gas networks.

4.7 Discussion

The applicability of a policy framework to reduce carbon emissions from one or more greenfield energy hubs depends on the political-economic structure of the jurisdiction where the energy hubs are to be built. Framework 1 is the cheapest way to reach a given emissions target, but relies on the builder and operator's dedication to meeting the emissions target, during both construction and operation, when alternative investment and operation decisions are cheaper. Framework 2 is more effective at economically incentivizing the construction and operation of a hub able to meet emissions targets, because the cost of emissions is internalized. However, implementing carbon taxes can be politically risky and the total cost of construction and operation can be significantly higher than with Framework 1, especially for mid-range emissions reduction targets. Framework 3 is able to achieve emissions targets without the use of carbon taxes, even when the operator only pursues minimum cost operation, but the overall cost can be significantly higher for aggressive emissions reduction targets. Framework 4 is the most complex, but it enables a mandate that a carbon price be considered in investment decisions without requiring a politically sensitive carbon price to be paid during operation.

Table 4.5: Tax rates required to meet emissions goals in Framework 4

Emissions reduction target	SCoC rate (¥/ton)	Total cost (B¥)	Investment cost (B¥)	Net operate cost (B¥)	Total SCoC (B¥)
None	N/A	3.49	1.64	1.85	0
5%	5	3.50	1.79	1.71	0.034
10%	66	3.55	1.86	1.69	0.363
25%	87	3.58	2.12	1.45	0.448
50%	346	3.92	3.20	0.722	1.242
75%	794	5.49	6.39	-0.896	0.584
90%	2,754	6.31	7.76	-1.44	0.572

Carbon emissions targets are usually pledged on a per-year basis. A constraint on the maximum annual emissions (whether via an explicit constraint or via a strategic tax) may only bind against the emissions in a single year. However, the decisions made in order to meet commitments for the critical year (either infrastructure investment or tax rate) will also reduce emissions in all other years. Optimizing to constrain *lifetime* emissions is an alternate approach that would result in different investment and operation decisions, but is less compatible with the annual emissions pledges which are most common today.

4.8 Conclusion

This paper describes and illustrates four low-carbon energy hub design frameworks, using a new formulation of the network constraints for the greenfield energy hub problem. The single-actor cooperative framework results in the lowest overall cost for any given carbon emissions target, while the bi- and tri-level problems are more expensive due to the lack of cooperation from lower-level actors. Using these frameworks, the impact of various policy decisions on the construction and operation of energy hubs can be investigated. Policy questions which

can be aided by these frameworks include:

- How should campuses be compensated for electricity exported to the grid, based on their contributions of energy as well as reductions in grid emissions?
- What secondary effects can be anticipated in response to investments in new grid-scale electricity and district heat assets, which will change the price and carbon intensity of grid-sourced energy?
- To what extent do limitations in regional energy transmission reduce the ability of energy hubs to meet emissions targets, or increase their cost of doing so?

Holistically investigating questions such as these can bring society closer to affordable, sustainable power systems.

Nomenclature

Abbreviations and Symbols

tCO_2e	Metric tons of greenhouse gases (GHG) converted to CO_2 equivalent.
¥	Chinese yuan (RMB).

Sets and indices

G	Set of equipment (power conversion and storage devices), indexed by g.
G^{C}	Set of power conversion devices ($G^{\mathrm{C}} \subset G$).
G^{S}	Set of storage devices ($G^{\mathrm{S}} \subset G$).
L	Set of branch flows, indexed by l.
M	Set of energy types, indexed by m.
N^{A}	Set of input power capacity discretization binaries, indexed by n^a.
N^{B}	Set of storage energy discretization binaries, indexed by n^b.

N^{C} Set of storage power discretization binaries, indexed by n^c.

N^{D} Set of converter count discretization binaries, indexed by n^d.

P Set of equipment ports, indexed by p.

P^{out} Set of equipment output ports ($P^{\mathrm{out}} \subset P$).

P_g Set of ports of equipment g ($P_g \subset P$).

S Set of representative days, indexed by s.

T Set of time periods, indexed by t.

Y Set of years, indexed by y.

Topology Matrices

$\boldsymbol{A}$ Network topology matrix, dimension $(P \times L)$. When subscripted, $\boldsymbol{A}_g$ refers to the rows of the matrix corresponding to the ports of equipment g.

$\boldsymbol{H}$ Converter efficiency matrix, dimension $(P^{\mathrm{out}} \times P)$. When subscripted, $\boldsymbol{H}_g$ refers to the rows of the matrix corresponding to the output ports of equipment g.

$\boldsymbol{J}$ 'Limiting' port matrix, dimension $(G \times P)$.

$\boldsymbol{K}$ Branch directionality vector, dimension (L).

$\boldsymbol{U}$ Input port matrix, dimension $(M \times L)$.

$\boldsymbol{W}$ Output port matrix, dimension $(M \times L)$.

$\boldsymbol{Z}$ Network efficiency matrix, dimension $(P^{\mathrm{out}} \times L)$.

Topology matrix values are defined in Appendix A.

Fixed Parameters

C_g^{unit} Cost of one piece of equipment of energy conversion device g (¥).

C_g^{power} Per-unit cost of power for storage device g (¥/MW).

C_g^{energy} Per-unit cost of energy for storage device g (¥/MWh).

C_m^{cap} Cost of input capacity for energy m (¥/MW).

$E^{\max}$ Annual GHG emissions limit (tCO_2e).

i Discount rate for calculating net-present value.

Δt Time interval length (hours).

π_s Probability of representative day s.

Time-Varying Energy Parameters

Subscripted $_{m,s,t,y}$ for energy m at time t on day s in year y.

$\boldsymbol{B}$ Power availability of input energy relative to its input capacity. For electricity generated by renewable sources, $0 \leq B_{m,s,t,y} \leq 1$. For seasonally available energy flows (*e.g.* district heating), $B_{m,s,t,y} \in \{0, 1\}$. For all other energy flows, $B_{m,s,t,y} = 1$.

$\boldsymbol{e}$ Marginal emissions rate (tCO_2e/MWh).

$\boldsymbol{f}$ Input energy price (¥/MWh).

$\boldsymbol{h}$ Grid energy feed-in price (¥/MWh).

$\boldsymbol{L}$ End-use power demand (MW).

Carbon Pricing Variables

P^{CO_2} Tax rate for GHG emissions (¥/tCO_2e).

$SCoC$ Social cost of carbon rate (¥/tCO_2e).

Investment Variables

C^{invest} Total investment cost (¥).

$D_g^{\max}$ Rated power for equipment g, for one piece of equipment for conversion devices, or total capacity for storage devices (MW).

I_g Number of pieces of equipment purchased for energy conversion device g.

$P_m^{\max}$ Purchased input power capacity for energy m (¥).

$Q_g^{\max}$ Purchased energy capacity for storage device g (MWh).

Operational Variables

Hub operations during each representative day s in each year y are independent, so these indices are omitted when possible for brevity.

C^{operate} Hub operating cost (¥).

E^{operate} GHG emissions from hub operation (tCO_2e).

$P_{m,t}$ Power flow into the energy hub from the grid for energy m at time t (MW).

$Q_{g,t}$ State of charge of storage device g at time t (MWh).

$r_{m,t}$ Power flow out of the energy hub to the grid for energy m at time t (MW).

T^{operate} Tax bill for GHG emissions (¥).

$V_{l,t}$ Power flow within the energy hub for branch l at time t (MW).

Dual Variables

$\alpha_{p,t}$ Dual variable for network power balance constraints at port p during time t.

$\beta_{g,t}$ Dual variable for conservation of energy constraints for storage device g at time t.

$\underline{\gamma}_{g,t}, \overline{\gamma}_{g,t}$ Dual variables for {lower, upper} state of charge constraint for storage device g at time t.

$\zeta_{g,t}$	Dual variable for maximum power constraints for converter g at time t.
$\underline{\kappa}_{g,t}, \overline{\kappa}_{g,t}$	Dual variables for {lower, upper} power constraint for storage device g at time t.
$\rho_{m,t}$	Dual variable for input capacity constraints for energy flow m at time t.
$\mu_{m,t}$	Dual variable for hub outflow constraints for energy flow m at time t.
$\underline{\phi}_{m,t}, \overline{\phi}_{m,t}$	Dual variables for {lower, upper} grid sales constraint for energy flow m at time t.
$\sigma_{l,t}$	Dual variable for branch flow non-negativity constraint for branch l at time t.

Chapter 5

PROFITABLE EMISSIONS-REDUCING ENERGY STORAGE

5.1 Introduction

Increasing the penetration of renewable energy is a popular solution to decarbonization of power systems; for example, many jurisdictions have renewable portfolio standards, and pricing of greenhouse gas (GHG) emissions incentivizes more installation of renewable generation. However, the most abundant sources of cost-effective renewable energy–wind and solar photovoltaic–suffer from uncertainty and variability in their power production. Grid-scale energy storage is often seen as a promising solution for the intermittency of renewable resources, and therefore a valuable contribution towards broader decarbonization efforts (in combination with other approaches such as demand response). Unfortunately, while storage *can* be used to reduce the carbon intensity of power system operations, studies have shown that under current market structures and generation mixes the use of energy storage can increase overall GHG emissions. In the absence of a price on GHG emissions, estimates of the impact include a range of 104-407 kg/MWh for grid-scale storage [170] and 75-270 kg/MWh for behind-the-meter storage [171]. This paper investigates the impact of an emissions-neutrality constraint on investment in storage and the resulting power system emissions.

The modeling of energy storage operation and its impact on grid emissions has been studied using a wide variety of power systems models and modes of energy storage participation; consequently, findings on emissions impacts are varied as well.

Energy storage has been modeled as providing energy [172, 173, 174, 175, 176, 170, 177, 178, 179], reserves [180, 181, 182], or both energy and reserves [183, 184, 185, 171, 186, 187]. Storage providing energy has been shown to be capable of increasing emissions [172, 173, 174, 175], or can either increase or decrease emissions depending on charge-scheduling heuristics

[178, 177, 176] and generation mixture [178, 177, 170, 179]. In [173], higher penetrations of renewables amplify this emission-increasing effect. Storage providing reserves has been shown to be capable of increasing emissions [181], decreasing emissions [180], or can either increase or decrease emissions depending on reserve quantity, storage quantity, and reserve scheduling rules [182]. Storage providing both energy and reserves has been shown to be capable of increasing emissions [187, 171], decreasing emissions [183, 185, 184], or can either increase or decrease emissions depending on changing generation mixes [186]. In [187], emissions are increased even in the presence of a 30 €/ton price on GHG emissions, although increasing wind penetration mitigates this effect.

When modeling storage's participation in power systems, many studies have treated the system's marginal emissions rate as fixed, and determined exogenously [178, 180, 174, 170, 171, 179, 175, 176]. This may be a reasonable approximation for small-scale energy storage, but larger quantities of energy storage will have the ability to change the marginal unit(s) of generation. More sophisticated approaches use an economic dispatch model [177, 173, 182] or a unit commitment [185, 187, 184, 186, 181, 183, 172]. Inclusions of the transmission network as in [184, 182, 181, 183, 172] is also significant, as locationality affects storage operations in a transmission-constrained system.

Previous work has investigated the emissions impact of storage participating in a market environment, but hasn't looked at how a daily emissions-neutrality constraint can impact storage investment decisions and resulting emissions. Lin *et al.* [182] introduces an emissions-neutrality constraint for storage providing reserves, but only considers single-period economic dispatch, and do not assess the impact on storage profitability. Several papers have investigated storage expansion planning for low-carbon emissions goals [188, 189, 190], but they do not address the emissions impact of adding storage to current market environments or storage profitability. A comprehensive review of storage expansion planning for low-carbon power systems is given in [191].

By contrast, this paper investigates the impact of an emissions-neutrality constraint (ENC) on the profitability of various quantities of storage, and therefore the optimal quantity

of storage to invest in, and finally the resulting GHG emissions impact. Profitability is assessed from two merchant storage perspectives: a profit-maximizing storage investor (PMSI) or a 'philanthropic' investor (PhSI) who only requires a specified minimum return on investment to cover installation costs. An example of an entity which may want to participate as a philanthropic storage investor would be a government with an interest in reducing costs and/or emissions from the power system in its jurisdiction while participating in a competitive energy market. Alternatively, a philanthropic emissions-neutral storage investor may be a public-private partnership; a governmental organization may offer low-cost financing, tax incentives, or other cost-reducing measure to a private storage investor in exchange for a commitment to offer storage dispatch control to the system operator with an ENC. These merchant energy storage perspectives are compared with a vertically-integrated utility (VIU) perspective, concerned only with overall costs and not storage profitability.

Though investments in energy storage by a system operator or a PMSI have reciprocal impacts on profitability [192], in this framework we look at just one or the other in order to more clearly see the impact of the ENC. Although storage may earn revenue by participating in reserves, including reserves in power systems modeling introduces sensitivity to required reserves quantity and scheduling rules [182]. Therefore, reserves are omitted in order to focus on how an ENC impacts a system where energy participation can increase emissions.

The specific contributions of this paper are:

- The formulation of two bi-level models ('philanthropic' and 'profit-maximizing') to optimize merchant storage investments in light of emissions-neutrality constraints in commitment and dispatch.

- Development of a heuristic to quickly obtain good feasible solutions to this inherently non-convex and computationally difficult problem.

- Analysis of solution quality of the 'philanthropic' problem using a relaxation that allows the evaluation of solution quality with reduced computational burden.

- Demonstration of these methods on a detailed case study.

- Sensitivity analysis showing the effect of governmental incentives or taxes on the optimal quantity of energy storage and the resulting operational impacts.

5.1.1 Organization

The rest of this chapter is organized as follows: Section 5.2 describes the power system model, Section 5.3 describes the various storage investor optimization perspectives, Section 5.4 presents heuristics to find good solutions to these computationally difficult bi-level problems, Section 5.6 describes a test system used to evaluate the impact of the emissions-neutrality constraint, Section 5.7 presents the results, and 5.8 concludes. Appendix A provides the formulation of the dual problem of transmission-constrained economic dispatch, and a nomenclature section follows at the end of the chapter.

5.2 Power System Model

A transmission-constrained unit commitment formulation is used to model a system operator's choice of online generators, the dispatch quantities of generators and energy storage, and the resulting prices. This formulation is embedded into a multi-level optimization model used by an energy storage investor to decide the quantities and locations to install storage.

5.2.1 System Operational Constraints

Operational constraints for the system operator's unit commitment problem are given in (5.1)-(5.13). The constraints in this section apply for each representative day $a \in A$, however the index a is omitted for brevity. Dual variables for each dispatch constraint are given in parentheses to the right of the equation.

$$v_{i,t} - z_{i,t} = u_{i,t} - u_{i,t-1} \,;\, \forall i \in I, t \in T \tag{5.1}$$

$$\sum_{\tau=t-\mathrm{g}_i^{\mathrm{up}}+1}^{t} v_{i,\tau} \leq u_{i,t}\,;\, \forall t \in T, i \in I \tag{5.2}$$

$$\sum_{\tau=t-\mathrm{g}_i^{\mathrm{down}}+1}^{t} z_{i,\tau} \leq 1 - u_{i,t}\,;\, \forall t \in T, i \in I \tag{5.3}$$

$$0 \leq g_{i,s,t} \leq g_{i,s}^{\max} u_{i,t} \quad \forall i \in I, s \in S, t \in T \quad \left(\underline{\delta}, \overline{\delta}\right) \tag{5.4}$$

$$0 \leq s_{b,t}^{\mathrm{ren}} \leq w_{b,t} \quad \left(\underline{\phi}, \overline{\phi}\right) \tag{5.5}$$

$$Q_{b,t} = Q_{b,t-1} + \eta J_{b,t}^{\mathrm{chg}} - \frac{1}{\eta} J_{b,t}^{\mathrm{dis}} \quad \forall b \in B, t \in T \quad (\kappa) \tag{5.6}$$

$$0 \leq Q_{b,t} \leq Q_b^{\max} \quad \forall b \in B, t \in T \quad \left(\underline{\xi}, \overline{\xi}\right) \tag{5.7}$$

$$0 \leq J_{b,t}^{\mathrm{chg}} \leq J_b^{\max} \quad \forall b \in B, t \in T \quad \left(\underline{\rho}^{\mathrm{chg}}, \overline{\rho}^{\mathrm{chg}}\right) \tag{5.8}$$

$$0 \leq J_{b,t}^{\mathrm{dis}} \leq J_b^{\max} \quad \forall b \in B, t \in T \quad \left(\underline{\rho}^{\mathrm{dis}}, \overline{\rho}^{\mathrm{dis}}\right) \tag{5.9}$$

$$\sum_{i \in I} m_{i,b}^{\mathrm{unit}} g_{i,t} + J_{b,t}^{\mathrm{dis}} - \sum_{l \in L} m_{l,b}^{\mathrm{line}} f_{l,t} + w_{b,t} - s_{b,t}^{\mathrm{ren}} =$$

$$d_{b,t} + J_{b,t}^{\mathrm{chg}}\,;\, \forall b \in B, t \in T \quad (\lambda) \tag{5.10}$$

$$f_{l,t} = y_l \sum_{b \in B} m_{l,b}^{\mathrm{line}} \theta_{b,t}\,;\, \forall l \in L, t \in T \quad (\beta) \tag{5.11}$$

$$-f_l^{\max} \leq f_{l,t} \leq f_l^{\max}\,;\, \forall l \in L, t \in T \quad \left(\underline{\gamma}, \overline{\gamma}\right) \tag{5.12}$$

$$E^{\mathrm{total}} \leq \chi E^{\mathrm{baseline}} \quad (\alpha) \tag{5.13}$$

$$g_{i,t} := g_i^{\min} u_{i,t} + \sum_{s \in S} g_{i,s,t}\,;\, \forall i \in I, t \in T$$

$$E^{\mathrm{total}} := \sum_{i \in I} \sum_{t \in T} \left(E_i^{\min} u_{i,t} + E_i^{\mathrm{su}} v_{i,t} + \sum_{s \in S} h_{i,s} g_{i,s,t} \right)$$

Eqs. (5.1)-(5.3) constrain the generator commitment variables. Eq. (5.1) relates status, startup, and shutdown variables ($u_{i,t}$, $v_{i,t}$, $z_{i,t}$, respectively). Eq. (5.2) ensures that minimum up-times are respected, while (5.3) ensures that minimum down-times are respected. Generator heat rate curves are represented by piecewise-linear segments. Eq. (5.4) constrains the power in each segment $g_{i,s,t}$ to its segment capacity limit $g_{i,s}^{\max}$. Renewable spillage $s_{b,t}^{\mathrm{ren}}$ is constrained in (5.5) to be non-negative and not more than the maximum renewable generation available $w_{b,t}$. Energy storage charging $J_{b,t}^{\mathrm{chg}}$ and discharging $J_{b,t}^{\mathrm{dis}}$ are constrained in

(5.6)-(5.9), where (5.6) tracks the state-of-charge of energy storage $Q_{b,t}$, (5.7) constrains the state-of-charge based on energy capacity $Q_b^{\max}$, and (5.8)-(5.9) constrain charging and discharging based on power capacity $J_b^{\max}$. Storage charge and discharge efficiency are given by η. The transmission network is represented by the DC power flow model in (5.10)-(5.12). Network topology is defined by matrices $m_{i,b}^{\text{unit}}$ for generators and $m_{l,b}^{\text{line}}$ for transmission lines. Eq. (5.10) ensures power balance at each node in the network, (5.11) relates flows $f_{l,t}$ to bus angles $\theta_{b,t}$ via line admittances y_l, and (5.12) constrains each line's power flow to its maximum magnitude $f_l^{\max}$. Finally, (5.13) represents the emissions-neutrality constraint (ENC), ensuring that GHG emissions E^{total} (based on generator emissions at minimum power $E_i^{\min}$, startup emissions E_i^{su}, and marginal emissions rates $h_{i,s}$) are not increased, relative to the emissions of the baseline (no-storage) solution E^{baseline}. To solve with a non-binding ENC, the value of χ is set to a large constant.

5.2.2 System Operator's Problem

The goal of the system operator is to minimize the total cost of supplying the demand of the system C^{gen} (based on generator cost at minimum power $C_i^{\min}$, startup costs C_i^{su}, and marginal costs $b_{i,s}$), subject to the operational constraints; this problem is formalized in (5.14)-(5.15).

$$\min_{\Omega^{\text{C}},\Omega^{\text{D}}} C^{\text{gen}} \tag{5.14}$$

$$C^{\text{gen}} := \sum_{t\in T}\sum_{i\in I}\left(C_i^{\min}u_{i,t} + C_i^{\text{su}}v_{i,t} + \sum_{s\in S} b_{i,s}g_{i,s,t}\right)$$

subject to:

$$\text{Eqs. (5.1)-(5.13)} \tag{5.15}$$

5.3 Investment Models

The question of how much storage is 'optimal' to install depends on the perspective taken. The simplest case is for a vertically-integrated utility (VIU), whose only objective is minimizing overall social cost. This perspective is simplest as decisions on storage investment Ω^{S}, generator commitment Ω^{C}, and dispatch Ω^{D} are conducted simultaneously. This perspective is formalized in (5.16)-(5.17). Storage investment costs are determined by the amoritized per-MWh storage energy cost c^{Q} and per-MW storage power cost c^{J} for a given storage quantity, while π_a represents the frequency of each representative day.

$$\min_{\Omega^{\mathrm{C}},\Omega^{\mathrm{D}},\Omega^{\mathrm{S}}} C^{\mathrm{batt}} + \sum_{a\in A} \pi_a C_a^{\mathrm{gen}} \tag{5.16}$$

subject to:

$$\text{Eqs. (5.1)-(5.13)} \tag{5.17}$$

$$C^{\mathrm{batt}} := \sum_{b\in B} \left(c^{\mathrm{Q}} Q_b^{\max} + c^{\mathrm{J}} J_b^{\max}\right)$$

This is contrasted with a centralized power market structure, in which a storage investor earns revenue based on locational marginal prices (LMPs), obtained from the commitment and dispatch solution determined by the system operator. A storage owner's net profit is determined by LMPs $\lambda_{b,t,a}$, power dispatch, and storage investment costs C^{batt}, as in (5.18).

$$Profit := \sum_{a\in A}\left[\pi_a \sum_{b\in B}\sum_{t\in T} \lambda_{b,t,a}\left(J_{b,t,a}^{\mathrm{dis}} - J_{b,t,a}^{\mathrm{chg}}\right)\right] - C^{\mathrm{batt}} \tag{5.18}$$

A purely self-interested storage investor would have the sole objective of choosing storage investments to maximize their net profit, while LMPs are determined by a lower-level system operator determining unit commitment and dispatch. This perspective is formalized in (5.19)-(5.20), and is referred to as the profit-maximizing storage investor (PMSI). Although owners of large geographically-dispersed storage installations may coordinate bids to maximize their energy-market profit [193], the PMSI formulation assumes that once the storage investments

are made, the energy market is competitive enough to be modeled with a cost-minimization problem.

$$\max_{\Omega^{\mathrm{S}}} Profit \tag{5.19}$$

subject to:

$$\boldsymbol{\lambda} \in \arg \min_{\Omega^{\mathrm{C}},\Omega^{\mathrm{D}}} \left\{ C^{\mathrm{gen}}; \text{subject to: Eqs. (5.1)-(5.13)} \right\} \tag{5.20}$$

By contrast, there may be a storage investor who is less concerned with maximizing net profit than with lowering the overall social cost, subject to the constraint that enough energy market revenue is collected to cover the annualized investment cost [194]. We refer to this perspective as a 'philanthropic' storage investor (PhSI). Entities which may take this perspective include governmental or not-for-profit entities participating in a competitive energy market. This perspective is formalized in (5.21)-(5.23). Both the PMSI and PhSI are bi-level optimization problems, and are illustrated in Fig. 5.1.

$$\min_{\Omega^{\mathrm{S}}} C^{\mathrm{batt}} + \sum_{a \in A} \pi_a C_a^{\mathrm{gen}} \tag{5.21}$$

subject to:

$$Profit \geq 0 \tag{5.22}$$

$$C^{\mathrm{gen}}, \boldsymbol{\lambda} \in \arg \min_{\Omega^{\mathrm{C}},\Omega^{\mathrm{D}}} \left\{ C^{\mathrm{gen}}; \text{subject to: Eqs. (5.1)-(5.13)} \right\} \tag{5.23}$$

5.4 Solution Method

Solving the VIU perspective is a relatively straightforward MILP problem, since all decisions are made in a single level. However, the inclusion of energy market profit in the bi-level models complicates the solution process, since storage investment decisions influence energy market prices and energy market prices influence storage investment decisions. Bi-level optimization problems are inherently non-convex and NP-hard, even with a linear lower level

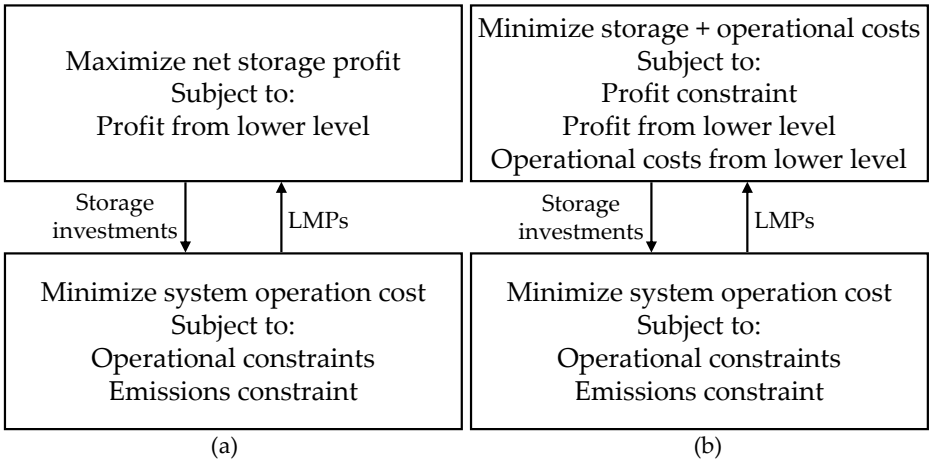

Figure 5.1: Bi-level formulations of merchant energy storage: (a) a profit-maximizing storage investor, (b) a 'philanthropic' storage investor.

[166]; problems where the lower level is non-convex (*e.g.* unit commitment) are even more challenging. For the purpose of this paper, we develop an iterative heuristic (Alg. 1) in order to determine good candidate solutions to both bi-level problems in a reasonable amount of time. The quality of these solutions is evaluated in Section 5.5.

All storage quantities between zero and the optimal VIU quantity are evaluated, and the resulting net storage profit and social cost for each quantity are evaluated once the unit commitment is solved. Finally, the profitable storage quantity with lowest social cost is chosen as the best candidate for the PhSI case, and the storage quantity with greatest net profit is chosen as the best candidate for the PMSI case.

Algorithm 1 Heuristic solution algorithm

1: DEFINE(VIU model, Lower-level model)
2: $q^{\max} \leftarrow \infty$ ▷ q is the system's total storage quanta
3: SOLVE(VIU model)
4: RECORD(q, NetStorageProfit, SocialCost)
5: $q^{\max} \leftarrow (q-1)$
6: **for** $i \leftarrow 1$ **to** $q^{\max}$ **do**
7: FIX($q = i$)
8: SOLVE(Lower-level model)
9: RECORD(q, NetStorageProfit, SocialCost)
10: **end for**
11: $q^{\text{philanthropic}} \leftarrow$SELECT($q$)
$q \in \{\text{argmin SocialCost}(q), \text{NetStorageProfit}(q) \geq 0\}$
12: $q^{\text{profit-max}} \leftarrow$SELECT($q \mid q \in \text{argmax NetStorageProfit}(q)$)

5.5 Assessing Solution Quality

As the PhSI and PMSI problems are inherently non-linear and non-convex, evaluating the quality of candidate solutions (relative to a global lower bound) is not straightforward. However, there are two MILP relaxations of the PhSI problem, which can be used to find an upper bound for the optimality gap of candidate solutions. The first is the simply the VIU, since the profit constraint and the lower-level optimality constraint are both relaxed. The second relaxes the lower-level optimality constraint on the unit commitment variables to create a formulation which can be transformed into a profit-constrained single-level equivalent (PCSLE).

5.5.1 Creating a Profit-Constrained Single-Level Equivalent

Though the PhSI objective (5.21) and operational constraints (5.1)-(5.13) can be formulated as a single-level MILP problem, the profit definition (5.18) contains both primal and dual decision variables; therefore, these variables must be optimized simultaneously. The system operator's unit commitment problem is necessarily non-convex due to binary commitment variables; strong duality does not in general hold for non-convex problems. However, if the binary variables and constraints are moved to the upper-level of the bi-level formulations described in Section 5.4, the lower level becomes a transmission-constrained economic dispatch (TCED) problem, which can be represented linearly using the DC power flow approximation. A linear (and therefore convex) lower-level problem can be replaced by a series of constraints in an upper-level problem, creating a single-level equivalent of the profit-constrained storage investment problem [194].

Moving the binary variables and constraints from the lower-level to the upper-level represents a relaxation of the original bi-level problem, since the values of the binary variables are no longer constrained by the lower-level unit commitment problem, and no additional constraints are introduced. Therefore, the best lower bound on the relaxed problem provides a lower bound for the best value of the original PhSI problem.

Since the original TCED problem is linear, strong duality is guaranteed, so the value of the primal and dual objective functions are equal for a set of primal and dual variables (Ω^{λ}) that are primal and dual optimal, respectively. The dual problem of the TCED is described in Appendix A. The strong duality constraint for the TCED problem is given in (5.24). Although this single-level equivalent contains bi-linear terms, Section 5.5.2 demonstrates how a MILP approximation can be obtained, which can provide a lower-bound on the optimum.

$$\hat{C}^{\text{dual}} = \hat{C}^{\text{primal}} := \sum_{i \in I} \sum_{s \in S} \sum_{t \in T} b_{i,s} g_{i,s,t} \tag{5.24}$$

Therefore, the profit-constrained single-level equivalent of the relaxed PhSI problem is given by the original objective function (5.25), the upper-level profit constraint (5.26), unit

commitment constraints (5.27), and lower-level constraints (5.28)-(5.30).

$$\min_{\Omega^{\mathrm{C}},\Omega^{\mathrm{D}},\Omega^{\mathrm{S}},\Omega^{\lambda}} C^{\mathrm{batt}} + \sum_{a\in A} C_a^{\mathrm{gen}} \tag{5.25}$$

subject to:

$$\text{Equation (5.22)} \tag{5.26}$$

$$\text{Equations (5.1)-(5.3)} \qquad \forall a \in A \tag{5.27}$$

$$\text{Equations (5.4)-(5.13)} \qquad \forall a \in A \tag{5.28}$$

$$\text{Equation (5.24)} \qquad \forall a \in A \tag{5.29}$$

$$\text{Equations (5.35)-(5.41)} \qquad \forall a \in A \tag{5.30}$$

5.5.2 Creating a MILP Approximation

The profit-constrained single-level equivalent presented in (5.25)-(5.30) contains several nonlinear terms. The profit definition (5.18) contains the product of continuous lower-level dual variables ($\boldsymbol{\lambda}$) and primal variables ($\boldsymbol{J}^{\mathrm{chg}}, \boldsymbol{J}^{\mathrm{dis}}$), while the strong duality constraint contains products of continuous lower-level dual variables and upper-level binary and continuous variables. First, the profit constraint can be converted from a product of lower-level primal and dual variables to a product of lower-level dual and upper-level variables using complementary slackness conditions, as shown in (5.31) [194].

$$\sum_{b\in B}\sum_{t\in T} \lambda_{b,t,a}\left(J^{\mathrm{dis}}_{b,t,a} - J^{\mathrm{chg}}_{b,t,a}\right) = \sum_{b\in B}\sum_{t\in T}\left[Q_b^{\max}\overline{\xi}_{b,t} + J_b^{\max}\left(\overline{\rho}^{\mathrm{dis}}_{b,t} + \overline{\rho}^{\mathrm{chg}}_{b,t}\right)\right] \tag{5.31}$$

Next, the continuous upper-level variables $Q_b^{\max}$ and $J_b^{\max}$ can be approximated by integer variables representing discrete storage quantities. These integer variables can be equivalently represented by a summation of binary variables in order to convert the products of integer and

continuous variables to the products of binary and continuous variables. A binary expansion is used in (5.32)-(5.33) to reduce dimensionality as compared to a unary expansion. Although the representation of integer variables by a binary expansion is not in general more efficient than an integer representation [195], this allows the use of the big-M method, and has been shown to be more effective than non-linear solvers or the use of McCormick envelopes in solving bi-linear problems containing the product of continuous and integer variables in constraints [196].

$$Q_b^{\max} \approx \sum_n 2^n x_{b,n}^a \Delta Q \tag{5.32}$$

$$J_b^{\max} \approx \sum_n 2^n x_{b,n}^b \Delta J \tag{5.33}$$

After discretization and binary expansions of the storage variables, the only non-linear terms remaining are products of continuous lower-level dual variables and upper-level binary variables. These products are linearized using the big-M approximation method, and the problem reduces to a MILP approximation of the original non-linear problem.

5.5.3 Limitations of the Single-Level MILP Approximation

Although the MILP approximation of the original bi-level problem provides a relaxation which can assess the quality of the heuristic-found solutions, this formulation is not without its drawbacks: first and foremost is computational tractability. As mentioned in Section 5.4, single-level equivalents of bi-level problems are inherently NP-hard. In practice, solving problems with big-M approximations can be challenging, as the values of M must be large enough to capture the full range of the continuous variables, but values which are too large cause difficulties for MILP solvers.

Second, as the MILP formulation is a relaxation, it may include integral solutions which are cheaper than the heuristic-found solution, but are not valid solutions to the original bi-level problem. A storage quantity which is not found to be profitable in the original bi-level

problem may be profitable in this single-level relaxation, since unit commitment variables are no longer constrained to be part of the minimum-cost solution of the original lower-level problem. In essence, the single-level equivalent assumes that all decisions (storage quantity, unit commitments) are made simultaneously, and so a storage quantity which would lower total costs but otherwise be unprofitable can be made profitable by selection of a sub-optimal unit commitment solution. Therefore, the true optimum of the original bi-level problem may be greater than than the best lower-bound found by the single-level equivalent, and therefore the optimality gap for a given heuristic-found solution can only overestimate the true optimality gap.

5.6 Case Study

A case study is conducted using the Reliability Test System of the Grid Modernization Laboratory Consortium (RTS-GMLC) [197]. The RTS-GMLC is based on the 1996 IEEE Reliability Test System, with an updated generation fleet, the addition of renewable generation, and 365 days of hourly profiles for load and renewable generation. This system has a high penetration of renewables: over the course of the year, hydro represents 10.8% of total energy demand, utility-scale solar PV 10.0%, rooftop PV 5.7%, and wind 19.0%.

For the planning problem, a set of five representative days is developed by using a k-means clustering algorithm on the 365 daily profiles, after their dimension was reduced by principal component analysis [198]: 95% of variance is captured via 13 principal components. When transforming the representative days back to full dimension, negative values of load or renewable generation are clipped to 0. Multi-period constraints in the system operator's problem (i.e. (5.1)-(5.3), (5.6)) are enforced cyclically; initial conditions are not assumed *a priori*, but assumed to reflect the end of the current day [53], and the net load in the first and last hours of the day are smoothed to avoid introducing unrealistic midnight ramps.

Dimensionality of the storage investment problem is reduced by fixing the storage power and energy ratios at a 4-hour duration, and by limiting storage investment to 10 candidate buses (out of the original 72); these candidate buses were selected by collecting a pool of

candidate solutions to the VIU planning problem, and selecting all buses which had storage investment in any candidate solution. Each optimization problem was solved to an optimality gap of 0.1% or better, and the heuristic algorithm typically completed within 4 hours.

5.7 Results

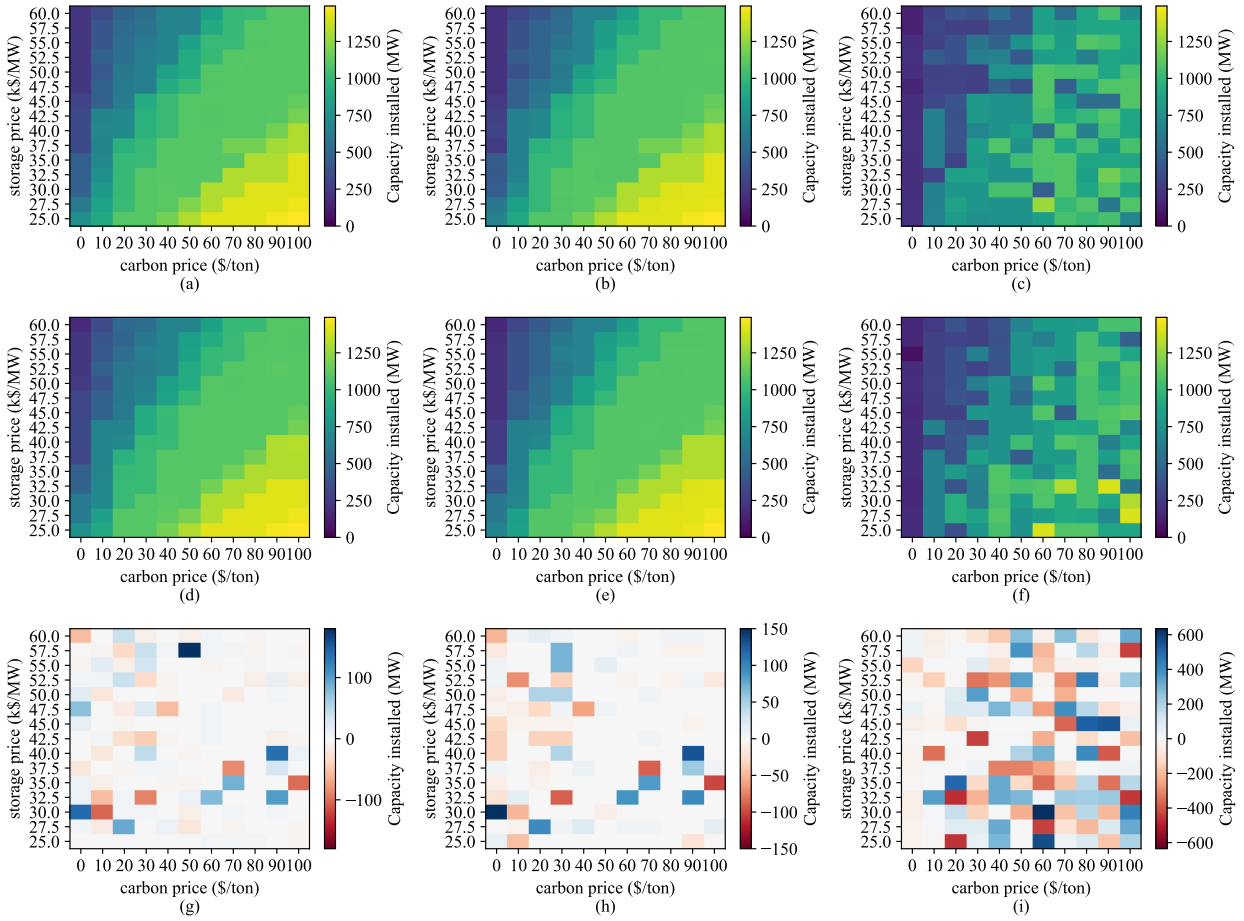

Figure 5.2: Optimal storage power as a function of investment perspective and emissions constraint. Rows: emissions unconstrained (a), (b), (c); emissions constrained (d), (e), (f); emissions constraint impact (g), (h), (i). Columns: vertically-integrated utility (a), (d), (g); philanthropic storage investor (b), (e), (h), profit-maximizing storage investor (c), (f), (h).

Fig. 5.2 shows the optimal storage quantities found by a vertically integrated utility, a

philanthropic storage investor, and a profit-maximizing storage investor, with sensitivity to both the effective price of energy storage (amoritized, per MW) and the price of carbon emissions. The first row shows the storage quantity without the emissions-neutrality constraint (ENC), the second row shows the storage quantity with the ENC, and the third row shows the difference from the ENC.

Decreasing storage quantities and increasing carbon price quantities both tend to increase the optimal storage quantity, for all perspectives, both with and without an ENC. On average, the PhSI installs nearly as much storage as the VIU (97.8% without the ENC, 97.3% with the ENC), but the PMSI installs significantly less (74.1% without the ENC, 73.9% with the ENC). The ENC does not have a strong impact on the quantity of storage installed by a VIU or PhSI (<0.5% on average for both), but tends to increase the quantity of storage purchased by a PMSI by an average of 5.0%, as shown in Table 5.1. This seemingly counter-intuitive results is due to the fact that storage dispatch and generator unit commitment are considered simultaneously, so the emissions constraint applies to the unit commitment variables which, once-fixed, define the time- and location-varying generator supply curves. The optimal storage quantity is ultimately a function of these supply curves, and in these case studies the ENC seems to result in supply curves which offer maximum PMSI profitability at greater storage quantities.

Although the ENC tends to increase the optimal storage quantity of a PMSI on average, there is significant variance for specific combinations of storage quantity and carbon price under all perspectives. In the VIU and PhSI cases, the constraint can alter the optimal storage quantity by >23% in both directions (with standard deviations of >4.8%), while in the PMSI case the impact ranges from -68% to +167% (standard deviation of 36.3%). This illustrates the non-convex nature of the storage investment problem, and shows the importance of conducting sensitivity analyses to illustrate the 'true' impact of this constraint on storage investment quantities.

Fig. 5.3 shows the emissions impact of the storage quantities shown in Fig. 5.2. Although the emissions impact of storage is generally beneficial (reducing emissions), in the case of un-

Table 5.1: Impact of Emissions-Neutrality Constraint on optimal investment quantity

Investment perspective	Average change	Worst case	Best case	Standard deviation
VIU	+0.46%	-23%	+31%	5.2%
PhSI	-0.08%	-23%	+34%	4.8%
PMSI	+5.0%	-68%	+167%	36%

priced GHG emissions the impact is only weakly beneficial or even detrimental, as shown in Figs. 5.3(a), 5.3(b), and 5.3(c). The impact of the ENC is to significantly reduce the system emissions in the un-priced GHG cases (on average 2.6% for the VIU, 3.1% for the PhSI, 3.0% for the PMSI), while having little effect on the emissions in the priced GHG cases (on average $\leq$0.1% change in all perspectives), as shown in Figs. 5.3(g), 5.3(h), and 5.3(i). This emissions reduction in the un-priced GHG case is achieved with minor cost increases: on average 0.12% for the VIU, 0.14% for the PhSI, 0.19% for PMSI, and no significant change in the priced GHG cases (on average $\leq$0.05% change in all perspectives).

The ENC can have a detrimental effect on emissions in some price scenarios by resulting in solutions with storage quantities and/or unit commitment variables such that although emissions in each day are not worse than the baseline, they are not reduced by *as much* as in the emissions-unconstrained investment-and-operation case. A binding ENC in just one representative day can impact the optimal storage quantity, and therefore operations in all days. As with the storage quantity, this demonstrates the non-convexity of the investment problems, caused by integer variables in all perspectives and bi-level structures in the PhSI and PMSI.

The quality of the PhSI solutions can be evaluated by investigating the lower bound of the two relaxations described in Section 5.5. The solutions found by the heuristic in Algorithm 1 are typically within 0.1% of the best lower bound found by the VIU relaxation. Although the PCSLE formulation is a tighter relaxation of the PhSI problem, in practice the progress of the

best lower-bound is relatively slow; the best lower bound found by the PCSLE formulation after 24 hours is still below the best lower bound of the VIU, which typically solves to 0 optimality gap within one hour.

5.8 Conclusion

Without a price on GHG emissions, the operation of energy storage can have a minimally beneficial or even detrimental effect on system emissions, even in power systems with very high penetrations of renewable resources. This effect persists over a wide range of energy storage prices, suggesting that policies which subsidize energy storage installation may not result in lowered emissions. If pricing GHG emissions is not feasible (*e.g.* due to political obstacles), then adding an emissions-neutrality constraint to the operation of energy storage can have a significant beneficial effect on system emissions, while not significantly impacting overall social costs or dissuading investment in merchant energy storage in either the philanthropic (PhSI) or profit-maximizing storage investment (PMSI) cases. In fact, the emissions-neutrality constraint tends to increase storage investment in the PMSI case. A philanthropic storage investor tends to invest in significantly more energy storage than a profit-maximizing storage investor, illustrating the benefits that a socially-minded storage investment entity can provide, even in the presence of profitability and emissions-neutrality constraints.

An efficient heuristic for this inherently non-convex problem is demonstrated, and an assessment of the PhSI solution quality using two MILP relaxations is demonstrated. Although the relaxation that moves commitment variables into the investment problem (a profit-constrained single-level equivalent, as in [194]) is tighter than the vertically-integrated utility (VIU) relaxation, the best lower bound found via the VIU relaxation shows that the heuristic finds solutions which are very close to the true optimum, and shows this with much less computational effort than the PCSLE relaxation.

While these effects have been shown in this particular case study, future work can examine the sensitivity of these results to more general cases. Factors which may contribute to different

outcomes in terms of storage investment and emissions may include:

- differences in market design, such as participation of energy storage in the reserves market(s),
- varying total penetrations of non-emitting resources, or varying ratios of solar, wind, and nuclear generation, and
- consideration of different storage durations, or of investment in a mixture of storage with varying durations.

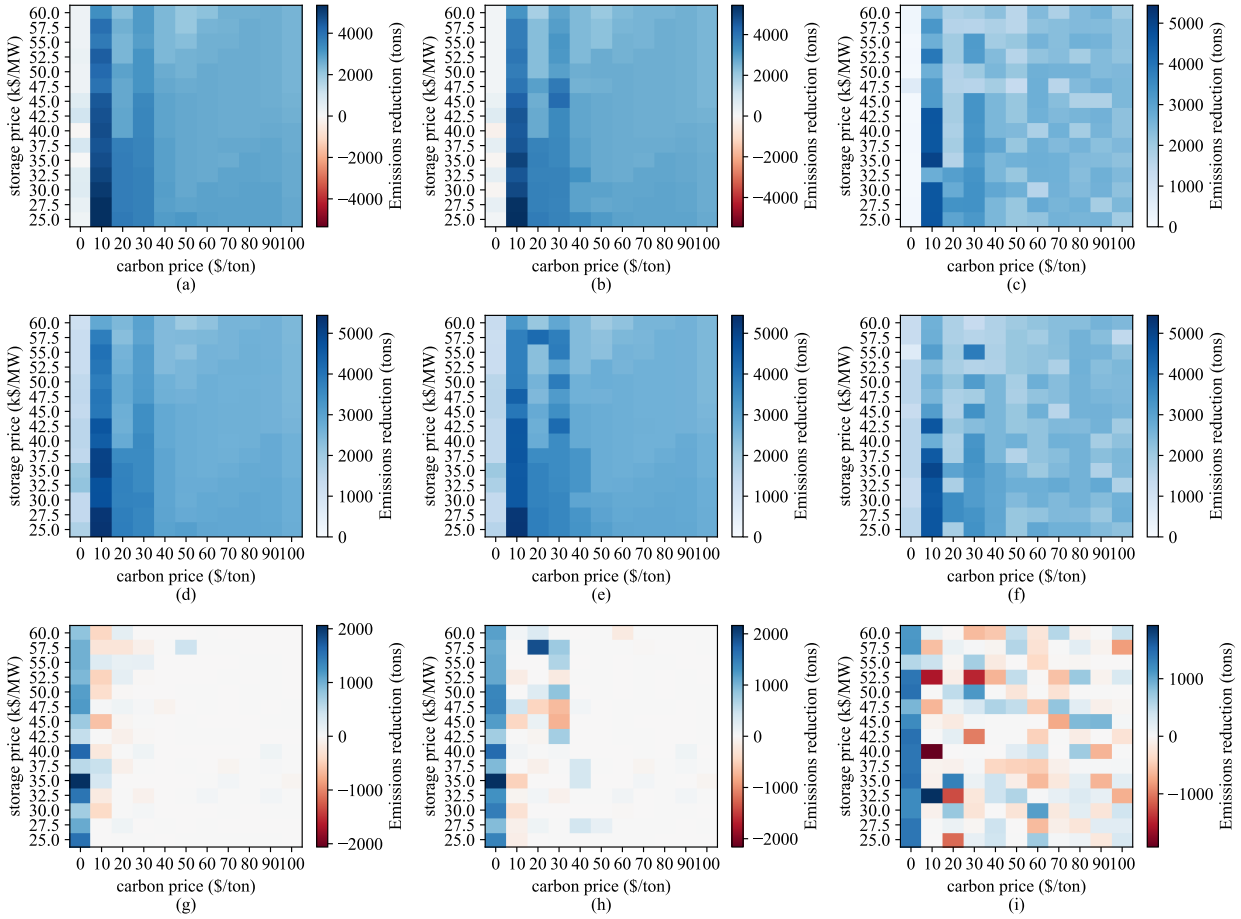

Figure 5.3: Emissions impact from storage as a function of investment perspective and emissions constraint. Rows: emissions unconstrained (a), (b), (c); emissions constrained (d), (e), (f); emissions constraint impact (g), (h), (i). Columns: vertically-integrated utility (a), (d), (g); philanthropic storage investor (b), (e), (h), profit-maximizing storage investor (c), (f), (h).

Nomenclature

Sets and Indices

A Set of representative days, indexed by a.

B Set of transmission network buses, indexed by b.

I Set of generating units, indexed by i.

L Set of transmission lines, indexed by l.

S Set of generator power output blocks, indexed by s.

T Set of time intervals, indexed by t or τ.

Parameters

$b_{i,s}$ Marginal cost of block s of generator i (\$/MWh).

$C_i^{\min}$ Minimum cost of generator i (\$/h).

C_i^{su} Start-up cost of generator i (\$).

$d_{b,t,a}$ Demand at bus b, time t, day a (MW).

$E^{\max}$ Regulator's GHG emission target (tons).

$E_i^{\min}$ Minimum GHG emissions of generator i (tons/h).

E_i^{su} Start-up GHG emissions of generator i (tons).

$f_l^{\max}$ Capacity of transmission line l (MW).

$g_i^{\max}$ Maximum power output of generator i (MW).

$g_i^{\min}$ Minimum power output of generator i (MW).

$g_{i,s}^{\max}$ Maximum power output of block s, generator i (MW).

g_i^{down} Minimum down-time of generator i (h).

g_i^{up} Minimum up-time of generator i (h).

$h_{i,s}$ Marginal GHG emissions of block s, generator i (tons/MWh).

$m_{l,b}^{\text{line}}$ Line connection map. $m_{lb}^{\text{line}} = 1$ if line l starts at bus b, $= -1$ if line l ends in bus b, 0 otherwise.

$m_{i,b}^{\text{unit}}$ Unit map. $m_{i,b}^{\text{unit}} = 1$ if generator i is located at bus b, 0 otherwise.

P^{CO_2} GHG emissions tax rate (\$/ton-CO_2e).

P^{load} Load shed penalty (\$/MWh).

P^{ren} Renewable generation shed penalty (\$/MWh).

$w_{b,t}$ Renewable generation at bus b, time t (MW).

x_l Reactance of line l (Ω).

π_a Probability of day a.

Primal Variables

C^{gen} System operator's generation cost (\$).

C^{shed} System operator's shed cost (\$).

E_a GHG Emissions for day a (tons).

E^{total} Total GHG emissions (tons).

$f_{l,t,a}$ Power flow on line l, time t, day a (MW).

$g_{i,t,a}$ Power output of generator i, time t, day a (MW).

$g_{i,s,t,a}$ Power output of generator i, block s, time t, day a (MW).

$s_{b,t,a}^{\text{load}}$ Load shed at bus b, time t, day a (MWh).

$s_{b,t,a}^{\text{ren}}$ Renewable generation shed at bus b, time t, day a (MWh).

$u_{i,t,a}$ Binary variable for the commitment status of generator i, time t, day a.

$v_{i,t,a}$ Binary variable for the start-up of generator i, time t, day a.

$z_{i,t,a}$ Binary variable for the shut-down of generator i, time t, day a.

$\theta_{b,t,a}$ Voltage phase angle of bus b, time t, day a (rad).

Dual Variables

$\underline{\delta}_{i,s,t}$ Dual variable for generator segment lower limit constraint.

$\overline{\delta}_{i,s,t}$ Dual variable for generator segment upper limit constraint.

$\underline{\phi}_{i,t}$ Dual variable for renewable shedding lower limit constraint.

$\overline{\phi}_{i,t}$ Dual variable for renewable shedding upper limit constraint.

$\kappa_{b,t}$ Dual variable for storage state-of-charge tracking constraint.

$\underline{\xi}_{b,t}$ Dual variable for storage state-of-charge lower limit constraint.

$\overline{\xi}_{b,t}$ Dual variable for storage state-of-charge upper limit constraint.

$\underline{\rho}^{\text{chg}}_{b,t}$ Dual variable for storage charging power lower limit constraint.

$\overline{\rho}^{\text{chg}}_{b,t}$ Dual variable for storage charging power upper limit constraint.

$\underline{\rho}^{\text{dis}}_{b,t}$ Dual variable for storage discharging power lower limit constraint.

$\overline{\rho}^{\text{dis}}_{b,t}$ Dual variable for storage discharging power upper limit constraint.

$\lambda_{b,t}$ Dual variable for power balance constraint.

$\underline{\gamma}_{l,t}$ Dual variable for line flow lower limit constraint.

$\overline{\gamma}_{l,t}$ Dual variable for line flow upper limit constraint.

$\beta_{l,t}$ Dual variable for DC power flow constraint.

α Dual variable for emissions constraint.

Variable Sets

Ω^{C} Set of binary commitment variables.

Ω^{D} Set of dispatch variables.

Ω^{λ} Set of dual dispatch variables.

Ω^{S} Set of storage investment variables.

Appendix A: Dual problem of Transmission Constrained Economic Dispatch

The dual problem of the TCED is given in (5.34)-(5.41), with the primal variables to which each dual constraint corresponds listed in parentheses.

$$\begin{aligned}\max_{\Omega^{\mathrm{D}}} \hat{C}^{\mathrm{dual}} := \alpha \left[\sum_{t\in T}\sum_{i\in I} E_i^{\min} u_{i,t} + E_i^{\mathrm{su}} v_{i,t} - \chi E^{\mathrm{baseline}}\right] \\ - \sum_{l\in L}\sum_{t\in T}\left[f_l^{\max}\left(\underline{\gamma}_{l,t} + \overline{\gamma}_{l,t}\right)\right] - \sum_{i\in I}\sum_{s\in S}\sum_{t\in T} g_{i,s}^{\max} u_{i,t}\overline{\delta}_{i,s,t} \\ + \sum_{b\in B}\sum_{t\in T}\left[\lambda_{b,t}\left(d_{b,t} - w_{b,t} - \sum_{i\in I} m_{i,b}^{\mathrm{unit}} g_i^{\min} u_{i,t}\right)\right. \\ \left. - Q_b^{\max}\overline{\xi}_{b,t} - J_b^{\max}\left(\overline{\rho}_{b,t}^{\mathrm{chg}} + \overline{\rho}_{b,t}^{\mathrm{dis}}\right) - w_{b,t}\overline{\phi}_{b,t}\right]\end{aligned} \tag{5.34}$$

subject to:

$$\alpha h_{i,s} + b_{i,s} - \sum_{b \in B} \left[m_{i,b}^{\text{unit}} \lambda_{b,t} \right] - \underline{\delta}_{i,s,t} + \overline{\delta}_{i,s,t} = 0 \quad (g_{i,s,t}) \tag{5.35}$$

$$\frac{1}{\eta^{\text{dis}}} \kappa_{b,t} + \overline{\rho}_{b,t}^{\text{dis}} - \underline{\rho}_{b,t}^{\text{dis}} - \lambda_{b,t} = 0 \quad \left(J_{b,t}^{\text{dis}} \right) \tag{5.36}$$

$$\lambda_{b,t} + \overline{\rho}_{b,t}^{\text{chg}} - \underline{\rho}_{b,t}^{\text{chg}} - \eta^{\text{chg}} \kappa_{b,t} = 0 \quad \left(J_{b,t}^{\text{chg}} \right) \tag{5.37}$$

$$\sum_{l \in L} y_l m_{l,b}^{\text{line}} \beta_{l,t} = 0 \quad (\theta_{b,t}) \tag{5.38}$$

$$\sum_{b \in B} \left(m_{l,b}^{\text{line}} \lambda_{b,t} \right) + \beta_{l,t} - \underline{\gamma}_{l,t} + \overline{\gamma}_{l,t} = 0 \quad (f_{l,t}) \tag{5.39}$$

$$\kappa_{b,t} - \kappa_{b,t+1} + \overline{\xi}_{b,t} - \underline{\xi}_{b,t} = 0 \quad (Q_{b,t}) \tag{5.40}$$

$$\lambda_{b,t} + \overline{\phi}_{b,t} - \underline{\phi}_{b,t} = 0 \quad \left(s_{b,t}^{\text{ren}} \right) \tag{5.41}$$

$$\alpha, \gamma, \delta, \zeta, \xi, \rho, \phi \geq 0$$

Chapter 6
FUTURE WORK

To complement the approaches presented in the preceding chapters, four additional low-carbon planning and policy approaches are proposed. Each of these potential approaches is categorized in Figure 6.1 based on the categorizations discussed in Section 1.6. These projects are:

- Emissions-Aware Tariff Design
- Operation of a Closed-Loop Carbon Cycle Power System
- Planning Low-Carbon District Energy Systems
- Comparing a Carbon Tax with Emissions Trading in Power Systems Operation

Each is described at more length in the following sections of this chapter.

6.1 Emissions-Aware Tariff Design

Although many jurisdictions have implemented pricing of carbon emissions [19], in many places these emissions are still un-priced. However, political will for carbon pricing is often present in small pockets of larger regions in which this will does not exist. The utility companies in these small pockets therefore have an opportunity to offer an electricity tariff which includes carbon pricing, in an effort to reduce induced carbon emissions from the wholesale power market in which it buys energy. Tariff design can have a significant impact on emissions induced by customer demand profiles, as shown in [199] by comparing customer load shifting using energy storage system to respond to various types of retail tariffs.

If the marginal emissions from the wholesale generation/transmission network can be reliably estimated in advance, then utility rates can have an added charge proportional to

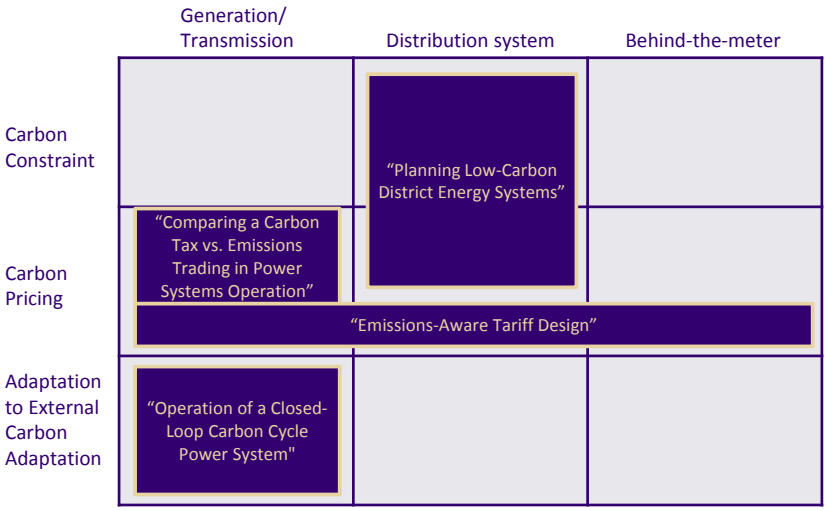

Figure 6.1: Proposed low-carbon power system design models, organized by method and point(s) of application

these marginal emissions. This change in the price vector presented to customers will tend to shift electricity consumption toward periods with lower marginal emissions, depending on the rate of the emissions charge and the customer flexibility in load scheduling. The question becomes: if a utility would like to reduce emissions by a certain quantity, *how high should the emissions charge be in order to reach an emissions target, anticipating the reaction of utility customers to changes in the price vector?*

This approach can be modeled as a bi-level problem, with the utility in the upper-level aiming to minimize the emissions-charge, subject to achieving a certain level of emissions reductions, as shown in Figure 6.2. The lower-levels represent the customers of this utility, reacting to the price vector being presented to them (a linear function of the emissions charge) [59], similarly to Chapter 2. If the behavior of the customers can be estimated

accurately, then the utility can solve this multi-level problem using the bisection method, iteratively guessing an emissions charge and comparing the induced emissions (resulting from the demand vectors of the lower-level customers) to the emissions target. This can avoid potential 'braided cobweb' effects of using historical data to set real-time prices without anticipating customer reactions to these prices [200].

This approach can be made revenue-neutral for the utility by offering customers a 'rebate' on each kWh of electricity, equal to the total emissions charge revenue divided by the total electricity consumption (an approach often referred to as a *feebate*). If the total energy consumption of the customers is assumed to be inflexibile (i.e., customers will shift energy through the day but will not reduce their overall consumption), then the solutions will be equivalent, as the total rebate will be a fixed value and therefore not impact the optimization. The end result of the charge and the rebate is that time periods with lower-than-average marginal emissions would have lowered prices, and vice versa. Since the collected revenue is re-distributed, the customers would see an increase in net cost only from the cost of generating energy using more expensive (but lower-emitting) power plants, not from the emissions charge itself.

If, on the other hand, the share of customers responding to this emissions-aware tariff is large enough to impact the dispatch of the power system, then the marginal emissions rates cannot be reliably estimated in advance and the dispatch of the power system in response to the changing loads must also be modeled by the utility. This structure is shown in Figure 6.3. To solve this more complicated structure, the customers' reactions to price vectors and the economic dispatch problems should both be modeled as linear approximations (assuming a pre-defined unit commitment), and each lower-level optimization problem transformed into a set of constraints based on strong duality. Then, the emissions charge can be selected from a discrete set of values, allowing products of upper-level and lower-level variables to be approximated using a MILP formulation.

Though revenue neutrality can easily be achieved for the customers participating in this tariff via the same 'rebate' approach discussed earlier, the cost of supplying electricity to the

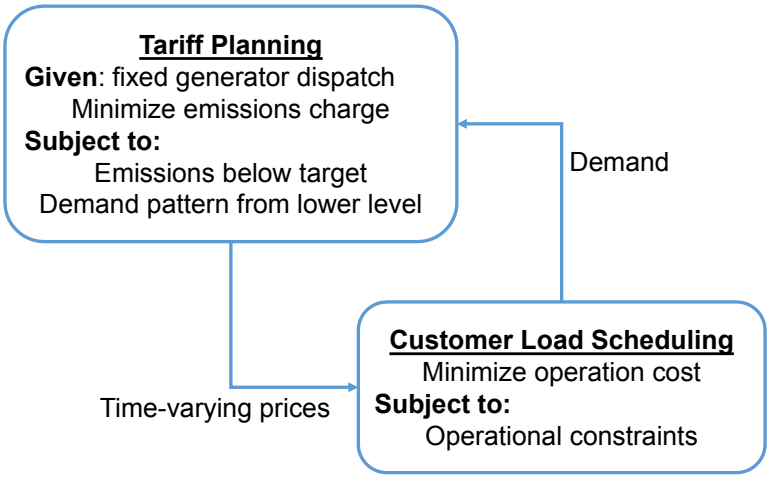

Figure 6.2: Bi-level model of emissions-aware tariff optimization, marginal penetration

remaining share of customers (not exposed to emissions pricing) may change. Additionally, there may be a change in the emissions induced by this share of customers, since the load-shifting by responsive customers will change which generators are being used to satisfy the demand of the non-responsive customers. These potential shifts in costs and emissions must be accounted for when considering the overall effects of such an emissions-aware tariff.

6.2 Operation of a Closed-Loop Carbon Cycle Power System

The current state of carbon capture and sequestration (CCS) technology and carbon pricing is not resulting in large deployment of CCS for the power sector [201]. A few demonstration projects have been implemented, but CCS in power generation is the exception rather than the rule. However, given the increased awareness of climate change and political will to combat it, a future with widespread use of CCS technologies may be possible. The prices of solar and wind generation, as well as energy storage, continue to fall and these technologies

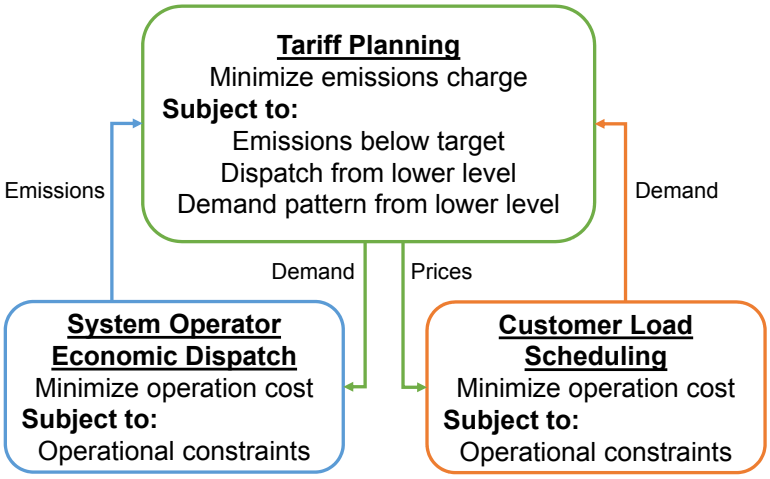

Figure 6.3: Bi-level model of emissions-aware tariff optimization, larger penetration

will play an increasing role in our generation mixture, but fossil-fuel generation may still play a role for some time due to its on-demand generation capabilities, absence of short-to-medium-term energy limitations (unlike many energy storage technologies), and natural inertial response [202].

Carbon-capture power plants (CCPPs) have additional power flexibility compared to the same plants without carbon-capture [203, 204, 205]. This is because the net power generation of the entire plant is the difference between the gross generation power and the power demand for the exhaust scrubbing and solute stripping processes, the latter of which can be flexibly scheduled based on the capabilities of on-site storage of both carbon-lean and carbon-rich solute. However, eventually the captured CO_2 must be stripped from the carbon-rich solute and conveyed to a sequestration site. Given wider adoption of CCS technologies, these may be a conveyance network to transport this CO_2, captured from geographically dispersed thermal generators, to a relatively smaller number of suitable sequestration points (or toward

industrial usage). Therefore, *planning for the operation of power systems with high penetration of CCS thermal generation must adequately model not only the flexibility of the CCS side, but also the constraints of the CO_2 network.*

Coordination of the electricity and natural gas networks has been extensively studied [206, 207], and there has been some work done in optimal design of a CO_2 network [208, 209], but there has been no work on the design or operation of a combined electricity and post-capture CO_2 network. One significant difference between the modeling of this network and similar modeling of combined natural gas and electricity networks is that the added flexibility of CCPPs relies on the capacity of the downstream CO_2 network, not the upstream fuel network. Additionally, CCPPs have the technical capacity to continue operation when faced with network constraints, bypassing carbon-capture processes and venting to the atmosphere, while there is no alternative to the gas network for natural gas generators. These distinctions add a different character to the operation of combined electricity and gas networks.

6.3 Planning Low-Carbon District Energy Systems

Chapter 4 explores the design of low-carbon campus energy hubs, but implicitly assumes that the district-level energy systems have pre-defined energy conversion equipment (e.g. district heat generation) and infinite distribution capacity (e.g. conveyance of electricity, natural gas, and district heat). An optimization of the wider-scale district level energy system planning could include non-idealities ignored in the campus energy hub model, including:

- the non-linear behavior of natural gas conveyance,
- losses present in conveyance of district heat, and
- the provision of adequate distribution capacity of electricity, natural gas, and district heat.

Planning decisions can also be expanded from those in the model in Chapter 4 to include: the selection of equipment for generating and distributing district heat, energy efficiency

options for construction of new buildings, and investment in electrification of regional transportation. The resulting model would be similar to that of [210], with the inclusion of a wider variety of energy flows and conversion and storage equipment (e.g. power-to-gas conversion, battery energy storage systems).

Once the underlying district energy system model is developed, it could be used to evaluate the relative efficiency of various decarbonization policies, as is demonstrated in Chapter 4. Potential policies could include:

- improving the thermal efficiency of the built environment and the electrical efficiency of loads which reside inside it,
- switching district heating boilers to equipment with lower carbon intensity,
- providing subsidies for decarbonization projects which would otherwise not be cost-effective, and
- carbon pricing policies, which can be applied at various points in the district energy network (e.g. to the customers, to the district network operators, or a mandate that a social cost of carbon be considered during planning).

6.4 Comparing a Carbon Tax with Emissions Trading in Power Systems Operation

In many respects, a tax on carbon emissions and an emissions trading scheme are very similar, as both reduce overall emissions by creating a price on carbon. An emissions trading scheme provides surety on overall emissions while implicitly creating a price, and a carbon tax provides surety on price while implicitly reducing emissions (for a more thorough discussion of commonalities and differences, see Section 1.3). One prominent drawback of emissions trading schemes is that the future price of emissions allowances is unknown; even once a market price has been established, that market price is subject to change as realizations of future uncertainty (such as technological progress, and demand for carbon-intensive goods

and services) differ from expectations. *Given that the price of emissions allowances has an uncertain trajectory, does this uncertainty meaningfully impact the cost of operating power systems, as compared to operation under a fixed carbon tax?*

The cost of operating a power system is a highly non-linear function of the price of carbon emissions, even when ignoring the overall emissions bill, as shown in Chapter 3. Additionally, operation of power systems is fairly 'lumpy' (non-convex) due to binary unit commitment variables. Therefore, the cost of operating a power system experiencing a range of carbon prices may be significantly different than the cost of operating at the average experienced price. An investigation into the operational effects of different pricing schemes could include:

- trajectories of carbon prices that follow statistical properties observed in real carbon allowance markets (for wide-ranging emissions trading schemes),

- feedback between power systems operations and price trajectories (for more narrow emissions trading schemes, in which the rate of 'consumption' of allowances by a power system can have a meaningful impact on prices), and

- investigating the relationship between emissions quotas and power systems dynamics (as there may be a number of 'break point' prices which provide a large degree of operational change relative to a small change in carbon price, as seen in Chapter 3).

Chapter 7
CONCLUSION

This dissertation describes several approaches to developing policies and planning for low-carbon power systems, and proposes several additional approaches for future study. Both sets of approaches are mapped onto categorizations by domain and method in Figure 7.1, as originally described in Section 1.6. In some cases these policies have no overlap, in other cases there may be overlap in either method or domain or both. The relative economic efficiency of these policies in achieving a given emission reduction target varies, but policy decisions in democratic societies are often made for reasons besides just economic efficiency. By presenting a full suite of policy options for power systems decarbonization to policy-makers, complete with analyses of their anticipated effects, it is hoped that policy-makers can better weigh the tradeoffs between efficiency, emissions, and likelihood of successfully implementing and maintaining these policies.

7.1 Research Conclusions

For 'adaptation' approaches, power systems must plan to react to exogenous decarbonization efforts. By contrast, designing regulatory policies to promote decarbonization by independent stakeholders requires solving multi-level Stackelberg models. Though these structures are more complex, and require regulators to approximate the perspectives of other stakeholders who will react to policy decisions, for certain types of analyses these structures are tractable and result in more accurate quantitative policy decisions for given emissions targets. Specifically:

1. If a lower-level problem can be modeled linearly, it can be optimized within an upper-level problem as a mixed-integer single-level equivalent using the strong duality theorem

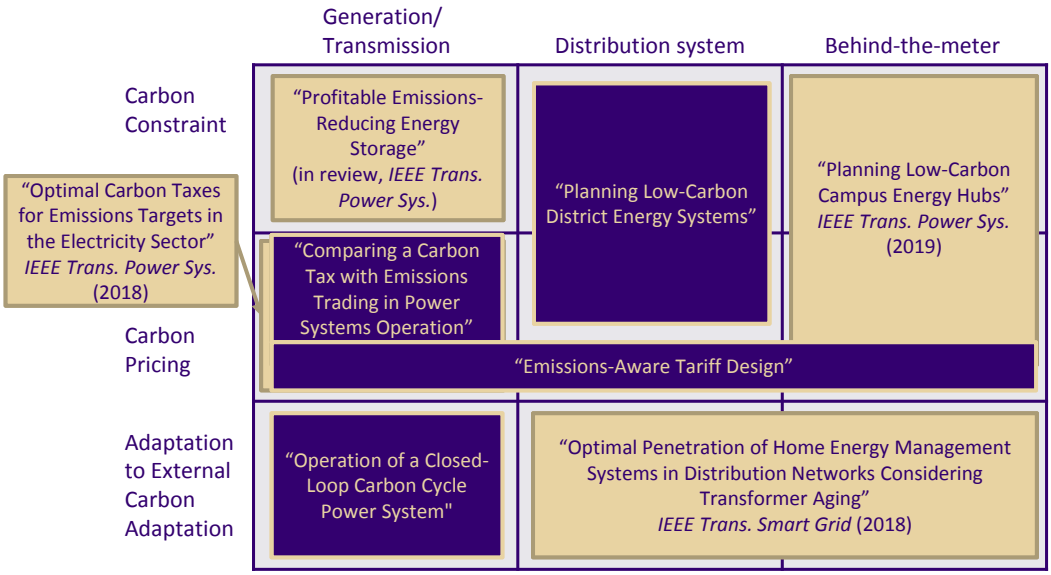

Figure 7.1: Low-carbon power system design models, described and proposed, organized by method and point(s) of application

[127], using an integer approximation of continuous upper-level decision variables as necessary, and

2. If a lower-level problem optimizes for cost minimization, while an upper-level problem optimizes for carbon price minimization (subject to emissions from the lower-level meeting an upper-level emissions target), the problem can be solved iteratively using the bisection method. This approach is only as computationally complex as the lower-level problem, e.g. if the lower-level problem is MILP, then solving the two problems

together is an iterative method of successive MILP optimizations. Convergence of the bisection method to a final solution is relatively slow (linear) compared to other root-finding methods, but convergence is guaranteed.

In general, power systems designed and operated for lower carbon have higher operational costs than the case in which emissions are not considered. The cost increase depends on both the strictness of the emissions target and on the structure of the emissions reduction approach. For a given target, single-level frameworks are cheapest, while multi-level models result in higher costs because the upper-level regulator has only indirect control over carbon emissions. However, multi-level models in which the distinct objectives of multiple stakeholders are modeled are more representative of market environments. Using these sorts of frameworks, regulator decisions can also be optimized considering multiple independent lower-levels. For example:

- A carbon price can be optimized that will apply to multiple power systems in order to meet a given combined emissions target (an extension of the work in Chapter 3). This can be accomplished since the emissions from each power system are monotonically non-increasing with respect to a carbon price, and the sum of multiple monotonically non-increasing functions is also monotonically non-increasing.

- The design of energy infrastructure for multiple campus energy hubs can be considered together, in light of a target for their combined emissions (an extension of the work in Chapter 4). This can be accomplished because although investment decision variables may be non-convex, they can be considered together as one master problem while the linear operation problem of each energy hub can be still incorporated into a single-level equivalent using the strong duality theorem.

7.2 Broader Conclusions

Although adoption of emissions-reducing policies will likely result in increased costs to investors and operators of power systems, if the cost increases are outweighed by emissions reductions valued at the social cost of carbon then the overall (planetary) social welfare is still increased. Even policies which are estimated to be more expensive than the social cost of carbon may be worthwhile, if there is a reasonable likelihood that their implementation will induce further cooperation from regulators in other jurisdictions.

Higher prices for electricity reduce overall demand and increase the value proposition for investment in new cleaner generation, transmission, and grid-scale energy storage, as well as technologies that generate or consume electricity more efficiently. Carbon capture and sequestration projects also become more attractive. Conversely, investment in equipment and policies which reduce the grid's carbon intensity reduce the strictness of subsequent policies (e.g. clean energy mandates, carbon prices, or operational constraints) required to achieve a given emissions target.

For policies involving carbon pricing, the carbon price collects revenue that can be used to invest in projects to reduce GHG emissions, adapt to climate change, and/or provide economic relief to communities which are negatively impacted by taxation of carbon, such as those heavily reliant on coal-mining. This revenue stream could also be used to offset tax reductions elsewhere to obtain revenue neutrality. However, the question of what should be done with revenue from carbon pricing is a political one, not a technical one, and is outside of the scope of this dissertation.

Alfred Marshall, who in 1890 described how society could improve social welfare by inducing economic actors towards activities which would "add the most to the sum total of happiness", nevertheless also described how political forces could successfully impede these changes, due to their relative advantage in this fight:

> A few people who have been strongly interested on one side have raised their voices loudly, persistently, and all together; while little has been heard from the great mass of people whose interests have lain in the opposite direction; for, even if their attention has been fairly called to the matter, few have cared to exert themselves much for a cause in which no one of them has more than a small stake. The few therefore get their way, although if statistical measures of the interests involved were available, it might prove that the aggregate of the interests of the few was only a tenth or a hundredth part of the aggregate of the interests of the silent many. (Marshall 1890, p. 470)

The transition to a low-carbon society, complete with low-carbon power systems, will likely be messy. There is much rhetoric on both sides of the debate, and far-reaching financial and equity impacts from just about every available policy option. Therefore, careful understanding and design of policies is vital, in order to bring emissions to sustainable levels with minimal disruption to the rest of society. Only by fully understanding the most cost-efficient ways to reduce power system GHG emissions can we make the best choices about our path forward, and successfully design a sustainable future.

BIBLIOGRAPHY

[1] *Climate Change 2014: synthesis Report. Contribution of Working Groups I, II and III to the Fifth Assessment Report of the Intergovernmental Panel on Climate Change*. Tech. rep. Intergovernmental Panel on Climate Change, 2014.

[2] *Global Warming of 1.5°C. An IPCC Special Report on the impacts of global warming of 1.5°C above pre-industrial levels and related global greenhouse gas emission pathways, in the context of strengthening the global response to the threat of climate change, sustainable development, and efforts to eradicate poverty*. Tech. rep. Intergovernmental Panel on Climate Change, 2018.

[3] Climate Action Tracker. *Temperatures*. 2018.

[4] Frederick P. Landers Jr. "The Black Market Trade in Chlorofluorocarbons: The Montreal Protocol Makes Banned Refrigerants a Hot Commodity". In: *George Journal of International and Comparative Law* 26.2 (1997), pp. 457–485.

[5] William Foster Lloyd. "W. F. Lloyd on the Checks to Population". In: *Population and Development Review* 6.3 (1980), pp. 473–496. DOI: 10.2307/1972412.

[6] Henry Sidgwick. *The Principles of Political Economy*. 2nd Ed. New York: MacMillan and Co., 1887.

[7] Alfred Marshall. *Principles of Economics*. London: MacMillan and Co., 1890.

[8] Arthur Cecil Pigou. *The Economics of Welfare*. McMillan and Company, 1920.

[9] Milton Friedman and Rose Friedman. *Free to Choose*. Harcourt Brace Jovanovich, 1980.

[10] R. H. Coase. "The Problem of Social Cost". In: *The Journal of Law and Economics* 3 (1960), pp. 1–44. DOI: 10.1086/466560.

[11] John Maynard Keynes. "The General Theory of Employment, Interest and Money". In: (1936).

[12] Herbert A Simon. "Models of man; social and rational". In: (1957).

[13] George A Akerlof. "The Market for "Lemons": Quality Uncertainty and the Market Mechanism". In: *The Quarterly Journal of Economics* 84.3 (1970), pp. 488–500.

[14] Michael Spence. "Job Market Signaling*". In: *The Quarterly Journal of Economics* 87.3 (Aug. 1973), pp. 355–374. DOI: 10.2307/1882010.

[15] Joseph E Stiglitz. "The theory of "screening," education, and the distribution of income". In: *The American economic review* 65.3 (1975), pp. 283–300.

[16] William J Baumol and Wallace E. Oates. *The theory of environmental policy*. 2nd Ed. Cambridge university press, 1988.

[17] William J Baumol and Wallace E Oates. "The use of standards and prices for protection of the environment". In: *The economics of environment*. Springer, 1971, pp. 53–65.

[18] Ellison S. Burton and William Sanjour. "A simulation approach to air pollution abatement program planning". In: *Socio-Economic Planning Sciences* 4.1 (1970), pp. 147–159. DOI: 10.1016/0038-0121(70)90036-4.

[19] Céline Ramstein et al. *State and Trends of Carbon Pricing 2019*. Tech. rep. World Bank, 2019.

[20] Enzo Sauma. "The impact of transmission constraints on the emissions leakage under cap-and-trade program". In: *Energy Policy* 51 (2012), pp. 164–171. DOI: 10.1016/j.enpol.2012.08.057.

[21] Antoine-Augustin Cournot. *Recherches sur les Principes Mathématiques de la Théorie des Richesses [Researches into the Mathematical Principles of the Theory of Wealth]*. chez L. Hachette, 1838.

[22] J v Neumann. "Zur Theorie der Gesellschaftsspiele [On the Theory of Games of Strategy]". In: *Mathematische annalen* 100.1 (1928), pp. 295–320.

[23] John Nash. "Non-Cooperative Games". PhD thesis. Princeton, 1950.

[24] Heinrich Von Stackelberg. *Marktform und gleichgewicht*. J. springer, 1934.

[25] Harry Singh. *Game Theory Applications in Electric Power Markets*. Tech. rep. TP-136-0. IEEE Power and Energy Society, 1999.

[26] M. R. Gent and J. W. Lamont. "Minimum-Emission Dispatch". In: *IEEE Transactions on Power Apparatus and Systems* PAS-90.6 (Nov. 1971), pp. 2650–2660. DOI: 10.1109/TPAS.1971.292918.

[27] J. K. Delson. "Controlled Emission Dispatch". In: *IEEE Transactions on Power Apparatus and Systems* PAS-93.5 (Sept. 1974), pp. 1359–1366. DOI: 10.1109/TPAS.1974.293861.

[28] J. Zahavi and L. Eisenberg. "Economic-Enviromental Power Dispatch". In: *IEEE Transactions on Systems, Man, and Cybernetics* SMC-5.5 (Sept. 1975), pp. 485–489. DOI: 10.1109/TSMC.1975.5408370.

[29] J. H. Talaq, F. El-Hawary, and M. E. El-Hawary. "A summary of environmental/economic dispatch algorithms". In: *IEEE Transactions on Power Systems* 9.3 (Aug. 1994), pp. 1508–1516. ISSN: 0885-8950. DOI: 10.1109/59.336110.

[30] F. N. Lee. "The coordination of multiple constrained fuels". In: *IEEE Transactions on Power Systems* 6.2 (May 1991), pp. 699–707. DOI: 10.1109/59.76715.

[31] F. N. Lee, J. Liao, and A.M. Breipohl. "Adaptive fuel allocation using pseudo fuel prices". In: *IEEE Transactions on Power Systems* 7.2 (May 1992), pp. 487–496. DOI: 10.1109/59.141750.

[32] J. Gardner, E. Leslie, and D. Todd. "Summary of the panel session 'Coordination Between Short-Term Operation Scheduling and Annual Resource Allocations'". In: *IEEE Transactions on Power Systems* 10.4 (Nov. 1995), pp. 1879–1889. DOI: 10.1109/59.476053.

[33] Benjamin F. Hobbs. "Optimization methods for electric utility resource planning". In: *European Journal of Operational Research* 83.1 (1995), pp. 1–20. DOI: doi.org/10.1016/0377-2217(94)00190-N.

[34] William H Golove and Joseph H Eto. *Market barriers to energy efficiency: a critical reappraisal of the rationale for public policies to promote energy efficiency*. Tech. rep. Lawrence Berkeley Lab., CA (United States), 1996.

[35] J. L. C. Meza, M. B. Yildirim, and A. S. M. Masud. "A Model for the Multiperiod Multiobjective Power Generation Expansion Problem". In: *IEEE Transactions on Power Systems* 22.2 (May 2007), pp. 871–878. ISSN: 0885-8950. DOI: 10.1109/TPWRS.2007.895178.

[36] E. Denny and M. O'Malley. "Wind generation, power system operation, and emissions reduction". In: *IEEE Transactions on Power Systems* 21.1 (Feb. 2006), pp. 341–347. ISSN: 0885-8950. DOI: 10.1109/TPWRS.2005.857845.

[37] A. K. Kazerooni and J. Mutale. "Transmission Network Planning Under Security and Environmental Constraints". In: *IEEE Transactions on Power Systems* 25.2 (May 2010), pp. 1169–1178. DOI: 10.1109/TPWRS.2009.2036800.

[38] Lu Wang, Yi-Ming Wei, and Marilyn A. Brown. "Global transition to low-carbon electricity: A bibliometric analysis". In: *Applied Energy* 205 (2017), pp. 57–68. ISSN: 0306-2619. DOI: 10.1016/j.apenergy.2017.07.107.

[39] Galen L. Barbose. *U.S. Renewables Portfolio Standards: 2018 Annual Status Report*. Tech. rep. Nov. 2018.

[40] X. Chen et al. "Power System Capacity Expansion Under Higher Penetration of Renewables Considering Flexibility Constraints and Low Carbon Policies". In: *IEEE Transactions on Power Systems* 33.6 (Nov. 2018), pp. 6240–6253. ISSN: 0885-8950. DOI: 10.1109/TPWRS.2018.2827003.

[41] L. Deng, B. F. Hobbs, and P. Renson. "What is the Cost of Negative Bidding by Wind? A Unit Commitment Analysis of Cost and Emissions". In: *IEEE Transactions on Power Systems* 30.4 (July 2015), pp. 1805–1814. DOI: 10.1109/TPWRS.2014.2356514.

[42] Jeremiah X. Johnson and Joshua Novacheck. "Emissions Reductions from Expanding State-Level Renewable Portfolio Standards". In: *Environmental Science & Technology* 49.9 (2015), pp. 5318–5325. DOI: 10.1021/es506123e.

[43] Chris Hope. *The PAGE09 integrated assessment model: A technical description*. Tech. rep. 04/2011. Cambridge Judge Business School, University of Cambridge, Apr. 2011.

[44] Chris Hope. *The Social Cost of CO2 from the PAGE09 Model*. Tech. rep. 05/2011. Cambridge Judge Business School, University of Cambridge, June 2011.

[45] Chris Hope. *New Insights from the PAGE09 Model: The Social Cost of CO2*. Tech. rep. 08/2011. Cambridge Judge Business School, University of Cambridge, July 2011.

[46] David Anthoff and Richard S. J. Tol. "The uncertainty about the social cost of carbon: A decomposition analysis using FUND". In: *Climatic Change* 117.3 (Apr. 2013), pp. 515–530. DOI: 10.1007/s10584-013-0706-7.

[47] William Nordhaus. "Evolution of modeling of the economics of global warming: changes in the DICE model, 1992-2017". In: *Climatic Change* 148.4 (June 2018), pp. 623–640. DOI: 10.1007/s10584-018-2218-y.

[48] Energy Innovation. *Energy Policy Simulator*. https://us.energypolicy.solutions/. 2019.

[49] Hal Harvey, Robbie Orvis, and Jeffrey Rissman. *Designing Climate Solutions: A Policy Guide for Low-Carbon Energy*. Island Press, 2018.

[50] Josh A. Taylor, Sairaj V. Dhople, and Duncan S. Callaway. "Power systems without fuel". In: *Renewable and Sustainable Energy Reviews* 57 (2016), pp. 1322–1336. DOI: 10.1016/j.rser.2015.12.083.

[51] B. Kroposki et al. "Achieving a 100% Renewable Grid: Operating Electric Power Systems with Extremely High Levels of Variable Renewable Energy". In: *IEEE Power and Energy Magazine* 15.2 (Mar. 2017), pp. 61–73. DOI: 10.1109/MPE.2016.2637122.

[52] D. J. Olsen, M. R. Sarker, and M. A. Ortega-Vazquez. "Optimal Penetration of Home Energy Management Systems in Distribution Networks Considering Transformer Aging". In: *IEEE Transactions on Smart Grid* 9.4 (July 2018), pp. 3330–3340. DOI: 10.1109/TSG.2016.2630714.

[53] D. J. Olsen et al. "Optimal Carbon Taxes for Emissions Targets in the Electricity Sector". In: *IEEE Transactions on Power Systems* 33.6 (Nov. 2018), pp. 5892–5901. DOI: 10.1109/TPWRS.2018.2827333.

[54] D. J. Olsen et al. "Planning Low-Carbon Campus Energy Hubs". In: *IEEE Transactions on Power Systems* (2019). DOI: 10.1109/TPWRS.2018.2879792.

[55] D. J. Olsen and D. S. Kirschen. "Profitable Emissions-Reducing Energy Storage". In: (2019). Submitted to *IEEE Transactions on Power Systems*.

[56] R. Sioshansi, R. O'Neill, and S. S. Oren. "Economic Consequences of Alternative Solution Methods for Centralized Unit Commitment in Day-Ahead Electricity Markets". In: *IEEE Transactions on Power Systems* 23.2 (May 2008), pp. 344–352. ISSN: 0885-8950. DOI: 10.1109/TPWRS.2008.919246.

[57] P. Samadi et al. "Optimal Real-Time Pricing Algorithm Based on Utility Maximization for Smart Grid". In: *2010 1st IEEE Int. Conf. on Smart Grid Commun. (SmartGridComm)*. Oct. 2010, pp. 415–420. DOI: 10.1109/SMARTGRID.2010.5622077.

[58] A.-H. Mohsenian-Rad and A. Leon-Garcia. "Optimal Residential Load Control With Price Prediction in Real-Time Electricity Pricing Environments". In: *IEEE Trans. Smart Grid* 1.2 (Sept. 2010), pp. 120–133. DOI: 10.1109/TSG.2010.2055903.

[59] M.R. Sarker, M.A. Ortega-Vazquez, and D.S. Kirschen. "Optimal Coordination and Scheduling of Demand Response via Monetary Incentives". In: *IEEE Trans. Smart Grid* 6.3 (May 2015), pp. 1341–1352. DOI: 10.1109/TSG.2014.2375067.

[60] M. Pipattanasomporn, M. Kuzlu, and S. Rahman. "An Algorithm for Intelligent Home Energy Management and Demand Response Analysis". In: *IEEE Trans. Smart Grid* 3.4 (Dec. 2012), pp. 2166–2173. DOI: 10.1109/TSG.2012.2201182.

[61] D.S. Callaway and I.A. Hiskens. "Achieving Controllability of Electric Loads". In: *Proceedings of the IEEE* 99.1 (Jan. 2011), pp. 184–199. DOI: 10.1109/JPROC.2010.2081652.

[62] N. G. Paterakis et al. "Optimal Household Appliances Scheduling Under Day-Ahead Pricing and Load-Shaping Demand Response Strategies". In: *IEEE Trans. Ind. Informa.* 11.6 (Dec. 2015), pp. 1509–1519. DOI: 10.1109/TII.2015.2438534.

[63] D. J. Hammerstrom et al. *Pacific Northwest GridWise testbed demonstration projects. Part I. Olympic Peninsula project*. Tech. rep. PNNL-17167. Pacific Northwest National Laboratory, 2007.

[64] "IEEE Guide for Loading Mineral-Oil-Immersed Transformers and Step-Voltage Regulators". In: *IEEE Std C57.91-2011 (Revision of IEEE Std C57.91-1995)* (Mar. 2012), pp. 1–123. DOI: 10.1109/IEEESTD.2012.6166928.

[65] P.J. Balducci et al. "An Examination of the Costs and Critical Characteristics of Electric Utility Distribution System Capacity Enhancement Projects". In: *2005/2006 IEEE PES Transmission and Distribution Conf. and Exhibition*. May 2006, pp. 78–86. DOI: 10.1109/TDC.2006.1668461.

[66] I. Gecils. *PY2013 Statewide AC Cycling Programs Process Evaluation*. Tech. rep. PGE0368.01. California Measurement Advisory Council, 2014.

[67] Katherine F. et al. "Saving energy cost-effectively: a national review of the cost of energy saved through utility-sector energy efficiency programs". In: *American Council for an Energy-Efficient Economy* (Sept. 2009).

[68] KEMA Inc. *Appliance Recycling Program Impact Evaluation*. Tech. rep. CPU0092.01. California Measurement Advisory Council, 2014.

[69] J. Taylor et al. "Evaluations of plug-in electric vehicle distribution system impacts". In: *2010 IEEE Power and Energy Soc. General Meeting*. July 2010, pp. 1–6. DOI: 10.1109/PES.2010.5589538.

[70] C. Farmer et al. "Modeling the Impact of Increasing PHEV Loads on the Distribution Infrastructure". In: *2010 43rd Hawaii Int. Conf. on Syst. Sci. (HICSS)*. Jan. 2010, pp. 1–10. DOI: 10.1109/HICSS.2010.277.

[71] Y. O. Assolami and W. G. Morsi. "Impact of Second-Generation Plug-In Battery Electric Vehicles on the Aging of Distribution Transformers Considering TOU Prices". In: *IEEE Trans. on Sustain. Energy* 6.4 (Oct. 2015), pp. 1606–1614. DOI: 10.1109/TSTE.2015.2460014.

[72] A.D. Hilshey et al. "Estimating the Impact of Electric Vehicle Smart Charging on Distribution Transformer Aging". In: *IEEE Trans. Smart Grid* 4.2 (June 2013), pp. 905–913. DOI: 10.1109/TSG.2012.2217385.

[73] K.J. Yunus et al. "Impacts of Stochastic Residential Plug-In Electric Vehicle Charging on Distribution Grid". In: *2012 IEEE PES Innovative Smart Grid Technol. (ISGT)*. Jan. 2012, pp. 1–8. DOI: 10.1109/ISGT.2012.6175691.

[74] M. R. Sarker, D. J. Olsen, and M. A. Ortega-Vazquez. "Co-Optimization of Distribution Transformer Aging and Energy Arbitrage Using Electric Vehicles". In: *IEEE Transactions on Smart Grid* 8.6 (Nov. 2017), pp. 2712–2722. DOI: 10.1109/TSG.2016.2535354.

[75] M.A. Cohen and D.S. Callaway. "Modeling the effect of geographically diverse pv generation on California's distribution system". In: *2013 IEEE Int. Conf. on Smart Grid Commun. (SmartGridComm)*. Oct. 2013, pp. 702–707. DOI: 10.1109/SmartGridComm.2013.6688041.

[76] R. Singh and A. Singh. "Aging of distribution transformers due to harmonics". In: *2010 14th Int. Conf. on Harmonics and Quality of Power (ICHQP)*. Sept. 2010, pp. 1–8. DOI: 10.1109/ICHQP.2010.5625347.

[77] M. Humayun et al. "Utilization Improvement of Transformers Using Demand Response". In: *IEEE Trans. Power Del.* 30.1 (Feb. 2015), pp. 202–210. DOI: 10.1109/TPWRD.2014.2325610.

[78] Q. Gong et al. "PEV Charging Control Considering Transformer Life and Experimental Validation of a 25 kVA Distribution Transformer". In: *IEEE Trans. Smart Grid* 6.2 (Mar. 2015), pp. 648–656. DOI: 10.1109/TSG.2014.2365452.

[79] M. Lodl and R. Witzmann. "Operation strategies of hybrid energy storages in low-voltage distribution grids with a high degree of decentralized generation". In: *2012 3rd IEEE PES Int. Conf. and Exhibition on Innovative Smart Grid Technol. (ISGT Europe)*. Oct. 2012, pp. 1–7. DOI: 10.1109/ISGTEurope.2012.6465750.

[80] S.M.M. Agah and H.A. Abyaneh. "Distribution Transformer Loss-of-Life Reduction by Increasing Penetration of Distributed Generation". In: *IEEE Trans. Power Del.* 26.2 (Apr. 2011), pp. 1128–1136. DOI: 10.1109/TPWRD.2010.2094210.

[81] A. Seier, P. D. H. Hines, and J. Frolik. "Data-Driven Thermal Modeling of Residential Service Transformers". In: *IEEE Trans. Smart Grid* 6.2 (2015), pp. 1019–1025. DOI: 10.1109/TSG.2015.2390624.

[82] D. Susa, M. Lehtonen, and H. Nordman. "Dynamic thermal modelling of power transformers". In: *IEEE Trans. Power Delivery* 20.1 (Jan. 2005), pp. 197–204. DOI: 10.1109/TPWRD.2004.835255.

[83] eMeter Strategic Consulting. *PowerCentsDC Program Final Report*. Tech. rep. Smart Meter Pilot Program, Inc, 2010.

[84] J. Wang, M. A. Biviji, and W. M. Wang. "Lessons learned from smart grid enabled pricing programs". In: *2011 IEEE Power and Energy Conf. at Illinois (PECI)*. Feb. 2011, pp. 1–7. DOI: 10.1109/PECI.2011.5740488.

[85] M. Alizadeh, T. H. Chang, and A. Scaglione. "Grid integration of distributed renewables through coordinated demand response". In: *2012 IEEE 51st IEEE Conf. on Decision and Control (CDC)*. Dec. 2012, pp. 3666–3671. DOI: 10.1109/CDC.2012.6426122.

[86] P. Wunderlich et al. "The Impact of Endogenous Motivations on Adoption of IT-Enabled Services: The Case of Transformative Services in the Energy Sector". In: *J. of Service Res.* 16.3 (2013), pp. 356–371. DOI: 10.1177/1094670512474841.

[87] E.M.L. Beale and J.A Tomlin. "Special facilities in a general mathematical programming system for non-convex problems using ordered sets of variables". In: *Proc. 5th Int. Conf. on Oper Res.* 1970, pp. 447–454.

[88] Pacific Northwest National Laboratory. *Feeder Taxonomy*. http://gridlab-d.sourceforge.net/wiki/index.php/Feeder_Taxonomy.

[89] William H. Kersting. *Distribution System Modeling and Analysis*. Boca Raton, Florida: CRC Press, 2012.

[90] Pecan Street Inc. *Dataport*. https://dataport.pecanstreet.org/.

[91] *2009 National Household Travel Survey*. Report. U.S. Department of Transportation, Federal Highway Administration, 2009.

[92] Electric Reliability Council of Texas. *Historical DAM Load Zone and Hub Prices*.

[93] NOAA National Climatic Data Center. *Quality Controlled Local Climatological Data*.

[94] GAMS Development Corporation. *GAMS—A User's Guide*. http://www.gams.com/dd/docs/bigdocs/GAMSUsersGuide.pdf. 2015.

[95] IBM. *User's Manual for CPLEX*. 2009.

[96] H. A. Gil and G. Joos. "On the Quantification of the Network Capacity Deferral Value of Distributed Generation". In: *IEEE Trans. Power Systems* 21.4 (Nov. 2006), pp. 1592–1599. DOI: 10.1109/TPWRS.2006.881158.

[97] D. Hammerstrom et al. "Standardization of a Hierarchical Transactive Control System". In: *Grid Interop 9*. 2009.

[98] *Valuing Climate Damages: Updating Estimation of the Social Cost of Carbon Dioxide*. Tech. rep. National Academies of Sciences, Engineering, and Medicine, 2017.

[99] Jarmo Vehmas. "Energy-related taxation as an environmental policy tool—the Finnish experience 1990–2003". In: *Energy Policy* 33.17 (2005), pp. 2175–2182.

[100] Christian Egenhofer. "The Making of the EU Emissions Trading Scheme: Status, Prospects and Implications for Business". In: *European Management Journal* 25.6 (2007), pp. 453–463.

[101] Reuven S. Avi-Yonah and David M. Uhlmann. "Combating Global Climate Change: Why a Carbon Tax is a Better Response to Global Warming than Cap and Trade". In: *Stanford Environmental Law Journal* 28.3 (2009).

[102] Gilbert E. Metcalf and David A. Weisbach. "The Design of a Carbon Tax". In: *University of Chicago Public Law & Legal Theory Working Paper* 254 (2009).

[103] Gilbert E. Metcalf. *Implementing a Carbon Tax*. Tech. rep. Resources For The Future, 2017.

[104] Warwick McKibbin et al. *The Potential Role of a Carbon Tax in U.S. Fiscal Reform*. Tech. rep. Brookings Institute, 2012.

[105] *Effects of a Carbon Tax on the Economy and the Environment*. Tech. rep. 4532. Congressional Budget Office, May 2013.

[106] John J. Conti et al. *Annual Energy Outlook 2014*. Tech. rep. U.S. Energy Information Administration, 2014.

[107] Carbon Brief. *Paris 2015: Tracking country climate pledges*. https://www.carbonbrief.org/paris-2015-tracking-country-climate-pledges. 2017.

[108] Antung Anthony Liu. "Tax evasion and optimal environmental taxes". In: *Journal of Environmental Economics and Management* 66.3 (2013), pp. 656–670.

[109] R. Ramanathan. "Emission constrained economic dispatch". In: *IEEE Transactions on Power Systems* 9.4 (Nov. 1994), pp. 1994–2000. DOI: 10.1109/59.331461.

[110] Yong Fu, M. Shahidehpour, and Zuyi Li. "Long-term security-constrained unit commitment: hybrid Dantzig-Wolfe decomposition and subgradient approach". In: *IEEE Transactions on Power Systems* 20.4 (Nov. 2005), pp. 2093–2106. DOI: 10.1109/TPWRS.2005.857286.

[111] M. Shao and W. T. Jewell. "CO2 emission-incorporated ac optimal power flow and its primary impacts on power system dispatch and operations". In: *IEEE PES General Meeting*. July 2010, pp. 1–8. DOI: 10.1109/PES.2010.5589724.

[112] Wei Wei et al. "Taxing Strategies for Carbon Emissions: A Bilevel Optimization Approach". In: *Energies* 7.4 (2014), pp. 2228–2245. DOI: 10.3390/en7042228.

[113] W. Wei, F. Liu, and S. Mei. "Nash Bargain and Complementarity Approach Based Environmental/Economic Dispatch". In: *IEEE Transactions on Power Systems* 30.3 (May 2015), pp. 1548–1549. DOI: 10.1109/TPWRS.2014.2346928.

[114] W. Wei, J. Wang, and S. Mei. "Convexification of the Nash Bargaining Based Environmental-Economic Dispatch". In: *IEEE Transactions on Power Systems* 31.6 (Nov. 2016), pp. 5208–5209. DOI: 10.1109/TPWRS.2016.2521322.

[115] *Operating Reserves and Variable Generation*. Tech. rep. NREL/TP-5500-51978. National Renewable Energy Laboratory, 2011.

[116] R. Fernández-Blanco, Y. Dvorkin, and M. A. Ortega-Vazquez. "Probabilistic Security-Constrained Unit Commitment With Generation and Transmission Contingencies". In: *IEEE Transactions on Power Systems* 32.1 (Jan. 2017), pp. 228–239. DOI: 10.1109/TPWRS.2016.2550585.

[117] *Western Wind and Solar Integration Study*. Tech. rep. NREL/SR-550-47434. National Renewable Energy Laboratory, 2010.

[118] Miguel Pérez de Arce and Enzo Sauma. "Comparison of incentive policies for renewable energy in an oligopolistic market with price-responsive demand". In: *The Energy Journal* 37.3 (2016), pp. 159–198.

[119] Kalyanmoy Deb, Karthik Sindhya, and Jussi Hakanen. "Multi-objective optimization". In: *Decision Sciences: Theory and Practice*. CRC Press, 2016, pp. 145–184.

[120] Graham R Wood. "The bisection method in higher dimensions". In: *Mathematical programming* 55.1-3 (1992), pp. 319–337.

[121] D. Krishnamurthy, W. Li, and L. Tesfatsion. "An 8-Zone Test System Based on ISO New England Data: Development and Application". In: *IEEE Transactions on Power Systems* 31.1 (Jan. 2016), pp. 234–246. DOI: 10.1109/TPWRS.2015.2399171.

[122] Energy Information Administration. *Monthly Energy Review*. 2016.

[123] Energy Information Administration. *How much carbon dioxide is produced when different fuels are burned?* 2016.

[124] Warren Katzenstein and Jay Apt. "Air Emissions Due To Wind And Solar Power". In: *Environmental Science & Technology* 43.2 (2009), pp. 253–258.

[125] B. D. Pitt. "Applications of Data Mining Techniques to Electric Load Profiling". PhD thesis. University of Manchester, 2000.

[126] H. Nosair and F. Bouffard. "Flexibility Envelopes for Power System Operational Planning". In: *IEEE Transactions on Sustainable Energy* 6.3 (July 2015), pp. 800–809. DOI: 10.1109/TSTE.2015.2410760.

[127] Stephen Boyd and Lieven Vandenberghe. *Convex optimization*. Cambridge university press, 2004.

[128] Patrick Billingsley. *Probability and Measure*. New York: Wiley, 1995.

[129] Mohsen Rahmani, Paulina Jaramillo, and Gabriela Hug. "Implications of environmental regulation and coal plant retirements in systems with large scale penetration of wind power". In: *Energy Policy* 95 (2016), pp. 196–210. DOI: 10.1016/j.enpol.2016.04.015.

[130] J. Qiu et al. "Low Carbon Oriented Expansion Planning of Integrated Gas and Power Systems". In: *IEEE Transactions on Power Systems* 30.2 (Mar. 2015), pp. 1035–1046. ISSN: 0885-8950. DOI: 10.1109/TPWRS.2014.2369011.

[131] *2014 Assessment of the ISO New England Electricity Markets*. Tech. rep. Potomac Economics, 2015.

[132] Research Into Action. *Process Evaluation of the 2013 Statewide Flex Alert Program*. Tech. rep. SCE0355. California Measurement and Advisory Council, 2014.

[133] Fernando J. de Sisternes, Jesse D. Jenkins, and Audun Botterud. "The value of energy storage in decarbonizing the electricity sector". In: *Applied Energy* 175 (2016), pp. 368–379. DOI: 10.1016/j.apenergy.2016.05.014.

[134] Yashen Lin, Jeremiah X. Johnson, and Johanna L. Mathieu. "Emissions impacts of using energy storage for power system reserves". In: *Applied Energy* 168 (2016), pp. 444–456. DOI: 10.1016/j.apenergy.2016.01.061.

[135] J. S. Heslin and B. F. Hobbs. "A multiobjective production costing model for analyzing emissions dispatching and fuel switching [of power stations]". In: *IEEE Transactions on Power Systems* 4.3 (Aug. 1989), pp. 836–842. DOI: 10.1109/59.32569.

[136] A. H. Milyani and D. S. Kirschen. "Optimally Designed Subsidies for Achieving Carbon Emissions Targets in Electric Power Systems". In: *2018 IEEE Power Energy Society General Meeting (PESGM)*. July 2018. DOI: 10.1109/PESGM.2018.8586055.

[137] Andrés Pereira, Enzo Sauma, and Juan Montero. "Impact of Carbon Tax Flexibility on the Chilean Power System Expansion Planning". In: *2019 IEEE Milano PowerTech*. June 2019.

[138] M. Geidl et al. "Energy hubs for the future". In: *IEEE Power and Energy Magazine* 5.1 (Jan. 2007), pp. 24–30.

[139] Christine Schwaegerl et al. "A multi-objective optimization approach for assessment of technical, commercial and environmental performance of microgrids". In: *European Transactions on Electrical Power* 21.2 (2011), pp. 1269–1288. DOI: 10.1002/etep.472.

[140] M. C. Bozchalui et al. "Optimal Operation of Residential Energy Hubs in Smart Grids". In: *IEEE Transactions on Smart Grid* 3.4 (Dec. 2012), pp. 1755–1766. DOI: 10.1109/TSG.2012.2212032.

[141] Ralph Evins. "Multi-level optimization of building design, energy system sizing and operation". In: *Energy* 90.Part 2 (2015), pp. 1775–1789. DOI: 10.1016/j.energy.2015.07.007.

[142] Ji Hyun Yi et al. "Impact of carbon emission constraint on design of small scale multi-energy system". In: *Energy* 161 (2018), pp. 792–808. DOI: 10.1016/j.energy.2018.07.156.

[143] Damien Picard and Lieve Helsen. "Economic Optimal HVAC Design for Hybrid GEOTABS Buildings and CO_2 Emissions Analysis". In: *Energies* 11.2 (2018). DOI: 10.3390/en11020314.

[144] C. Weber and N. Shah. "Optimisation based design of a district energy system for an eco-town in the United Kingdom". In: *Energy* 36.2 (2011), pp. 1292–1308. DOI: 10.1016/j.energy.2010.11.014.

[145] Boran Morvaj, Ralph Evins, and Jan Carmeliet. "Optimising urban energy systems: Simultaneous system sizing, operation and district heating network layout". In: *Energy* 116.Part 1 (2016), pp. 619–636. DOI: 10.1016/j.energy.2016.09.139.

[146] Yi Wang et al. "Mixed-integer linear programming-based optimal configuration planning for energy hub: Starting from scratch". In: *Applied Energy* 210 (2018), pp. 1141–1150.

[147] Modassar Chaudry et al. "Combined gas and electricity network expansion planning". In: *Applied Energy* 113 (2014), pp. 1171–1187. DOI: 10.1016/j.apenergy.2013.08.071.

[148] M. D. Galus, S. Koch, and G. Andersson. "Provision of Load Frequency Control by PHEVs, Controllable Loads, and a Cogeneration Unit". In: *IEEE Transactions on Industrial Electronics* 58.10 (Oct. 2011), pp. 4568–4582. DOI: 10.1109/TIE.2011.2107715.

[149] Pierluigi Mancarella. "MES (multi-energy systems): An overview of concepts and evaluation models". In: *Energy* 65 (2014), pp. 1–17. DOI: 10.1016/j.energy.2013.10.041.

[150] Garrett Hardin. "The Tragedy of the Commons". In: *Science* 162.3859 (1968), pp. 1243–1248. DOI: 10.1126/science.162.3859.1243.

[151] *Technical Support Document: Social Cost of Carbon for Regulatory Impact Analysis Under Executive Order 12866*. Tech. rep. U.S. Interagency Working Group on Social Cost of Carbon, 2010.

[152] *Technical Support Document: Technical Update of the Social Cost of Carbon for Regulatory Impact Analysis Under Executive Order 12866 [August 2016 revision]*. Tech. rep. U.S. Interagency Working Group on Social Cost of Greenhouse Gases, 2016.

[153] William D Nordhaus. "Revisiting the social cost of carbon". In: *Proceedings of the National Academy of Sciences* (2017), pp. 1518–1523.

[154] J. Vandewalle, K. Bruninx, and W. D'haeseleer. "Effects of large-scale power to gas conversion on the power, gas and carbon sectors and their interactions". In: *Energy Conversion and Management* 94 (2015), pp. 28–39.

[155] Jacques F Benders. "Partitioning procedures for solving mixed-variables programming problems". In: *Numerische mathematik* 4.1 (1962), pp. 238–252.

[156] Christodoulos A Floudas. *Nonlinear and mixed-integer optimization: fundamentals and applications*. Oxford University Press, 1995.

[157] Myriam De Saint Jean, Pierre Baurens, and Chakib Bouallou. "Parametric study of an efficient renewable power-to-substitute-natural-gas process including high-temperature steam electrolysis". In: *International Journal of Hydrogen Energy* 39.30 (2014), pp. 17024–17039.

[158] Ning Zhang et al. "Reducing curtailment of wind electricity in China by employing electric boilers for heat and pumped hydro for energy storage". In: *Applied Energy* 184 (2016), pp. 987–994.

[159] S. Wilcox and W. Marion. *Users Manual for TMY3 Data Sets*. Tech. rep. NREL/TP-581-43156. National Renewable Energy Laboratory, 2008.

[160] H. Pandžić et al. "Near-Optimal Method for Siting and Sizing of Distributed Storage in a Transmission Network". In: *IEEE Transactions on Power Systems* 30.5 (Sept. 2015), pp. 2288–2300.

[161] S.M. Hasnain. "Review on sustainable thermal energy storage technologies, Part II: cool thermal storage". In: *Energy Conversion and Management* 39.11 (1998), pp. 1139–1153.

[162] Audun Aspelund, Steinar P. Tveit, and Truls Gundersen. "A liquefied energy chain for transport and utilization of natural gas for power production with CO_2 capture and storage – Part 3: The combined carrier and onshore storage". In: *Applied Energy* 86.6 (2009), pp. 805–814.

[163] Brian Songhurst. *LNG plant cost escalation*. Tech. rep. The Oxford Institute for Energy Studies, 2014.

[164] Sven Werner. "International review of district heating and cooling". In: *Energy* (2017).

[165] Joshua S. Graff Zivin, Matthew J. Kotchen, and Erin T. Mansur. "Spatial and temporal heterogeneity of marginal emissions: Implications for electric cars and other electricity-shifting policies". In: *Journal of Economic Behavior & Organization* 107.Part A (2014), pp. 248–268.

[166] Stephan Dempe et al. "Bilevel programming problems". In: *Energy Systems. Springer, Berlin* (2015).

[167] Emilie Danna, Edward Rothberg, and Claude Le Pape. "Exploring relaxation induced neighborhoods to improve MIP solutions". In: *Mathematical Programming* 102.1 (2005), pp. 71–90.

[168] GAMS Development Corporation. *GAMS: Solver Usage*. `https://www.gams.com/latest/docs/UG_SolverUsage.html`. 2018.

[169] Banu Soylu and Gazi Bilal Yıldız. "An exact algorithm for biobjective mixed integer linear programming problems". In: *Computers & Operations Research* 72 (2016), pp. 204–213. DOI: 10.1016/j.cor.2016.03.001.

[170] Eric S. Hittinger and Inês M. L. Azevedo. "Bulk Energy Storage Increases United States Electricity System Emissions". In: *Environmental Science & Technology* 49.5 (2015), pp. 3203–3210. DOI: 10.1021/es505027p.

[171] Michael J. Fisher and Jay Apt. "Emissions and Economics of Behind-the-Meter Electricity Storage". In: *Environmental Science & Technology* 51.3 (2017), pp. 1094–1101. DOI: 10.1021/acs.est.6b03536.

[172] B. C. Ummels, E. Pelgrum, and W. L. Kling. "Integration of large-scale wind power and use of energy storage in the Netherlands' electricity supply". In: *IET Renewable Power Generation* 2.1 (Mar. 2008), pp. 34–46. DOI: 10.1049/iet-rpg:20070056.

[173] Ramteen Sioshansi. "Emissions Impacts of Wind and Energy Storage in a Market Environment". In: *Environmental Science & Technology* 45.24 (2011), pp. 10728–10735. DOI: 10.1021/es2007353.

[174] Richard T. Carson and Kevin Novan. "The private and social economics of bulk electricity storage". In: *Journal of Environmental Economics and Management* 66.3 (2013), pp. 404–423. DOI: 10.1016/j.jeem.2013.06.002.

[175] Oytun Babacan et al. "Unintended Effects of Residential Energy Storage on Emissions from the Electric Power System". In: *Environmental Science & Technology* 52.22 (2018), pp. 13600–13608. DOI: 10.1021/acs.est.8b03834.

[176] Menglian Zheng et al. "Economic and environmental benefits of coordinating dispatch among distributed electricity storage". In: *Applied Energy* 210 (2018), pp. 842–855. DOI: 10.1016/j.apenergy.2017.07.095.

[177] Scott B. Peterson, J. F. Whitacre, and Jay Apt. "Net Air Emissions from Electric Vehicles: The Effect of Carbon Price and Charging Strategies". In: *Environmental Science & Technology* 45.5 (2011), pp. 1792–1797. DOI: 10.1021/es102464y.

[178] Christopher G. Hoehne and Mikhail V. Chester. "Optimizing plug-in electric vehicle and vehicle-to-grid charge scheduling to minimize carbon emissions". In: *Energy* 115 (2016), pp. 646–657. DOI: 10.1016/j.energy.2016.09.057.

[179] Laura M. Arciniegas and Eric Hittinger. "Tradeoffs between revenue and emissions in energy storage operation". In: *Energy* 143 (2018), pp. 1–11. DOI: 10.1016/j.energy.2017.10.123.

[180] Mehdi Noori et al. "Light-duty electric vehicles to improve the integrity of the electricity grid through Vehicle-to-Grid technology: Analysis of regional net revenue and emissions savings". In: *Applied Energy* 168 (2016), pp. 146–158. DOI: 10.1016/j.apenergy.2016.01.030.

[181] Nicole A. Ryan et al. "Use-Phase Drives Lithium-Ion Battery Life Cycle Environmental Impacts When Used for Frequency Regulation". In: *Environmental Science & Technology* 52.17 (2018), pp. 10163–10174. DOI: 10.1021/acs.est.8b02171.

[182] Yashen Lin, Jeremiah X. Johnson, and Johanna L. Mathieu. "Emissions impacts of using energy storage for power system reserves". In: *Applied Energy* 168 (2016), pp. 444–456. DOI: 10.1016/j.apenergy.2016.01.061.

[183] D. J. Swider. "Compressed Air Energy Storage in an Electricity System With Significant Wind Power Generation". In: *IEEE Transactions on Energy Conversion* 22.1 (Mar. 2007), pp. 95–102. DOI: 10.1109/TEC.2006.889547.

[184] Trishna Das, Venkat Krishnan, and James D. McCalley. "Assessing the benefits and economics of bulk energy storage technologies in the power grid". In: *Applied Energy* 139 (2015), pp. 104–118. DOI: 10.1016/j.apenergy.2014.11.017.

[185] Ramteen Sioshansi and Paul Denholm. "Emissions Impacts and Benefits of Plug-In Hybrid Electric Vehicles and Vehicle-to-Grid Services". In: *Environmental Science & Technology* 43.4 (2009), pp. 1199–1204. DOI: 10.1021/es802324j.

[186] Michael T Craig, Paulina Jaramillo, and Bri-Mathias Hodge. "Carbon dioxide emissions effects of grid-scale electricity storage in a decarbonizing power system". In: *Environmental Research Letters* 13.1 (2018).

[187] A. Tuohy and M. O'Malley. "Pumped storage in systems with very high wind penetration". In: *Energy Policy* 39.4 (2011), pp. 1965–1974. DOI: 10.1016/j.enpol.2011.01.026.

[188] Markus Haller, Sylvie Ludig, and Nico Bauer. "Decarbonization scenarios for the EU and MENA power system: Considering spatial distribution and short term dynamics of renewable generation". In: *Energy Policy* 47 (2012), pp. 282–290. DOI: 10.1016/j.enpol.2012.04.069.

[189] Michaela Fürsch et al. "The role of grid extensions in a cost-efficient transformation of the European electricity system until 2050". In: *Applied Energy* 104 (2013), pp. 642–652. DOI: 10.1016/j.apenergy.2012.11.050.

[190] Ana Mileva et al. "Power system balancing for deep decarbonization of the electricity sector". In: *Applied Energy* 162 (2016), pp. 1001–1009. DOI: 10.1016/j.apenergy.2015.10.180.

[191] J. Haas et al. "Challenges and trends of energy storage expansion planning for flexibility provision in low-carbon power systems – a review". In: *Renewable and Sustainable Energy Reviews* 80 (2017), pp. 603–619. DOI: 10.1016/j.rser.2017.05.201.

[192] K. Pandžić, H. Pandžić, and I. Kuzle. "Coordination of Regulated and Merchant Energy Storage Investments". In: *IEEE Transactions on Sustainable Energy* 9.3 (July 2018), pp. 1244–1254. DOI: 10.1109/TSTE.2017.2779404.

[193] H. Mohsenian-Rad. "Coordinated Price-Maker Operation of Large Energy Storage Units in Nodal Energy Markets". In: *IEEE Transactions on Power Systems* 31.1 (Jan. 2016), pp. 786–797. DOI: 10.1109/TPWRS.2015.2411556.

[194] Y. Dvorkin et al. "Ensuring Profitability of Energy Storage". In: *IEEE Transactions on Power Systems* 32.1 (Jan. 2017), pp. 611–623. DOI: 10.1109/TPWRS.2016.2563259.

[195] Jonathan H. Owen and Sanjay Mehrotra. "On the Value of Binary Expansions for General Mixed-Integer Linear Programs". In: *Operations Research* 50.5 (2002), pp. 810–819. DOI: 10.1287/opre.50.5.810.370.

[196] Akshay Gupte et al. "Solving mixed integer bilinear problems using MILP formulations". In: *SIAM Journal on Optimization* 23.2 (2013), pp. 721–744.

[197] *Reliability Test System of the Grid Modernization Laboratory Consortium*. https://github.com/GridMod/RTS-GMLC. 2018.

[198] A. Almaimouni et al. "Selecting and Evaluating Representative Days for Generation Expansion Planning". In: *2018 Power Systems Computation Conference (PSCC)*. June 2018. DOI: 10.23919/PSCC.2018.8442580.

[199] Benjamin Whitney Griffiths. "Reducing emissions from consumer energy storage using retail rate design". In: *Energy Policy* 129 (2019), pp. 481–490. DOI: 10.1016/j.enpol.2019.01.039.

[200] A. G. Thomas and L. Tesfatsion. "Braided Cobwebs: Cautionary Tales for Dynamic Pricing in Retail Electric Power Markets". In: *IEEE Transactions on Power Systems* 33.6 (Nov. 2018), pp. 6870–6882. DOI: 10.1109/TPWRS.2018.2832471.

[201] Dennis Y.C. Leung, Giorgio Caramanna, and M. Mercedes Maroto-Valer. "An overview of current status of carbon dioxide capture and storage technologies". In: *Renewable and Sustainable Energy Reviews* 39 (2014), pp. 426–443.

[202] Samuel C. Johnson et al. "Evaluating rotational inertia as a component of grid reliability with high penetrations of variable renewable energy". In: *Energy* 180 (2019), pp. 258–271. DOI: 10.1016/j.energy.2019.04.216.

[203] Q. Chen, C. Kang, and Q. Xia. "Modeling Flexible Operation Mechanism of CO_2 Capture Power Plant and Its Effects on Power-System Operation". In: *IEEE Transactions on Energy Conversion* 25.3 (Sept. 2010), pp. 853–861.

[204] Abdirahman M. Abdilahi et al. "Harnessing flexibility potential of flexible carbon capture power plants for future low carbon power systems: Review". In: *Renewable and Sustainable Energy Reviews* (2017).

[205] Xue Li et al. "Stochastic low-carbon scheduling with carbon capture power plants and coupon-based demand response". In: *Applied Energy* 210 (2018), pp. 1219–1228. ISSN: 0306-2619. DOI: 10.1016/j.apenergy.2017.08.119.

[206] A. Zlotnik et al. "Coordinated Scheduling for Interdependent Electric Power and Natural Gas Infrastructures". In: *IEEE Transactions on Power Systems* 32.1 (Jan. 2017), pp. 600–610.

[207] J. Yang et al. "Effect of Natural Gas Flow Dynamics in Robust Generation Scheduling under Wind Uncertainty". In: *IEEE Transactions on Power Systems* 33.2 (Mar. 2018), pp. 2087–2097.

[208] X. Wang et al. "A carbon capture and distribution network design problem for carbon emission reduction and utilization". In: *Proceedings of 2010 IEEE International Conference on Service Operations and Logistics, and Informatics*. July 2010, pp. 246–251.

[209] H. Y. Yun et al. "Networks optimization for capturing and transporting CO2". In: *2014 IEEE International Conference on Industrial Engineering and Engineering Management*. Dec. 2014, pp. 739–743.

[210] Boran Morvaj, Ralph Evins, and Jan Carmeliet. "Decarbonizing the electricity grid: The impact on urban energy systems, distribution grids and district heating potential". In: *Applied Energy* 191 (2017), pp. 125–140. DOI: 10.1016/j.apenergy.2017.01.058.